NBER WORKING PAPER SERIES

THE FRACTURED-LAND HYPOTHESIS

Jesús Fernández-Villaverde
Mark Koyama
Youhong Lin
Tuan-Hwee Sng

Working Paper 27774
http://www.nber.org/papers/w27774

NATIONAL BUREAU OF ECONOMIC RESEARCH
1050 Massachusetts Avenue
Cambridge, MA 02138
September 2020, Revised August 2022

We are grateful for comments from the editor, four referees, seminar audiences at Brown University, the NBER DAE meeting, the NBER EFDIS meeting, the Quantitative History Webinar Series hosted by Hong Kong University, the China Economics Summer Institute, Toulouse School of Economics, UC Irvine, Vancouver School of Economics, and CEIBS, and from discussions with Siwan Anderson, Emmanuelle Auriol, Roland Bénabou, Lisa Blaydes, Eric Bouteiller, Jean-Paul Carvalho, Latika Chaudhary, Dan Bogart, Zhiwu Chen, Felipe Valencia Caicedo, James Fenske, Oded Galor, Saum Jha, Nippe Lagerlöf, Chicheng Ma, Joel Mokyr, Gary Richardson, Mohamed Saleh, Paul Seabright, Stergios Skaperdas, Enrico Spolaore, Denis Tkachenko, Felipe Valencia, Joachim Voth, Yang Xie, Kan Xu, and Melanie Meng Xue. We are grateful to Kan Xu, Yidan Han, and Pei Zhi Chia for research support. The views expressed herein are those of the authors and do not necessarily reflect the views of the National Bureau of Economic Research.

The Fractured-Land Hypothesis
Jesús Fernández-Villaverde, Mark Koyama, Youhong Lin, and Tuan-Hwee Sng
NBER Working Paper No. 27774
September 2020, Revised August 2022
JEL No. H56,N40,P48

ABSTRACT

Patterns of state formation have crucial implications for comparative economic development. Diamond (1997) famously argued that "fractured land" was responsible for China's tendency toward political unification and Europe's protracted polycentrism. We build a dynamic model with granular geographical information in terms of topographical features and the location of productive agricultural land to quantitatively gauge the effects of fractured land on state formation in Eurasia. We find that topography alone is sufficient, but not necessary, to explain polycentrism in Europe and unification in China. Differences in land productivity, in particular the existence of a core region of high land productivity in northern China, also deliver the same result. We discuss how our results map into observed historical outcomes, assess how robust our findings are, and analyze the predictions of our model for Africa and the Americas.

Jesús Fernández-Villaverde
Department of Economics University
of Pennsylvania
The Ronald O. Perelman Center
for Political Science and Economics
133 South 36th Street Suite 150
Philadelphia, PA 19104
and CEPR
and also NBER
jesusfv@econ.upenn.edu

Mark Koyama
Center for the Study of Public Choice,
George Mason University
Fairfax, VA 22030
mkoyama2@gmu.edu

Youhong Lin
Center for Cliometrics Studies of China
Guangdong University of Foreign Studies
lin.youhong@foxmail.com

Tuan-Hwee Sng
National University of Singapore
Department of Economics
SINGAPORE 117570
tsng@nus.edu.sg

Here begins our tale. The empire, long divided, must unite; long united, must divide. Thus it has ever been.

Romance of the Three Kingdoms, Chapter 1.

1 Introduction

The economic rise of western Europe is often attributed to its polycentric state system (see, among others, Jones, 2003; Mokyr, 2016; and Scheidel, 2019). In this reading of the historical record, the European state system i) fostered intellectual pluralism, which made a competitive market for ideas possible (and, with it, the Scientific and Industrial Revolutions); and ii) created incentives for institutional innovation and incremental investment in state capacity. Correspondingly, many explanations of China's failure to achieve sustained economic growth focus on its long history as a centralized empire and the barriers to riches that such centralization induced. But what factors account for the prevalence of political polycentrism in Europe and the prominence of political centralization in China?

Researchers have proposed numerous mechanisms for the divergence in state systems across the two extremes of the Eurasia landmass. A popular mechanism, made famous by Diamond (1997, 1998), argues that "fractured land" such as mountain barriers, dense forests, indented coastlines, and rugged terrain impeded the development of large empires in Europe in comparison to other parts of Eurasia.

The fractured-land hypothesis is not without its critics. Hoffman (2015) points out that China is, in fact, more mountainous than Europe. Peter Turchin and Tanner Greer have advanced similar arguments.[1] Turchin goes so far as to claim that it is not Europe's fragmentation that needs explanation, but China's precocious and persistent unification. The fractured-land hypothesis has also been challenged for being static and overly deterministic. Hui (2005, p. 1) contests the idea that China was "destined to have authoritarian rule under a unified empire," while contending that Europe's political fragmentation was a highly contingent outcome. After all, China has not always been unified. As the opening lines of *The Romance of Three Kingdoms* above remind us, China has experienced long periods of fragmentation throughout its history.

[1] See, for details, http://peterturchin.com/cliodynamica/why-europe-is-not-china/ and http://scholars-stage.blogspot.com/2013/06/geography-and-chinese-history-fractured.html.

Besides, the degree of fragmentation in Europe has varied over time.[2]

This paper has two goals. First, we provide a quantitative investigation of the fractured-land hypothesis. We gauge why China became a large state early in history, whereas Europe experienced protracted polycentrism, by modeling the dynamic process of state-building and exploring how fractured land shaped inter-state competition in unexpected non-linear ways. Second, we illustrate the applicability of our model by studying state formation more generally. Using rich data on topography, climate, and land productivity, we simulate this model for the entire world, including Africa and the Americas, at a fine grid-cell geographical level and look at the resulting probability distributions of political structures.

Inspired by Crafts (1977) and Turchin et al. (2013), we focus on pattern predictions rather than replicating specific outcomes. We report probability distributions over outcomes because history is contingent. An independent event could interact with existing conditions to trigger unanticipated consequences. Absent that event, history may develop in a different direction. Our model allows for contingency in the outbreak and outcome of wars. Thus, our simulations are random, but with probabilities assigned by structural conditions. If and when a state emerges to dominate its neighbors is neither fluke nor destiny, but a balance of structure and contingency. Our model does not aim to capture the precise borders of specific countries—which are the product of chance events—but it *does* aim to generate patterns in border formation that correspond to what we observe historically.

Our main finding is that fractured land indeed provides a robust explanation for the political divergence observed at the two ends of Eurasia: a unified China and a polycentric Europe. In addition, our model allows us to distinguish between two versions of the fractured-land hypothesis. First, in a narrow sense, scholars have equated fractured land with the presence of mountainous and rugged topography. Second, a broader definition of fractured land considers the location of productive agricultural land.

We document that topography alone is sufficient, but not necessary, to explain polycentrism in Europe and unification in China. The location of Europe's mountain ranges ensured that

[2]There is a question about how we measure political fragmentation before the rise of the modern nation-state. Can we consider the Holy Roman Empire as a unified polity? Under Otto I (r. 962–973, all dates are CE unless otherwise noted), perhaps yes. Under Francis I (r. 1745–1765), most likely no. For operational purposes, and following the Weberian tradition, we will call a "polity" or "state" an organization that keeps a quasi-monopoly of violence over a fixed territory (Weber, 1972; Tilly, 1990).

there were several distinct geographical cores of equal size that could provide the nuclei for future European states. In contrast, China was dominated by a single vast plain between the Yangtze and the Yellow Rivers. But the presence of a dominant core region of high land productivity in China—in the form of the North China Plain—and the lack thereof in Europe can also explain political unification in China and division in Europe.

It is only when we neutralize the effects of fractured land in the broad sense that Europe and China cease to move at different paces toward political unification. Thus, geographical features that went beyond ruggedness might be crucial to understanding why China unified and Europe remained polycentric. Our analysis highlights the importance of having core geographical regions of high land productivity unbroken by major mountain, desert, or sea barriers.

Importantly, we establish that fractured land can explain why Europe was fragmented into medium-sized states rather than into a large number of tiny and fragile polities as in Southeast Asia. It is precisely this configuration of medium-sized polities that researchers have argued played a critical role in developing European institutions. Among the most influential contributions, Mokyr (2016) has emphasized how a politically fragmented Europe fostered a competitive "market for ideas" that led to the intellectual milieu that made the Industrial Revolution possible. In other words, polycentrism can set up the pre-conditions required for the technological change highlighted in Galor and Weil (2000) and Galor (2005, 2011). Scheidel (2019) makes similar points, although he highlights institutional innovation as well.

In comparison, a centralized empire like China could more easily suppress ideas that challenged the status quo through many channels, such as the civil service exam that dominated elite selection (Lin, 1995), the limits to the development of "useful knowledge" (Mokyr, 2016, pp. 316–317), or the prevailing patterns of social cooperation (Greif and Tabellini, 2017). Jami (2012, p. 389) has even talked about "the continued imperial monopoly of 'science as action'." Thus, political centralization might account for the "Needham Paradox" of why China did not experience an indigenous industrial revolution despite having most of the pre-conditions that existed in Great Britain in the 18th century.[3] More generally, Roland (2020) argues that world civilizations can be split into two cultural and institutional types, one statist and one market-oriented, and suggests that geography might play a role in determining which system predominates.

[3] Mokyr (2016, ch. 16), reviews other proposed explanations of the "Needham Paradox."

A critical insight of this interpretation is that the costs and benefits of China's state system varied according to the overall level of technology. Civil service examinations based on the rote memorization of Confucian classics can create an efficient bureaucracy to run a pre-industrial society based on extensive Smithian division of labor, but it cannot spawn a scientific revolution that triggers industrialization.

We assess how our quantitative results depend on the assumptions and calibration of the model through an extensive battery of robustness tests. These tests confirm the key role of fractured land in the broad sense.

Our dynamic model of state-building is also of methodological interest for two reasons. First, we can use it as a measurement device to identify those dimensions where a simple geographical explanation needs improvement. For example, we use our model to demonstrate how the slow diffusion of maize in the Americas slowed down political consolidation. Second, it is easy to extend our model, in future research, to incorporate other factors—such as religious, linguistic, genetic, and ethnic diversity or technological and climatic change—that have played a role in state formation. Arbatli et al. (2020) and Spolaore and Wacziarg (2016) have documented the importance of population diversity for the frequency of intrasocietal conflicts. Ashraf and Galor (2013, 2018) suggest that the "endowment" of greater genetic diversity in Europe than in China may drive polycentricity. Conversely, the standardization of the Chinese characters by Qin Shi Huang has been a unifying force throughout China's history. Olsson and Hansson (2011) suggest a long history of statehood is associated with less ethnolinguistic fractionalization. Our argument is not that these factors are not relevant, but that we can capture much of the dynamics of the data by relying only on our simple geographical mechanism.

Our model also ignores the role of improvement in military technology through inter-state competition highlighted by Hoffman (2015). According to Hoffman, a political-military tournament eradicated polities that were unable to compete and accelerated military and political innovation through learning-by-doing. Our results show that this is not necessary to account for the comparative political structures of Europe and China. In a richer model, the political-military tournament could be a complement to fractured land.

Our analysis contributes to several literatures. First, we build on Turchin et al. (2013), who pioneered the use of quantitative simulations to understand the causal link between geography and state fragmentation. However, both our question and findings differ. Turchin et al. (2013) focus

on the diffusion of cultural traits and military technology. They argue that the intensification of warfare—a process influenced by proximity to the Eurasian steppe and antagonistic relations between nomads and settled agriculturalists—selected for ultrasocial traits and large-scale states by pressuring premodern polities to strengthen and invest in state capacity. In comparison, we focus on the systematic differences in the size and pattern of state formation and offer a quantitative account for Europe's polycentricity.

Second, we complement a long-standing literature that attributes the rise of western Europe to its multi-state system by investigating the *causes* of Europe's political fragmentation. Without being exhaustive, the literature includes Hume (1752), Montesquieu (1989), Pirenne (1925), Hicks (1969), Jones (2003), Hall (1985), Rosenberg and Birdzell (1986), Baechler (1975), Cowen (1990), Tilly (1990), Chaudhry and Garner (2006), Mokyr (2007), Karayalcin (2008), Chu (2010), Olsson and Hansson (2011), Voigtländer and Voth (2013a), and Lagerlöf (2014).

Third, we add to the literature on state formation in China and Europe. One strand emphasizes the importance of the threat from the steppe in Chinese state development (Lattimore, 1940; Grousset, 1970; Huang, 1988; Barfield, 1989; Gat, 2006; Turchin, 2009; Bai and Kung, 2011; Chen, 2015; Ko et al., 2018). Other scholars contrast the greater absolutist power of Chinese rulers relative to their European counterparts (Fukuyama, 2011; Jia et al., 2020). Another strand considers military competition in European state formation (Parker, 1988; Tilly, 1990; Downing, 1992; Voigtländer and Voth, 2013b; Gennaioli and Voth, 2015; Becker et al., 2020), or the relative dearth of inter-state conflicts as a hindrance to the rise of representative government in China (Dincecco and Wang, 2018). Finally, the literature on the size of nations pioneered by Alesina and Spolaore (1997, 2003, 2005) relates state size to both conflict and trade.

Fourth, our study is related to work that investigates the relationship between agricultural productivity, state formation, and conflict (Mayshar et al., 2022, 2017). For instance, Iyigun et al. (2017) examine the link between a permanent rise in agricultural productivity and conflict between 1400 and 1900, while Acharya and Lee (2018) develop a model in which economic development generates rents that lead to the formation of territorial states.

Empirically, Kitamura and Lagerlöf (2019) find that mountain ranges and rivers have an influence on the location of political boundaries in Europe and the Near East. They link the stability of borders to higher levels of income. Other empirical tests of other parts of Diamond's hypothesis include Turchin et al. (2006), Laitin et al. (2012), and Pavlik and Young (2019).

Last, we contribute to the literature on the relationship between geography and economic and political outcomes. Geography can shape economic outcomes directly via access to trade routes or vulnerability to disease vectors (Sachs, 2001) or indirectly via its effect on ethnic fragmentation (Ahlerup and Olsson, 2012; Michalopoulos, 2012) or political institutions (Acemoglu et al., 2001, 2002, 2005). We provide an example of the latter phenomenon: geography mattered because it gave rise to a centralized state in China and polycentrism in Europe.

The remainder of the paper is organized as follows. Section 2 outlines the fractured-land hypothesis. Section 3 builds a model of inter-state competition that integrates geographical characteristics. Section 4 calibrates the model and Section 5 presents the quantitative results. Section 6 discusses some aspects of Chinese and European history in light of our model. Section 7 looks at the implications of our model for Africa and the Americas. Section 8 discusses extensions of the model. Section 9 concludes.

2 Fractured Land?

Anthropologists, geographers, historians, and sociologists have long argued that early states only formed when three conditions were satisfied. First, there was a sufficiently large area of productive agricultural land to generate the food surplus required to feed and clothe a political elite and its bureaucracy. Second, this food output needed to be appropriable (Mayshar et al., 2022). Third, there were geographical boundaries that made it possible to coerce the population into transferring food surpluses to the political elite (e.g., Carneiro, 1970). Indeed, agrarian states struggled to project power into rugged, hilly, or mountainous lands where coercion was too costly (Mayshar et al., 2017; Scott, 2017).

Based on these ideas, geographers built the concept of a geographical core to describe the nucleus of successful states (Whittlesey, 1944; Pounds and Ball, 1964; Hechter and Brustein, 1980). The cores of most early states were centered around self-contained regions that had fertile agricultural land and good transport connections, and that were defensible from external invasion. Conversely, geographical cores that satisfied the above conditions experienced earlier and faster state formation.

Many authors (e.g., Hume, 1752; Jones, 2003; Kennedy, 1987) have postulated that since Europe's topographical peculiarities were less favorable to the formation of early states, the

posterior history of the continent was plagued by fragmentation. The most influential formulation of this idea is the fractured-land hypothesis of Diamond (1997, 1998). Diamond makes three observations: (1) China was not threatened by the presence of large islands off its mainland (Taiwan and Hainan were too small and Japan too far away); (2) the Chinese coastline was smooth compared to the European coastline; and (3) most importantly, unlike Europe, China was not fractured by high mountains and dense forests.

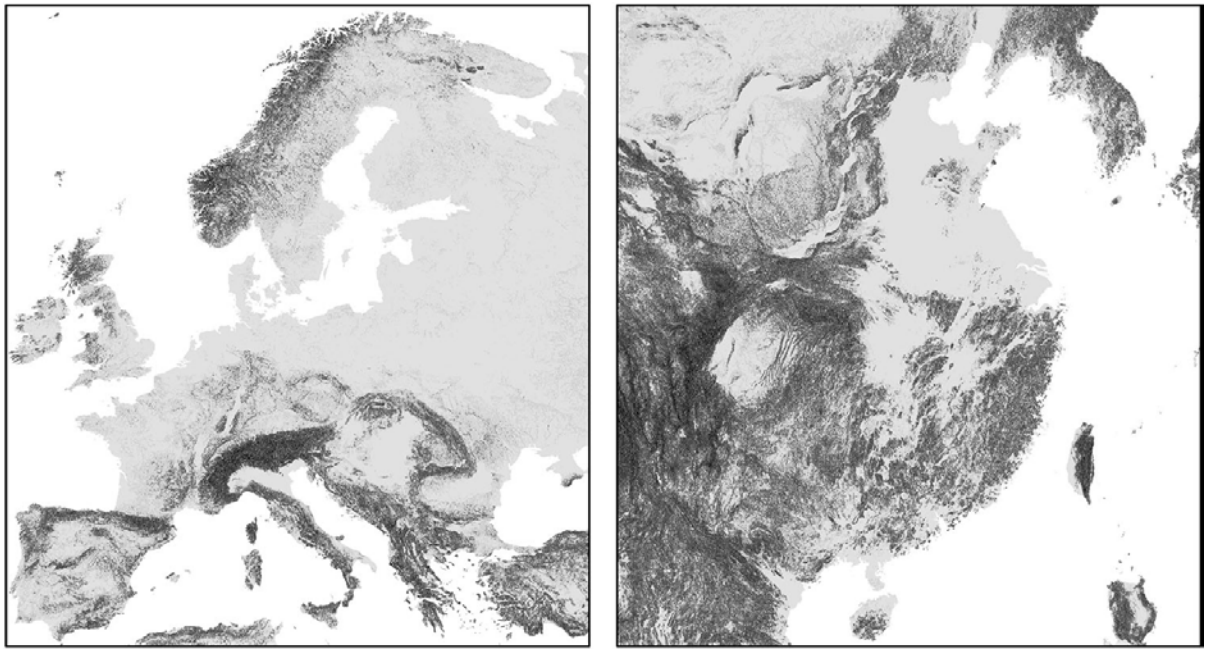

Figure 1: Ruggedness in Europe and China proper.

The claims of the fractured-land hypothesis have come under heavy criticism. Hoffman (2015, pp. 109–112) observes that China is significantly more mountainous than Europe (see Figure 1). Over 37% of modern China is defined as mountainous compared to little more than 10% of Europe. Even if one restricts attention to the so-called China proper, i.e., the traditionally agrarian part of China south of the Great Wall and east of the Tibetan plateau, more than 33% was elevated above 1,000 m. compared to only around 6% in Europe.

However, the crucial factor might not be the ruggedness of the terrain at large, but the location of either continent's mountainous regions. Beyond the total amount of ruggedness, Figure 1 illustrates that mountain ranges at or near the center of western Europe play an important role in separating Italy and Spain from France and making core regions of central Europe (Switzerland, Austria) difficult to conquer.[4]

[4]During World War II, Switzerland planned a retreat to a "réduit national" in the central part of Switzerland

Consequently, Europe comprises several cores: the British Isles, Scandinavia, the Iberian peninsula, and the Italian peninsula. France, the Low Countries, Germany, and Poland span what is known as the northern European plain. The easternmost part of this plain borders the Russian forest in the northeast, the steppe in the east, and the Carpathian mountains in the south; it corresponds loosely to modern Poland and the territory controlled by the Polish-Lithuanian Commonwealth in the early modern period. The central part of the plain corresponds to modern Germany, while France occupies the western part of the plain.

Meanwhile, the most mountainous regions in China are in the south and west, and they do not intersect the Central Plain in the north that historically played a crucial role in China's early unification. The Central Plain, centered on the Yellow River basin, is blocked from Korea in the northeast by the Changbai Mountains and the Taihang Mountains in the west. The plain itself is flat, except for the Taishan Mountains in Shandong and the Dabie Mountains of Anhui. southern China is more mountainous than the central Chinese plain. The Yunnan-Guizhou plateau has a particularly high elevation. Mountains and then dense forests divided Lingnan and Yunnan from Vietnam and Burma, respectively. Diamond (1997, p. 414) himself emphasizes the existence of a large core region capable of dominating the other regions in China:

> China's heartland is bound together from east to west by two long navigable river systems in rich alluvial valleys (the Yangtze and Yellow Rivers), and it is joined from north to south by relatively easy connections between these two river systems (eventually linked by canals). As a result, China very early became dominated by two huge geographic core areas of high productivity, themselves only weakly separated from each other and eventually fused into a single core.

The arguments in the previous pages are qualitative. As such, they cannot be assessed quantitatively (e.g., *how* rough must the terrain be to make a difference for political unification?) or used to measure the role of structure versus contingency in the observed outcomes (perhaps China's early leaders were luckier or better than their European counterparts?).

Can we bring quantitative data and a simple model of state formation and competition to the table and formally evaluate the fractured-land hypothesis and the range of distributions of probability that it can span? The next section introduces such a model.

in case of a German invasion. The 12 Battles of the Isonzo during World War I between the Italian and Austro-Hungarian armies suggest that taking over such a redoubt is extremely costly, even for a modern army.

3 Model

First, we describe how we divide the world into hexagonal cells. Second, we measure the geographical, climatic, and resource availability characteristics in each of those cells. Third, we highlight Eurasia, the region we will focus on for our baseline exercises. Fourth, we present a formal model of how polities evolve through conflict and secession by gaining or losing cells.

3.1 The Geographical Space

Our first step is to divide the Earth's landmass (excluding Antarctica, which is largely uninhabited even today) into 65,641 hexagonal cells of radius 28 kilometers, each potentially capable of sustaining a polity and allowing armies to pass through it (Figure 2). This radius corresponds to the distance that a healthy adult travels by foot per day on flat terrain.[5] As a result, a 28-kilometer hexagon roughly represents the surface that the simplest polities can monitor and defend with rudimentary Bronze Age technologies. Subsection 3.4 will motivate why we fill our geographical space with hexagons instead of other shapes.

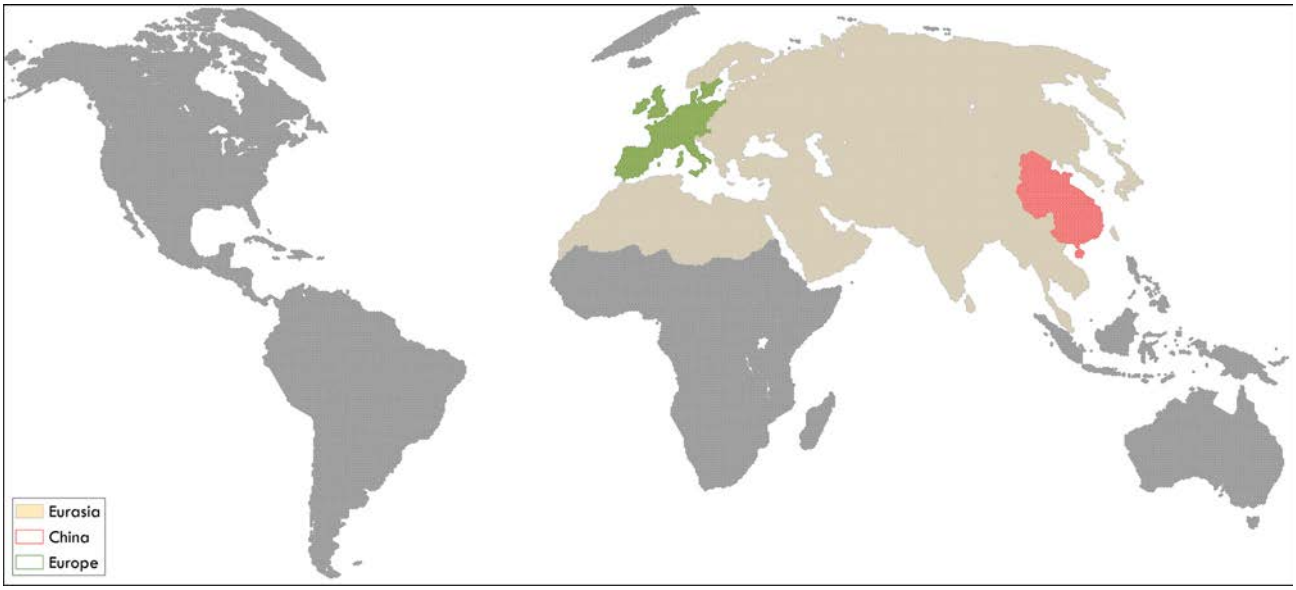

Figure 2: The world in hexagons.

[5]This distance assumes a 7-hour march at a leisurely pace of 4 km/h. In Roman times, recruits were required to complete about 30 km in 6 hours in loaded marches. In the U.S. Army, the average march rate for foot soldiers is estimated to be between 20 to 30 km per day. See Headquarters, Department of the Army (2017, Figure 1–2).

3.2 Geographical, Climatic, and Resource Availability Characteristics

Our second step is to measure, in each cell, a vector of geography and climate characteristics, $\mathbf{x}$, and historical resource availability, y. Such characteristics will allow us to test Diamond's hypothesis that geographical features are central to the likelihood that we observe the regional clustering of cells into empires.

Geography and Climate. In terms of geographical and climatic characteristics, we consider, first, terrain ruggedness, x_{rugged}. We measure ruggedness by the average standard deviation of elevation, an index of topographic heterogeneity. Plains and plateaus score low on this measure, while mountain ranges and valleys score high (Nunn and Puga, 2012). Figure 3 depicts x_{rugged}. There, we can see the high ruggedness of the Alps, the Balkans, the Caucasus, and the Himalayas and the low ruggedness of the northern European plain, much of Russia, the Indian subcontinent, and North China.

Second, we identify cells in hot and cold climates using the WorldClim 1.4 historical data on annual average monthly maximum and minimum temperatures during the mid-Holocene epoch (4000 BCE), which was relatively warm in historical context.[6] Hot and cold climates hinder the movement of large armies because exposure to extreme temperatures induces physiological stress that can impair body functions and cause death (Department of the Army, 2016; Sanford et al., 2017) and change the behavior of insect vectors (Bellone, 2020).

We set $x_{hot} = \log(t_{max} - 21)$ for tropical cells with an annual average maximum temperature t_{max} of 22°C or above, and $x_{hot} = 0$ otherwise.[7] We set $x_{cold} = \log(9 - t_{min})$ if the annual average minimum temperature t_{min} of a cell is below 8°C, and $x_{cold} = 0$ otherwise.[8] In Figure 4, cells with a minimum temperature below 8°C are depicted in gray. Most of these cells are in the northern frontier of our area of study or mountainous regions (the Himalayas, the Alps, the Caucasus). Cells with a maximum temperature above 22°C appear in red. Most of those are in the Indian subcontinent and Southeast Asia.

[6] In the appendix, as a robustness check, we rerun our simulations using climatic data from the 1960s.

[7] According to the Wet Bulb Globe Temperature (WBGT) index, the most widely used measure of heat stress risk, a temperature of 22 °C is equivalent to a WBGT of 25°C (assuming a relative humidity of 85%, a humidity level often observed in the tropics). Beyond this level, it is advisable to adjust outdoor activities accordingly (Surgeon General, 2008; Department of the Army, 2016).

[8] A temperature of 8°C or below is defined as fridge temperature under European Union regulations (see, for e.g., European Pharmacopoeia 10th Edition).

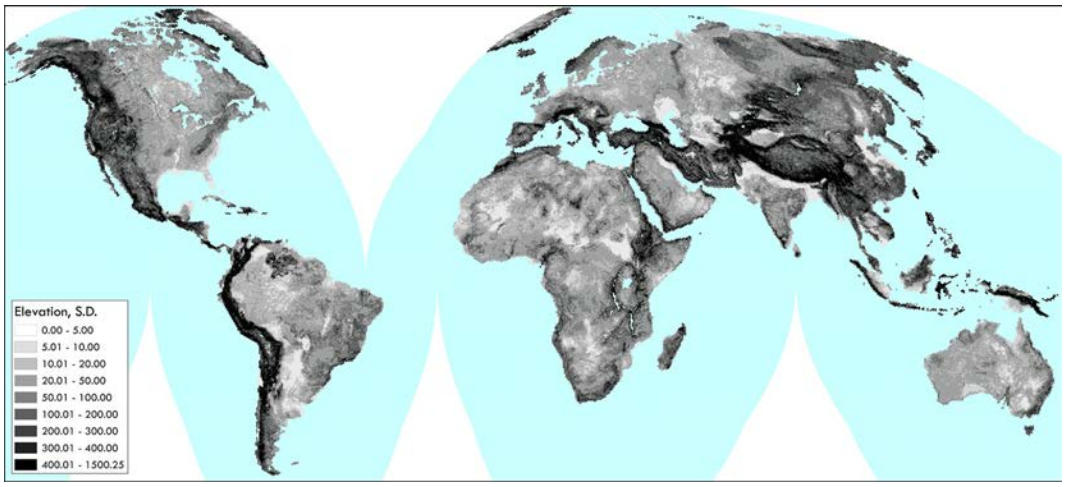

Figure 3: Terrain ruggedness (standard deviation of elevation).

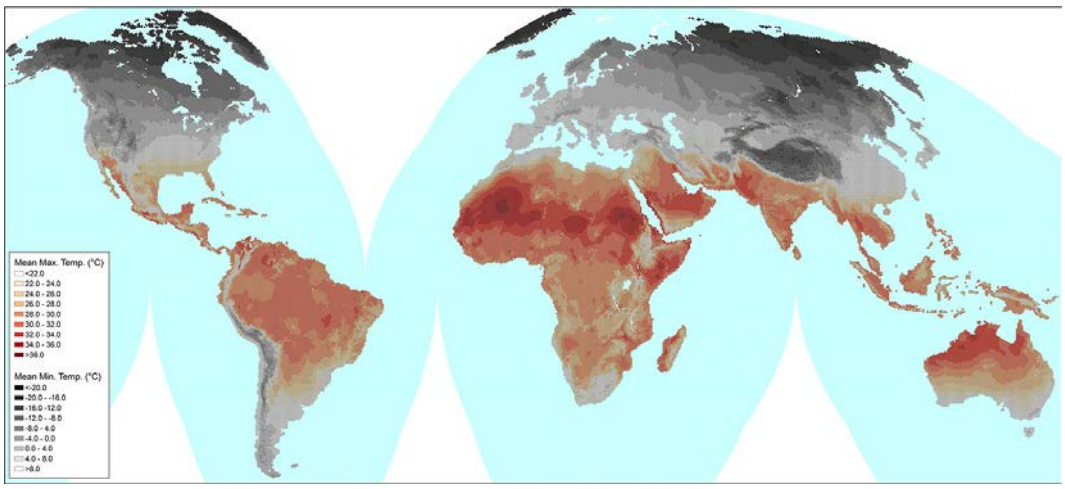

Figure 4: Annual average max. and min. Monthly temperatures.

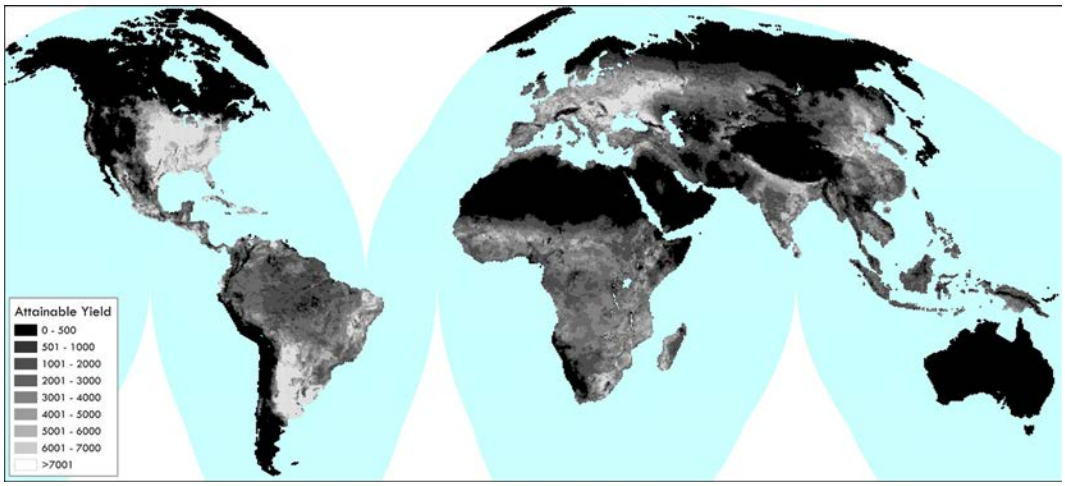

Figure 5: Attainable caloric yield based on pre-Columbian cereals (GAEZ v4).

We include these three continuous geographical variables in the vector $\mathbf{x} = \{x_{rugged}, x_{hot}, x_{cold}\}$. The vector $\mathbf{x}$ could be enriched with further geographical, climatic, cultural, and technological variables. We will return to this point later on.

Resource Availability. Our primary measure of historical resource availability is drawn from the Food and Agriculture Organization's Global Agro-Ecological Zones database, version 4 (henceforth GAEZ v4). The database divides the world's land surface into grid-cells of size 5' latitude/longitude (approximately 75 km^2). For each grid-cell, the dataset publishes the hypothetical annual yields (in tons per hectare) of different crops. We focus on cereal grains, which formed the basis of taxation in early states (Childe, 1936; Carneiro, 1970; Mayshar et al., 2017). Following Galor and Özak (2016), for each of our cells, we generate its highest attainable yield, y_{GAEZ}, in calories by (1) extracting the hypothetical yield of every cereal that existed in the continent where the cell is located before the Columbian Exchange, (2) converting the yields into calories, and (3) selecting the highest calorie-yielding cereal for the cell. Figure 5 shows the result of this exercise, with high densities in the Italian peninsula, India, and China and low densities in Russia, the Arabian peninsula, and inner Asia. In our model, productivity will determine the ability of the polity that controls it to mobilize resources for military purposes.

GAEZ v4 yields, however, might miss that agricultural states developed earlier along river corridors rich in alluvial soil, which is naturally irrigated by regular floods and not covered by thick forests. This soil is easy to work on with primitive tools and has the highest productivity among different soils (Fried, 1967; Driessen and Deckers, 2001).[9] The alluvium-rich regions of Mesopotamia (Tigris River), Egypt (Nile), the Indus Valley (Indus), and North China (Yellow River) were comparatively advanced in the exploitation of resources in 1000 BCE. To account for this phenomenon, we measure the percentage of alluvial soil in every cell based on the FAO Digital Soil Map of the World (DSMW) and denote it as r.

In our baseline model, we set $y_0 = r \cdot y_{GAEZ}$ at $t = 0$ and $y_{500} = y_{GAEZ}$ at $t = 500$, with the assumption that y grows at a constant rate between $t = 0$ and $t = 500$ for every cell. Later, as a robustness check, we will measure r using estimates from the KK10 Anthropogenic Land

[9] Scott (2017) argues that the concentration of grain and population on loess or alluvial soils enabled early state formation: "It was possible and not uncommon at the time to have sedentary farming populations on alluvial soils practicing irrigation without any state. But there was no such thing as a state that did not rest on an alluvial, grain farming population" (p. 117).

Cover Change database. Separately, we will check if ignoring initial developmental differences by setting $r = 1$ affects our results. We will also show that our findings are robust to the use of alternative measures of resource availability, including agricultural productivity (Ramankutty et al., 2002) and historical population estimates (Goldewijk et al., 2017).

3.3 Eurasia, China, and Europe

Our baseline exercises will report results from the 28,822 cells that include most of Europe, North Africa, the Middle East, Continental Asia, and Japan (cells with brown, red, and green borders in Figure 2). This area is often called Eurasia, the "Old World," or the Afro-Eurasian ecumene. We consider this space because, after the beginning of the Iron Age (c. 1200–1000 BCE), intense political, trade, and cultural contacts across Eurasia took off.[10]

As Hodgson (1954, p. 716) put it, our area of interest corresponds to:

> ...the various lands of urbanized, literate, civilization in the Eastern Hemisphere, in a continuous zone from the Atlantic to the Pacific, [that] have been in commercial and commonly in intellectual contact with each other, mediately or immediately.

What phenomena did Hodgson have in mind? For instance, the Roman Empire and Han China traded indirectly and knew of each other's existence. A Roman delegation visited China in 166 and the Chinese historian Yu Huan wrote a description of the Roman Empire—named *Daqin*—sometime between 239 and 265. Roman commerce with the Indian subcontinent was lively, with the tariffs on it accounting for as much as one-third of the empire's revenue (McLaughlin, 2010). Roman coins made their way to Japan and Buddhism was present in Rome.

Importantly, Eurasia has accumulated a large share of the world's population for most of history and has been the origin of many developments in technology and social and political forms (Kremer, 1993; Diamond, 1997). Understanding the dynamics of the political forms that evolved in this space is, hence, critical for global economic history.

Within the 28,822 Eurasian cells, 1,415 cells cover "China," defined as the lands south of the Great Wall (cells with red borders in Figure 2). This region corresponds to the historical core of Imperial China until the Qing expansion to the West (Perdue, 2005). Another 1,285 cells,

[10]The Iron Age starts at slightly different times over Eurasia, with the earliest transitions in the Middle East and the latest in northern Europe. For compactness of exposition, we ignore such heterogeneity.

highlighted with green borders in Figure 2, are in (western) "Europe," defined as the lands west of the Hajnal line running from Saint Petersburg to Trieste and delimiting the region of the so-called *European marriage pattern* (Hajnal, 1965). Many historians have used this marriage pattern as a proxy for close cultural and social similarities of the loosely called "western world."

Calling a cell "Eurasia," "China," or "Europe" has *no* implications for the model. It is just a label to build the statistics that summarize the outcomes from our simulations.

3.4 Evolution of Polities

We now take the hexagonal cells we have defined above, with their geographical, climatic, and resource availability characteristics, and consider how polities evolve in them over discrete periods $t = 0, 1, 2, \ldots$. At $t = 0$, each cell begins as an independent polity. Thus, the space is filled by a hexagonal tiling, with each cell bordering adjacent cells 1–6 (Figure 6). We consider a regular tiling to impose ex-ante homogeneity on the geographical shapes of polities. We prefer a hexagonal tiling to the other two regular tilings of the Euclidean plane because its vertex configuration is simpler than that of a triangular or square tiling. This simplicity better reflects the frontiers that most polities have had over time in our reading of the historical data.

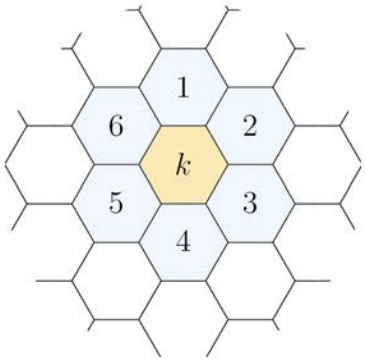

Figure 6: Cell k and adjacent cells.

Over time, some polities expand by conquering neighboring cells, while others lose control of cells. We describe now how the conquest and the secession of cells operate.

3.4.1 Conquest across land

In each period, a cell k finds itself in a border conflict with one of its adjacent cells with probability $\alpha \cdot y_k$, where $\alpha > 0$. For simplicity, we assume that, when a cell experiences a border

conflict, only one of its six borders is affected. Relaxing this assumption is straightforward, but it makes the model less transparent with little additional insight.

We make the probability of a border conflict depend on the productivity of the cell to capture the idea that more productive cells are more tempting for neighbors to exploit. This formulation is based on the Hobbesian thesis that states invade for gain, safety, and reputation; hence, productive lands are more likely to experience war. It also builds upon the circumscription theory and the Malthusian argument, which both see warfare as an outcome of population pressure. Studies of early states also suggest that the main objective of war was resources, including population (slaves) and properties. States more eagerly sought control of productive lands than poor terrains. Military expeditions were expensive, and soldiers would not fight well if they expected meager rewards even in victory (Scott, 2017).[11]

Most cells in our geographical space are inland. Conditional on inland cell k encountering a border conflict, the probability that its adversary is cell $\overline{k} \in \{1, 2, 3, 4, 5, 6\}$ is

$$\frac{y_{\overline{k}}}{y_1 + y_2 + y_3 + y_4 + y_5 + y_6},$$

where $y_1, ..., y_6$ are the respective productivities of the six adjacent cells (see Subsection 3.4.2 for the case where the cell has sea frontiers). This assumption follows the intuition explained above: two highly productive cells are more likely to be tempted into a conflict with each other than one low- and one high-productivity cell.

A conflict between cells has two interpretations. If a different polity controls each cell (as occurs, for sure, in $t = 0$), we consider this conflict a war. The victor of this war, to be determined in the next paragraph, annexes the losing cell. If the cells are controlled by the same polity (as may occur after previous annexations), we think about this conflict as a political struggle for resources within the polity. The unified government will resolve the conflict by reallocating resources or through other policies in a manner that is inconsequential to our model.

Victory in a war between two polities is given by a contest function that depends on (a) the aggregate productivity of the polities in conflict, and (b) the geographical characteristics $\mathbf{x}$ of the cells in conflict. Specifically, if a war takes place between polities i and j, which controlled

[11] See also Barfield (1989) and Cunliffe (2008) for discussions on how the search for booty led to the endless conflicts between poor and rich areas in the past and Liberman (1998), for evidence showing how military conquest of an industrial society pays high dividends.

cells k and $\overline{k}$, respectively, polity i wins with probability:

$$\pi_i = \frac{Y_{i,t}}{(Y_{i,t} + Y_{j,t}) \times (1 + max\{\Theta \cdot \mathbf{x}_k, \Theta \cdot \mathbf{x}_{\overline{k}}\}}, \tag{1}$$

where $Y_{i,t}$ ($Y_{j,t}$) denotes the sum of productivities of all cells controlled by polity i (j) at period t; $\mathbf{x}_k$ ($\mathbf{x}_{\overline{k}}$) denotes the geographical characteristics of cell k ($\overline{k}$); Θ is a parameter vector that controls the weights of each geographical and climatic characteristic, and $\Theta = \{\theta_{rugged}, \theta_{hot}, \theta_{cold}\}$.

The contest function (1) reflects two ideas. First, more productive polities win more often, but the vagaries of war might bring victory to the weaker side. This may be due to factors that we do not model, such as exceptional military leadership or strong state capability. Second, the relevant variable is the sum of productivities of the cells of a polity, not the average productivity. Estonia, in 1939, had higher income per capita than the Soviet Union (Norkus, 2019), but due to the difference in size, it could do next to nothing to resist annexation.

Second, the geographical and climatic variables make conquest harder or easier depending on the values of Θ, which mediate the probability of victory. The probability of the war ending with no victor and, thus, no annexation is:

$$1 - \pi_i - \pi_j = 1 - \frac{1}{1 + max\{\Theta \cdot \mathbf{x}_k, \Theta \cdot \mathbf{x}_{\overline{k}}\}},$$

which is strictly positive and is increasing in $max\{\Theta \cdot \mathbf{x}_k, \Theta \cdot \mathbf{x}_{\overline{k}}\}$. If $\theta_{rugged} >> 0$ (i.e., conquering very rough terrain is daunting, as scores of armies over millennia have discovered in Afghanistan), the probability of no annexation after a war that involves a cell with rough terrain is high.

Two secondary assumptions deserve further discussion. First, we assume that only the cell of the losing polity in the conflict is annexed, not the whole polity. While complete conquest sometimes occurs in history (think about the fall of the Sasanian Empire to the Arab invaders between 642 and 651), most conflicts end up by trading small pieces of land (recall the dynastic struggles that plagued Europe during the early modern period and the subsequent small exchanges of territories).

Second, since a polity may share borders with multiple polities, it may face simultaneous wars with several of them. We assume that a polity fighting more than one war will channel its resources proportionately according to the strengths of its adversaries. Otherwise, these wars

are independent of each other. A good example of simultaneous struggles, albeit a little later than the period for which our model is most appropriate, is the wars of Charles V, Holy Roman Emperor (r. 1519–1556), against his many enemies. The emperor always carefully weighted where to allocate his resources. His strategic choices were lamented by Francis I of France (r. 1515–1547) during his captivity in Madrid, but thoroughly enjoyed by the Elector John of Saxony (r. 1525–1532) while organizing the Schmalkaldic League.

We could generalize the previous two assumptions by allowing the annexation of larger parts (or the totality) of a polity and the correlation of wars across frontiers. In our example above, Francis I and Suleiman the Magnificent (r. 1520–1566) signed an improbable alliance in 1536 against Charles V. However, these generalizations require the introduction of many free parameters. Instead, we prefer to keep our model tightly parameterized and enhance its interpretability even if at the cost of some realism. We could also introduce strategic considerations (e.g., alliances and strategic conquests). Section 6 discusses these issues.

3.4.2 Conquest across the sea

Our model allows for conquest to take place across the sea. For our period of study (1000 BCE to 1500, see Section 4 for an explanation), invasions via the sea occasionally took place (e.g., the Roman conquest of Britain). Still, they were much less common than conquest over land for at least two reasons. First, ships were not stout enough for long-distance power projection across rough seas until the early 15th century, which saw the emergence of bigger, full-rigged ships with three masts (Clowes, 1932; Woodward, 2021). Second, until the development of better boats and more powerful guns, *and* the synthesis of the two into a new form of assault employed by the European powers against the non-Europeans during the Age of Sail, naval battles were essentially infantry battles fought on water or beach.[12] This setting disadvantaged the aggressor, whose capacity to conquer was constrained by the number of ships it could gather and survive the journey to the opposite shore (Padfield, 1979). While extensive maritime trade existed, there were no navies to dominate the oceans until the 16th century. Historically, no major naval battles were fought in the Indian, the Pacific, or the Atlantic Oceans before 1500. The exceptions were the straits and the Mediterranean Sea, almost entirely enclosed by land

[12]For example, the Battle of Sluys in 1344 was one of the largest naval battles of the Middle Ages. It took place at the port of Sluys and was contested by men-at-arms fighting from the platforms of static cogs.

and, thus, calmer and less dangerous to traverse than other seas. Yet, even an invasion across a narrow strait was militarily risky and logistically challenging (see Koyama et al., 2021).

We incorporate this "stopping power of water" for military conquest (Mearsheimer, 2001, p. 84) in two ways. First, consider a coastal cell k, which borders $l \in \{1, ...5\}$ cells by land and $6 - l$ by sea. Let L denote the set of cells that border cell k by land and let S denote the set of cells that lie no more than six cells ($\sim$330 km) from cell k by sea. We assume that, conditional on cell k encountering a border conflict, the probability that its adversary is cell $\overline{k}$ is:

$$\frac{y_{\overline{k}}}{\sum_{i \in L} y_i} \cdot \frac{l}{6}, \tag{2}$$

if $\overline{k} \in L$ and

$$\frac{y_{\overline{k}}}{\sum_{i \in S} y_i} \cdot \frac{6 - l}{6} \cdot \alpha_{sea}, \tag{3}$$

if $\overline{k} \in S$. In other words, we do not allow sea conquests in the model over more than $\sim$330 km.[13]

The parameter $\alpha_{sea} \in [0, 1]$ measures the likelihood of wars arising across the sea relative to land conflicts. For completeness, we will consider both the case $\alpha_{sea} < 1$, i.e., conflicts across the sea are less likely to take place than conflicts overland, and the case of $\alpha_{sea} = 1$, i.e., conflicts are as likely to take place across the sea as overland.

Second, if a polity controls two or more clusters of cells that are separated by sea, when war involving one of these clusters breaks out, the polity can mobilize the full resources of that cluster and a fraction $\sigma \in [0, 1]$ of the resources of the other clusters to fight the war. This accounts for the fact that moving large armies and supplies across a sea strait is capital intensive and depends on factors such as the possession of a large navy or the ability to mobilize a large merchant fleet and the availability of good harbors for loading and unloading. Circumstances such as unpredictable sea weather or changes in wind direction also affect the ability of troops and supplies to arrive in a timely manner (recall the "Protestant Wind" that favored William of Orange's invasion of England in 1688 while keeping James II's fleet in port). Again, for completeness, we will consider both the case $\sigma < 1$ and $\sigma = 1$.

[13]This upper limit is wider than the English Channel, the Irish Sea, the Sound, the Bosporus, the Strait of Sicily, the Red Sea, the Palk Strait, the Indonesian Straits, and the Korea and Taiwan Straits—the straits that witnessed sea conquests before 1500. It also allows for conquest through the Mediterranean Sea via island or coast hopping. As Abulafia (2011, loc. 412) puts it: "Conflicts for control of the Mediterranean thus have to be seen as struggles for mastery over its coasts, ports and islands rather than as battles over open spaces."

3.4.3 Secession

To reflect the historical tendency for border regions in large states to seek secession, we allow border cells to secede from the polity they belong to with strictly positive probability in each period. A border cell is defined as one that shares an edge with one or more cells ruled by another polity.

The border cell k's probability of secession is high if (a) the cell has a high $\Theta \cdot \mathbf{x}_k$ (i.e., geographical and climatic characteristics that make secession hard to suppress), (b) if the parent polity i controls a large number of cells (and is therefore heterogeneous), or (c) if polity i has a long frontier relative to its interior (which increases the difficulty of monitoring and controlling the population). Specifically, the probability of border cell k seceding from polity i is:

$$\beta \times \Theta \cdot \mathbf{x}_k \times \sum_{m}^{65,641} \mathbb{1}_i(m) \times \frac{\sum_{m}^{65,641} (\mathbb{1}_i(m) \cap \mathbb{1}_B(m))}{\sum_{m}^{65,641} \mathbb{1}_i(m)} = \beta \times \Theta \cdot \mathbf{x}_k \times \sum_{m}^{65,641} (\mathbb{1}_i(m) \cap \mathbb{1}_B(m)), \quad (4)$$

where $\beta > 0$ is a constant determining the likelihood of secession, $\mathbb{1}_i(m) = 1$ if cell m is ruled by polity i and $\mathbb{1}_i(m) = 0$ otherwise, and $\mathbb{1}_B(m) = 1$ if cell m is a border cell and $\mathbb{1}_B(m) = 0$ otherwise.

To simplify, we assume that if a polity is cut into disjoint parts due to war or secession, each part becomes a separate polity. The exception is when the disjoint parts are separated by sea by a distance no further than six cells (Subsection 3.4.2), in which case the polity survives. Geographically divided polities such as Pakistan between 1947 and 1971 seldom live long.

As before, for simplicity, we consider that each cell separates independently from other cells. However, since a polity might have several cells sharing edges with other polities, it may suffer the separation of several cells in the same period.

3.4.4 Summary

As conflicts between polities and unrest within polities occur, states consolidate over time as long as the probability of secession is not too high. Larger states have access to more resources, and, hence, are likely to consolidate further. However, some cells are more difficult to conquer than other cells due to their geographical and climatic characteristics. These features will lead to regular patterns of state formation.

To summarize, the timing of events is as follows:

1. At $t = 0$, each cell is a separate polity.
2. At each time period, the probability of conflict breaking out in cell k is $\alpha \cdot y_k$, where $\alpha > 0$ and y_k is the productivity of cell k.
3. If cell k encounters a border conflict, only one of its six borders is affected. The conditional probability that its adversary is cell $\overline{k}$ is given by equation (2) if $\overline{k}$ borders k by land, and by equation (3) if $\overline{k}$ is connected to k by sea.
4. If there is a conflict between cells controlled by different polities, a war takes place.
5. In a war between cells k and $\overline{k}$, controlled, respectively, by polity i and j, polity i wins and annexes cell $\overline{k}$ with the probability given by the contest function (1).
6. A polity may fight no war, one war, or multiple wars at any period. If it fights multiple wars, it splits its resources proportionally according to the resources of its adversaries.
7. Cell k secedes from polity i with the probability given by equation (4).

4 Calibration

To calibrate our model, we need to pick an initial and endpoint of the simulation, a time unit, and the values of seven parameters: α, α_{sea}, σ, θ_{rugged}, θ_{hot}, θ_{cold}, and β.

For the initial and endpoint of the simulation, our baseline exercises want to gauge whether our model can account for the evolution of the Eurasia polity structure between the beginning of the Iron Age (c. 1200–1000 BCE) and the dawn of the Age of Exploration in the second half of the 15th century. Thus, we pick 1000 BCE to 1500. These points give us a total of 2,500 years.[14]

At the start of the Iron Age, the "Old World" was nearly entirely fragmented. Even areas where larger polities existed previously, such as the Fertile Crescent, were recovering from the Late Bronze Age collapse: Egypt was transitioning through its third intermediate period, the palace economies of the Aegean had crumbled, and the Kassite dynasty of Babylonia and

[14]Later, we will discuss the implications of our model for Africa and the Americas during this period.

the Hittite Empire had disappeared.[15] The Shang in China had somewhat progressed toward unification, but the documentary record of how effective their territorial control was is scant (Campbell, 2018, ch. 4).

The Age of Exploration quickly integrated the whole world. Juan Sebastián Elcano completed the first circumnavigation of the globe in 1522, only 103 years after the Portuguese started the systematic exploration of the West African coast. And by 1565, the Manila galleons had opened a regular trade route between Europe, Asia, and the Americas (Giráldez, 2015).

Our choice of time unit must balance the need to have a detailed account of the evolution of political forms and the computational burden. Hence, we pick five years to get 500 simulation periods (2,500 years divided by 5). This time unit is also a reasonable approximation to the median length of many conflicts, which, in the data, have a huge variation.[16]

Fortunately, the values of all parameters in the model, except β, are time-independent. They represent the geographical relative attractiveness or difficulties of conquest, which are static properties.[17] Thus, our pick of an initial and end period and a five-year time unit only matters when mapping the lengths of outcomes in the model with the lengths of outcomes in the data.

We can move now to calibrate our seven parameters. Since $\alpha \cdot y_k$ determines the probability of conflict occurring in cell k, we set $\alpha = \frac{1}{y_{max}}$, where y_{max} is the productivity of the cell with the most resources in our dataset. In such a way, $\alpha \cdot y = 1$ for the cell with the highest value of y and $0 \leq \alpha \cdot y \leq 1$ for all other cells. We pick $\sigma = 0.33$, based on Dupuy (1979), a well-regarded source among military scholars and historians. Dupuy (1979) uses military history statistics to weight variables that predict war outcomes (these weights are used, for example, to calibrate war games at general staff colleges). We set $\alpha_{sea} = 0.1$ to account for the observation that about 10% of the historical battles listed on Wikipedia were sea battles.[18]

Drawing again from Dupuy (1979), we pick θ_{rugged} so that $\theta_{rugged} \cdot x_{rugged} = 2$ for the cell at the 90th percentile of the ruggedness ranking.[19] At this value, a war between two adversaries

[15] See the classic account of the Late Bronze Age collapse in Drews (1993), and, more recently, Cline (2014).

[16] Computing this variance becomes even more challenging once one realizes it is hard to agree on what constitutes a war. Think about the long conflict between the Spanish Empire and the Provinces of the Netherlands (1568–1648): Was it one long war or several consecutive ones?

[17] We do not model changes in military technology. Although some of those changes could be biased toward one geographical feature, there is not much evidence of this bias in the data (Dupuy, 1979).

[18] While Wikipedia data might have biases in its coverage, we checked that other sources, such as Phillips and Axelrod (2005), do not have more comprehensive datasets. In any case, our robustness exercises will document that the results of the model do *not* depend materially on the value of α_{sea}.

[19] According to Dupuy (1979), a formula that fits the historical data well is c (combat power) $= s$ (military

of equal strength fighting in this cell will end in a stalemate with a probability of $\frac{2}{3}$. Likewise, we pick θ_{hot} and θ_{cold} so that $\theta_{hot} \cdot x_{hot} = \theta_{cold} \cdot x_{cold} = 2$ for the respective cells at the 90th percentile of the annual average monthly maximum and minimum temperature rankings.

Finally, we set $\beta = 1 \times 10^{-5}$. Given Europe's long coastline compared with China's, European states tend to be non-compact in our simulation. Our low β prevents secession from being the main cause of Europe's fragmentation. At the calibrated β, a polity that comprises Europe's cells would have to annex territories at a rate of 90 cells (approximately the size of two Austrias) every 50 periods (250 years) to compensate for the loss of cells through secession. In comparison, a polity that controls China's cells would only need to annex approximately 22 cells (approximately half the size of Austria) every 50 periods to maintain its territorial size.

Parameter	Value
α	$\frac{1}{y_{max}}$
α_{sea}	0.1
σ	0.33
θ_{rugged}	$\frac{2}{x_{rugged}=90th \text{ percentile}}$
θ_{hot}	$\frac{2}{x_{hot}=90th \text{ percentile}}$
θ_{cold}	$\frac{2}{x_{cold}=90th \text{ percentile}}$
β	1×10^{-5}

Table 1: Baseline calibration of the model.

Table 1 summarizes the calibration. We will call this calibration our "baseline calibration." We will also have a "preferred specification," with the same parameter values, but we make our model more realistic by adding the roles of rivers, steppes, loess soil, and climate in state formation. Section 5 will show that both specifications deliver nearly the same quantitative results regarding the speed of state consolidation. But since the preferred specification requires additional discussion, we delay the presentation of its details until Subsection 5.4 and focus, first, on the more parsimonious and easier-to-analyze baseline calibration.

strength and other factors) $\times$ r (role, either attack or defense) $\times$ w (weather/terrain obstacles), where $r = 1$ for attack, $r = 1.3$ for defense, $w = 1$ for attack, and $w = 1.5$ for defense when obstacles are present. All else equal, this formula implies that the combat power of defense is approximately twice ($1.3 \times 1.5 \approx 2$) that of attack under unfavorable weather/terrain obstacles. This power of defense translates into a $\frac{2}{3}$ probability that the war ends with no conquest. An alternative approach is to incorporate topographical features in the Lanchester equations, a popular set of ODEs used to compare military forces (see Przemieniecki, 2000, ch. 4). Following this strategy, Engel (1954)—using combat data from the battle of Iwo Jima—and Weiss (1966)—using combat data from the U.S. Civil War—also estimate that weather/terrain obstacles roughly double the effectiveness of the defense.

In Subsection 5.3 and Appendix C, we conduct many sensitivity tests to document that our results are robust not only to changes in the values of the parameters in Table 1, but also to the use of alternative datasets and modifications to the conflict mechanism.

5 Quantitative Results

We are ready to simulate our model on the computer: we divide the world into hexagonal cells, feed in each cell's geographical and climate characteristics and historical resource availability, and draw random paths of conflicts and secession. Since the evolution of the model is stochastic, replicating the idea that history is a mix of structure and contingency, we simulate the model 30 times.[20] Based on this sample, we conduct bootstrap analysis to compute the mean Herfindahl indices of the areas we called "China" and "Europe" and their confidence intervals by drawing a sample of 30 simulations with replacement for 10,000 times. Our simulations cover the whole world. But for now, and only for *reporting* purposes, we will focus on the results for the Old World. We will discuss the results on Africa and the Americas in Section 7.

Despite its extreme simplicity (and the omission of many plausible mechanisms of state formation), our model generates patterns of political consolidation that resemble those observed in history. Panel A of Figure 7 depicts Eurasia in a representative simulation from our preferred specification in period 50 (i.e., 750 BCE). While nearly every cell is still an independent polity, we start seeing a consolidation of power in northern China resembling the core areas of the Shang and the Zhou dynasties. In comparison, no large polities appear in Europe.

Panel B of Figure 7 depicts the same simulation after 300 periods (i.e., 500 CE). In the east, a large polity has unified northern China, but has yet to fully control the southern half. In the west, we see polities that roughly resemble Spain or France (including a polity very similar to the Kingdom of the Suebi in the northwest of the Iberian peninsula, which existed between 409–585). The year 500 is around the time when the Germanic kingdoms that inherited the western Roman Empire were formed. The Indian subcontinent is divided into many polities (although with an emerging power in the north), while the Arabian peninsula, given the low productivity of its land, is fragmented (we will revisit this point in Section 8 and Appendix D.5).

[20] A short movie with a representative simulation can be seen here: https://www.dropbox.com/s/ftgcjqpetm22911/FracturedLandMovie220101.mp4?dl=0.

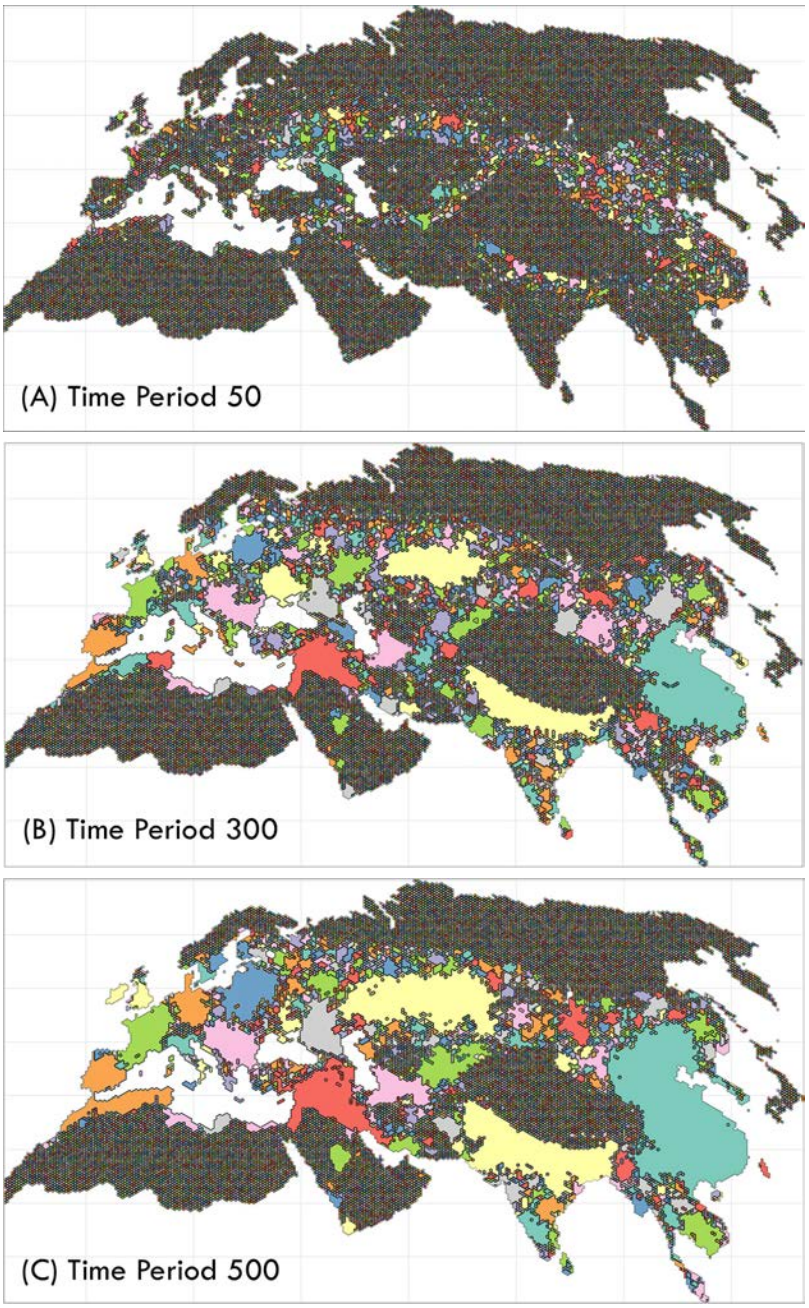

Figure 7: One representative simulation run.

Panel C of Figure 7 depicts the same simulation at the end of the simulation after 500 periods (i.e., 1500). The large polity occupying China and dominating East Asia has expanded to the south toward Vietnam and Yunnan. The polity controlling India has expanded toward the south, occupying an area similar to the Delhi Sultanate (1206–1526) at its peak. In Europe, we see a nearly unified Iberian peninsula (as happened between 1580 and 1640), polities resembling England, Scotland, and Ireland, a larger France, and the Ottoman Empire.

At the end of the simulation, European Russia and (in particular) Siberia are highly fragmented. Both observations match the historical record during the period we consider. The Grand Duchy of Moscow only started to grow quickly after 1300, and the conquest of Siberia did not commence until the 16th century and the arrival of gunpowder. However, our simulation misses anything resembling the Mongol Empire and its successor states, such as the Golden Horde, even if these unification processes were transient. Appendix D.2 discusses what we need to change in the model to generate states resembling the Mongol Empire.

5.1 Chinese Unification, European Polycentrism

Figure 7 is not an anomaly. The central result of our model is that larger polities emerge early in China and that this part of the world tends to become unified under a single state. In contrast, polycentrism is persistent over time in Europe. Figures 8 and 9 depict the evolution of the Herfindahl indices of political unification for China and Europe over 500 periods for the 10,000 bootstrap samples based on the 30 simulations under the baseline calibration.[21] We start with the baseline calibration to have the simplest scenario. The colored intervals denote the 95% confidence intervals of the estimated indices in each period.

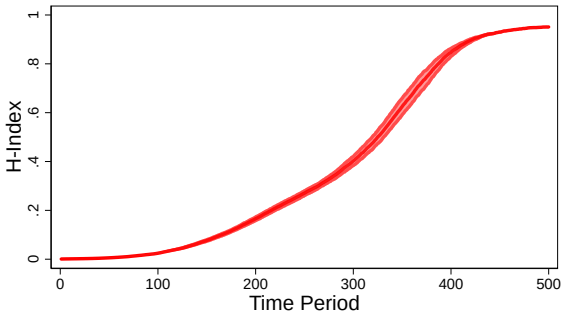

Figure 8: China. Fan chart for 30 simulations of the baseline specification.

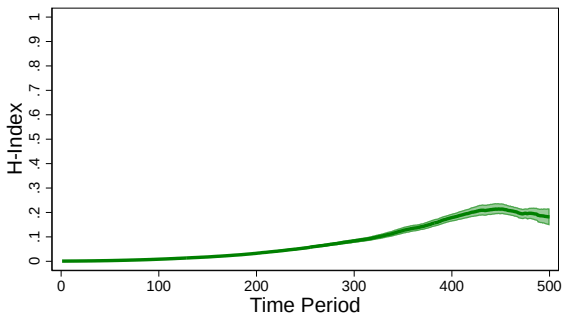

Figure 9: Europe. Fan chart for 30 simulations of the baseline specification.

Across all simulations, China centralizes quickly. The Herfindahl index for China crosses 0.5 after around 300 periods and converges to 1 toward the end of the 500 periods. In history, China was first unified in 221 BCE when the armies of Qin Shi Huang conquered the state of Qi, the last independent kingdom in northern China. Still, much of southern China continued

[21] We define the Herfindahl index of political unification of a region as $H_{pc} = \sum_{i=1}^{N} s_i^2$, where N is the number of polities existing in the region, and s_i is the percentage of the cells in the region controlled by polity i.

to be occupied by minorities such as the Yue and Man (Twitchett and Fairbank, 1986; Dien and Knapp, 2019). When the Han dynasty replaced the Qin, the present-day provinces of Fujian, Guangdong, Guangxi, Guizhou, and Yunnan were outside Chinese control (notice the similarities between Figure 33 in Appendix E and Panel B in Figure 7). Over time, the Chinese set up an increasing number of new counties in the south and replaced nominal suzerainty with actual bureaucratic control. Yunnan, the last of the provinces above to be brought under Chinese control, was officially incorporated into China only in 1276, close to the end of our study period. Hence, our model captures the consolidation of political power in China and its speed. In comparison, Europe always remains fragmented. The Herfindahl index for Europe stays as low as 0.2 as late as 500 periods into the simulations.

5.2 Inspecting the Mechanism

We inspect the mechanism behind Figures 8 and 9 by varying the parameter values of the obstacles and the productivities of the cells. First, we eliminate the role of climate in making conquest difficult by setting $\theta_{hot} = \theta_{cold} = 0$. This exercise, which we call "minimum set of obstacles," is motivated by Diamond (1997), who focuses on mountain ranges and seas, and irregular coastlines as barriers to conquest.[22] Panel A of Figure 10 shows that China unifies more rapidly than Europe. The main difference with respect to Figures 8 and 9 is that Europe unifies more by the end of the simulation.

We push the previous argument to its limit by eliminating the sea and geoclimatic obstacles to conquest: $\alpha_{sea} = 1$, $\sigma = 1$, and $\Theta = \mathbf{0}$. We call this exercise "no obstacles." In this case, cells will no longer secede as the probability of secession given by equation (4) is now always zero. Furthermore, indented coastlines no longer slow political consolidation as a war between two coastal cells across the sea is now as likely to occur and end up in annexation as a war between two neighboring cells on a flat plain. Panel B of Figure 10 shows that, absent geographical and climatic barriers to conquest, Europe still unifies later than China, but will end up in a similar situation a few centuries later as an empire from Eastern Europe emerges to conquer the West. European unification remains sluggish because China's core productive areas are more compact, facilitating early consolidation.

[22]Table 4 in Appendix B summarizes all the specifications reported by Figures 8–12. The two regions are comparable in resource availability across our different specifications.

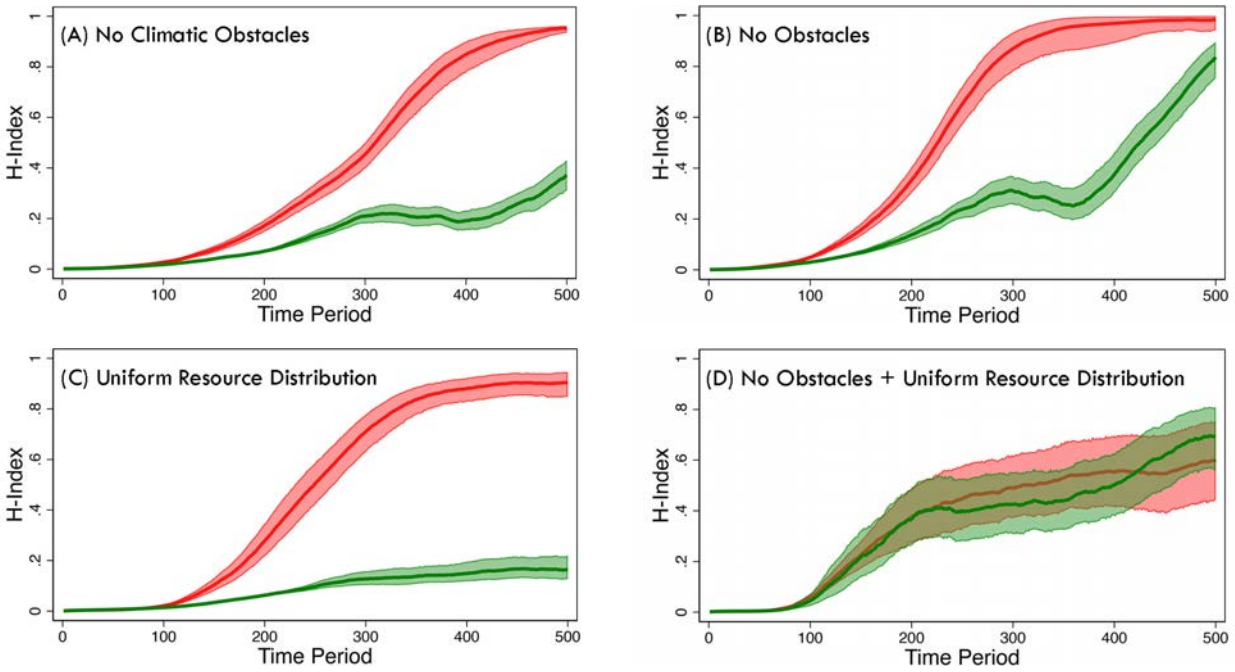

Figure 10: Varying parameter and productivity values. For each specification, we conduct the simulation exercise 30 times and display the average Herfindahl (unification) indices for China (red) and Europe (green). The shaded intervals depict the 0.95 bootstrap confidence interval.

Next, we assume that attainable caloric yield is uniform across our study area, with $y = 0.5$ for all cells. Thus, every cell is equally likely to engage in conflict. We call the third alternative exercise "uniform resource distribution." Panel C of Figure 10 is nearly the same as Figures 8 and 9, our baseline calibration.

Panel D of Figure 10 combines "no obstacles" and "uniform resource distribution." In this counterfactual, our geographical space is neither "fractured" by geographical and climatic obstacles, nor separated into land clusters of varying productivity levels. Panel D of Figure 10 shows that once we neutralize both aspects of fractured land, China no longer unifies earlier. Panel D is a key result in our paper. It indicates that non-linearities play a central role in accounting for patterns of state formation: only when we remove both geographical obstacles *and* differences in resources do China and Europe unify at a comparable pace.

5.3 Robustness

How robust to the details of our exercise is our central finding of fast Chinese unification and persistent European polycentrism? In the next pages, we conduct two sets of robustness tests,

but Appendix C reports the results of many additional tests.

Alternative Datasets. We choose the GAEZ v4 attainable caloric yields as our primary measure of productivity and the percentage of alluvial soil to account for early state formation because they are transparent and objective. However, they are not perfect (Appendix A discusses the strengths and weaknesses of the datasets used in the baseline simulations). For instance, the GAEZ v4 yields likely overestimated the productivity of Europe vis-à-vis China.[23] Also, focusing on alluvium overlooks a vital source of China's early agricultural advantage: the deep loess deposits along the upper reaches of the Yellow River, traditionally known as the cradle of Chinese civilization (Ho, 1975; Scott, 2017). These issues suggest that, under a better measurement, China's unification might be faster than in our baseline model.

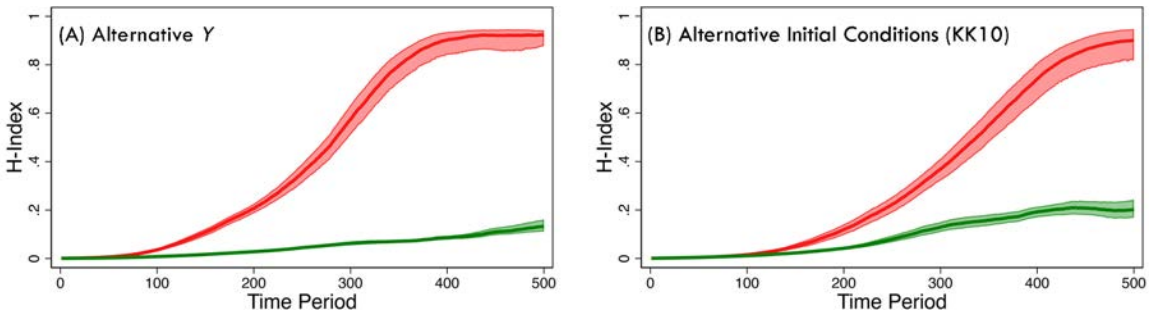

Figure 11: Alternative datasets. For each specification, we conduct the simulation exercise 30 times and display the average Herfindahl (unification) indices for China (red) and Europe (green). The shaded intervals depict the 0.95 bootstrap confidence interval.

Hence, we undertake two robustness checks. First, we replace the highest attainable yield based on the GAEZ v4 database with the Cropland Suitability Index computed by Ramankutty et al. (2002) as our y variable. The result is reported in Panel A of Figure 11. Under this alternative measurement, China completes its unification a bit earlier, while the consolidation of polities in Europe is even slower than in the baseline results in Figures 8 and 9.

Second, we use the KK10 Anthropogenic Land Cover Change dataset (henceforth KK10) in 1000 BCE (our $t = 0$) constructed by Kaplan and Krumhardt (2011) in place of the percentage of alluvial soil to capture the early lead that some areas enjoyed. The KK10 dataset estimates the fraction of land under human use in 1000 BCE (see Appendix A.2 for some potential problems

[23] If we take population density in 1950—when reasonably reliable population data became available worldwide—as a proxy for historical resource availability, Europe's GAEZ v4 figures are on average about 40% overestimated relative to China's. The actual overestimation may be higher as population growth in western Europe outstripped China between 1500 and 1950, in no small part due to the Industrial Revolution.

with the KK10 dataset). Panel B of Figure 11 shows that China unifies even faster than in the baseline specification.

Appendix C.2 presents more checks using alternative datasets, including the History Database of the Global Environment (HYDE) version 3.1, the FAO Harmonized World Soil Database version 1.2, and temperature data of the 1960s drawn from WorldClim 1.4. In each case, we see China unifying at a much faster pace than Europe.

Alternative Conflict Mechanisms. Our second set of robustness tests modifies how wars occur in our model. In the baseline model, a cell enters into a war with one of its neighbors with a probability that depends on the relative productivities of the neighboring cells: the more productive a neighbor, the higher the probability that conflicts arise along its border.

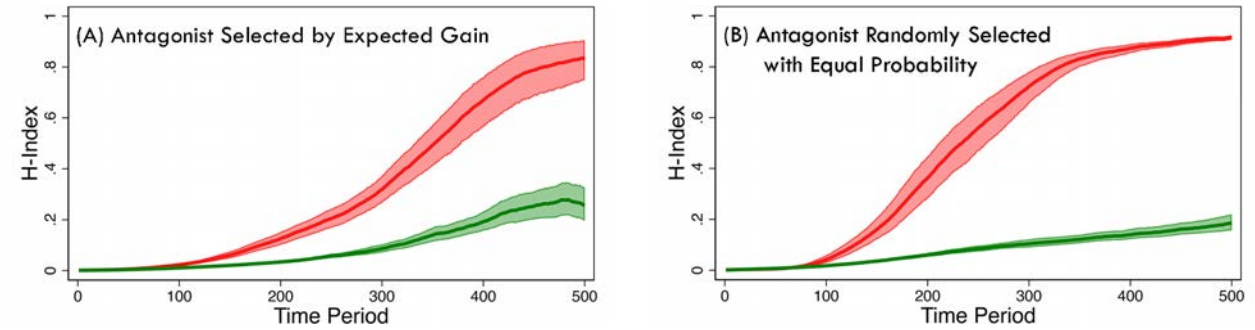

Figure 12: Alternative Conflict Mechanisms. For each specification, we conduct the simulation exercise 30 times and display the average Herfindahl (unification) indices for China (red) and Europe (green). The shaded intervals depict the 0.95 bootstrap confidence interval.

Figure 12 changes this probability. In Panel A, the adversary of the cell is the neighboring cell that offers the highest expected gain of conquest to the regime that controls cell k. In panel B, all the neighboring cells are potential adversaries with equal probability. In both instances, we continue to observe faster unification in China. Appendix C.3 implements two more alternative conflict mechanisms that consider the cost of transporting resources from where they originate to the location of fighting. The results are qualitatively the same.

5.4 Enriching the Model

Next, we add more realism to our model by considering the roles of rivers, the steppe, nomadic pastoralism, loess soils, the disease environment in the tropics, and the risk of hypothermia in

cold regions. We first consider these enrichments separately before taking them jointly into account. This last case will constitute our preferred specification mentioned in Section 4.

Scholars have linked riverine connectivity and state building. Diamond (1997, p. 331) noticed that "China's long east-west rivers (the Yellow River in the north, the Yangtze River in the south) facilitated diffusion of crops and technology between the coast and inland." The role of rivers in England's early development is widely discussed by medievalists and geographers (see Langdon, 1993; Jones, 2000). Armies used major rivers as a source of supply. For example, the Roman invasions of Persia often followed the Euphrates. Even as recently as the U.S. Civil War, most operations in the West followed rivers (the Mississippi, the Cumberland, etc.). At the same time, rivers separate basins and can impede movement between left and right banks. Historically, numerous battles took place by the crossing of an important river.[24]

Panel A of Figure 13 captures the role of rivers by increasing the probability of conquest when cells along the same river come into conflict and decreasing the probability of conquest when a riverine cell fights a non-riverine cell. The extension yields results similar to our baseline calibration, with only slightly slower political unification in China (see Appendix D for details about this and the following exercises in this subsection).

Panel B considers the early agricultural advantage enjoyed by areas with rich loess deposits and easy access to water (Scott, 2017). One such area is the loess plateau in the middle reaches of the Yellow River. This plateau was an important source—if not the crucial source—of Chinese civilization (Ho, 1975). Twenty thousand years ago, the region was covered mainly by grass (Jiang et al., 2013). This, coupled with the nature of loess soil—soft and stoneless—and easy access to water, made agriculture extremely rewarding even with primitive tools. Thus, we give cells with deep loess deposits a higher r, equivalent to alluvial areas having a head start in our baseline specification. While China unifies faster, the main findings remain unchanged.

The next two exercises focus on the Eurasian steppe as depicted in Ramankutty and Foley (2014). In the first exercise (Panel C, Figure 13), we consider the role of the steppe as a "highway of grass," i.e., a network of overland routes that facilitated the movement of caravans, pack animals, and people between Europe and Asia (Frachetti, 2008). We also engage with the

[24]Some notable examples include the Battle of Granicus (334 BCE), the Battle of Rhone Crossing (218 BCE), the Battle of the Medway (43), the Battle of Red Cliffs (208), the Battle of the Milvian Bridge (312), the Battle of Fei River (383), the Battle of Stamford Bridge (1066), and the Battle of Stirling Bridge (1297).

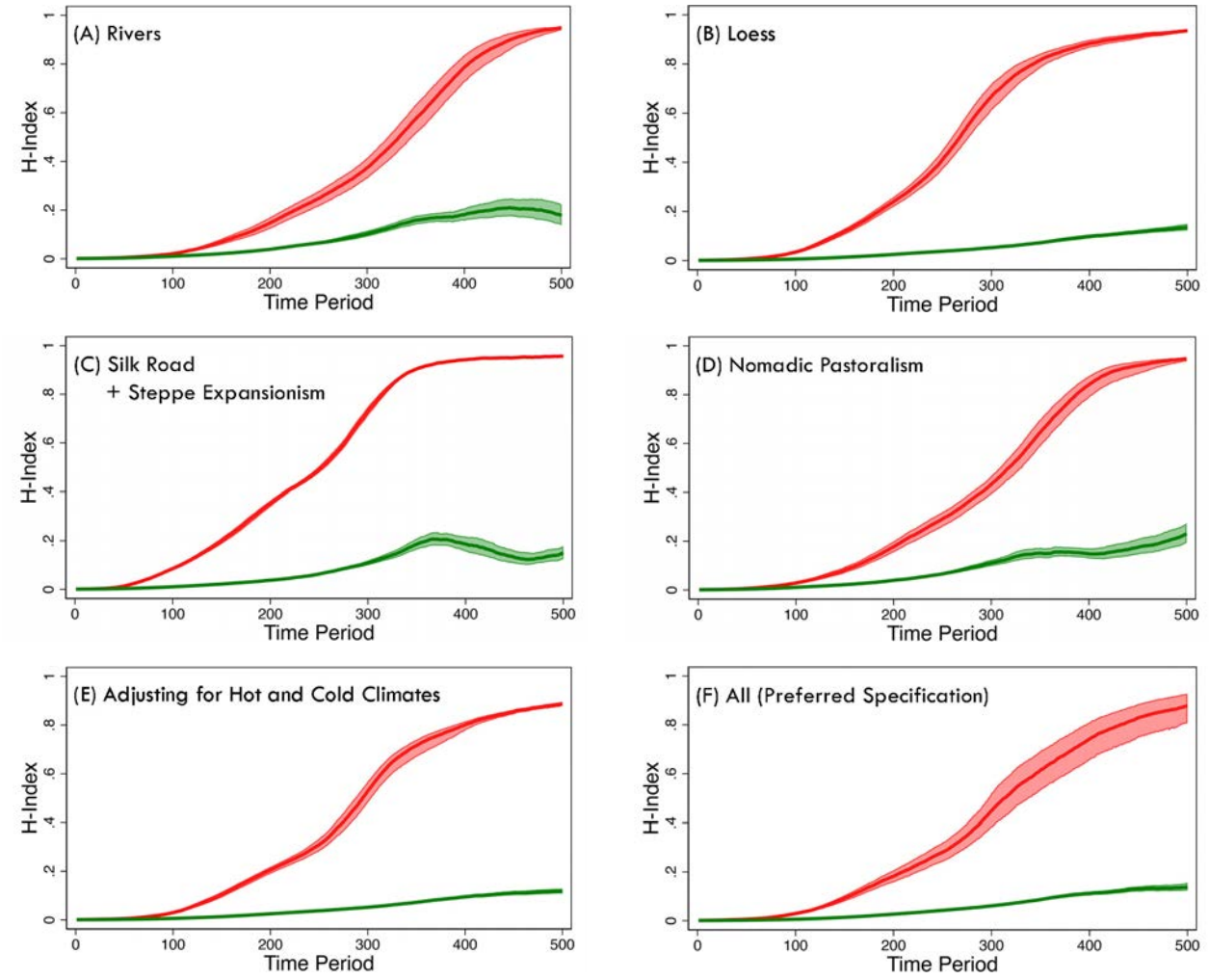

Figure 13: Enriching the model. For each specification, we conduct the simulation exercise 30 times and display the average Herfindahl (unification) indices for China (red) and Europe (green). The shaded intervals depict the 0.95 bootstrap confidence interval.

argument of Turchin et al. (2013), who note that the Eurasian steppe influenced state building both directly, because steppe nomads eliminated weaker and less cohesive polities, and indirectly, by developing and spreading technologies that intensified warfare. Barfield (1989) observed that the fragile ecology of the steppe helped shape a culture and practice of military expansionism.[25] The steppe east of the Altai Mountains, where temperature swings are greater than in any other part of the world, was especially prone to outward expansionism (Gibbon, 2003; Neparáczki

[25]According to Lattimore (1940), the struggle between the pastoral herders in the steppe and the settled populations in China was, first and foremost, an ecological one. The geography of Eurasia created a natural divide between the river basins of China and the Eurasian steppe. In the Chinese river basins, fertile alluvial soil, sufficient rainfall, and moderate temperatures encouraged the early development of intensive agriculture. In the steppe, pastoralism emerged as an adaptation to the arid environment. During periods of cold temperatures, when droughts led to catastrophic deaths among animal herds, the steppe nomads were often impelled to invade their settled neighbors for food (Bai and Kung, 2011).

et al., 2019; McNeill, 2021). Our second steppe exercise in Panel D adjusts the productivity of cells belonging to the Eurasian steppe to acknowledge the fact that nomadic pastoralism, rather than cereal cultivation, was the primary mode of livelihood in the steppe. In both exercises, we observe a slightly faster pace of unification in China, but otherwise no qualitative impact on our main findings. These modifications do not affect the productivity and barriers to the conquest of the core areas of state formation.

Panel E of Figure 13 allows for the influence of climate on pathogens and production. We discount the historical productivity values of cells in hot (>22°C for average monthly maximum temperature) and cold (<8°C for average monthly minimum temperature) regions, so that cells at the 75th (25th) percentile of the average monthly maximum (minimum) temperature scale have approximately the same 1950-population-density-to-productivity ratio as cells in the median. We do so because GAEZ v4 does not consider historical circumstances. In tropical regions, diseases limited the use of farm animals and lowered human health and capital. In cold regions, land had to be set aside for firewood in the winter and for pastoral activities, e.g., for meat (heme iron), fur, or wool to keep warm (Rosenzweig and Volpe, 1999). Hence, GAEZ v4 tends to overestimate historical resource availability in hot and cold regions.[26] Based on GAEZ v4, cold cells at the 25th percentile of the annual average monthly minimum temperature scale (-4°C) are about 30% more productive than cells around the median (10°C) of the scale, yet the population density of the former in 1950 is only a quarter of the latter. Likewise, based on GAEZ v4, hot cells at the 75th percentile (29.5°C) of the annual average monthly maximum temperature scale are as productive as those around the median (20°C), yet the population density of the former in 1950 is only a quarter of the latter. In this exercise, Europe's pace of political consolidation is somewhat slower, but the main results are unchanged.

Finally, in Panel F we consolidate the modifications in Panels A–E to construct our preferred specification. Comparing this panel with Figures 8 and 9 shows that our central result is roughly the same as with the baseline calibration and the preferred specification. The former is more transparent, the latter richer in details and, thus, our favorite choice.

[26]Consider Manchuria, the most productive region in modern-day China according to GAEZ v4. Traditionally, Manchuria was regarded as a place with low agricultural potential because of its cold climate. During the Three Kingdoms period, Sun Quan, emperor of the Wu kingdom, considered invading Manchuria but gave up after being persuaded by his advisors that the region was too cold to be agriculturally productive.

5.5 Taking Stock

This section has demonstrated that it is insufficient to compare average levels of ruggedness between China and Europe. Instead, what matters is the *distribution* of mountains and other geographical obstacles. While China is, indeed, more rugged than Europe, the location of geographical barriers promoted faster political unification in China. Furthermore, while topography alone is a sufficient condition to explain China's recurring unification and Europe's persistent polycentrism, it is not necessary. Take away topography, and we continue to observe more rapid unification in China. Only removing *both* geographical barriers and land productivity ensures that China and Europe unify at a comparable pace.

6 Historical Discussion Informed by the Model

We can now use our model to inform a discussion of China and Europe, the role of the balance of powers, and the feedback between economic prosperity and political polycentrism.

China. At first glance, it is not obvious why geography should contribute to China's recurring political unification. China's terrain is significantly more rugged than Europe's (Hoffman, 2015). Also, the climatic distinction between China's temperate north and subtropical south is stark. Different climatic conditions divided China into two agricultural zones: historically, millet, sorghum, and wheat were the staple crops in northern China, while rice was dominant in the south. Different crops, in turn, encouraged the development of different social organizations and cultural norms (Talhelm et al., 2014).

China's political unification intrigued the Chinese themselves. During the late Warring States period, Lü Buwei, the chancellor of the Qin kingdom, asked why the number of states in China had decreased from tens of thousands c. 2200 BCE to three thousand c. 1600 BCE to only a handful in his time (Sellmann, 2002). Not long after Lü's death, all but one of the remaining surviving states would perish as Qin built China's first unified empire in 221 BCE. While the Qin dynasty lasted only 15 years, it marked a watershed. From 221 BCE to the founding of the Chinese Republic in 1911, China was unified for 1142 years out of 2132 years (Ko and Sng, 2013). The record is unparalleled in world history.

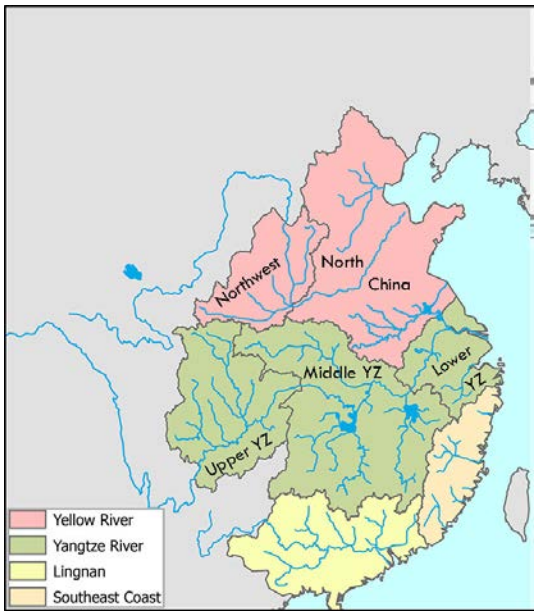

Figure 14: China's macroregions as defined by Skinner (1977).

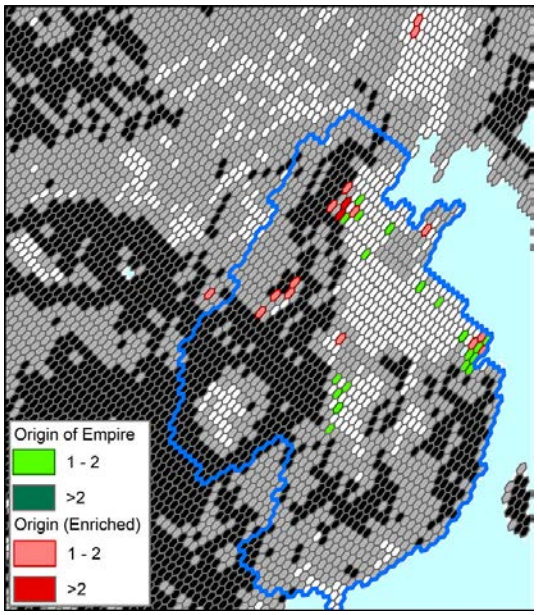

Figure 15: Flatness & centrality of North China (Background: Ruggedness).

Our model highlights the role of North China, referred to as the "Central Plain" in historical records, in driving these phenomena. While North China is only one of several macroregions of China (Figure 14), it played an outsized role in Chinese history. The silty and flood-prone Yellow River, China's "mother river," runs through the region. Regularly inundated by flooding, which replenished the soil, North China was agriculturally precocious and productive even with primitive agricultural tools (Huang, 1988). Notably, North China is close to the flat cores of Northwest China (Guanzhong Plain), Middle Yangzi (Jianghan Plain), and Lower Yangtze (Yangtze Delta), which, together with the Central Plain, form the heartland of traditional China. In 1943, Sha Xuejun, one of the first modern political geographers in China, used the term "the hub of China" to describe the centrality of North China and its contiguous plains (Sha, 1972). Paraphrasing Mackinder (1942), he remarked: "To control China, one needs to first control its heartland; To control China's heartland, one needs to first control its hub."

In our simulations, North China stands out for its flat terrain and high agricultural productivity. Its flatness facilitates military conquest and political consolidation (Figure 15 plots the cells from where the empire originates in each simulation). And once a unified state emerges in North China, the wealth of resources at its disposal makes it nearly impossible for the other Chinese regions—which find internal unification harder to achieve due to their rugged terrains—to resist conquest. This explains why the states of Qin and Jin could unify China

despite its adversaries' attempts to maintain a balance of power during the Warring States and the Three Kingdoms periods (see Section 6 for a discussion of balancing and bandwagoning).[27]

Unlike the North European Plain, which is non-compact and open to being invaded from multiple directions, North China was shielded by the Tibetan plateau and the Pacific Ocean on its two flanks. Meanwhile the steppe and deserts north of China limited the expansion of the Chinese state in that direction. In our simulations, the North Chinese state typically expands in a southerly direction until it hits the tropical rainforests of Indochina, and an increased probability of secession hinders further expansion. Thus, the resulting empire often approximates the shape of China proper.

Besides the size and flatness of North China, its proximity to the core areas of Northwest China, Middle Yangtze, and Lower Yangtze also allowed a single powerful state to overcome its rivals and build a centralized polity. In our baseline simulation run, all unifications of China originate from three contiguous plains: the Central Plain, the Jianghan Plain, and the Lower Yangtze Delta (Figure 15). The proximity of North China to the Mongolian steppe likely provided a further martial impetus to China's unification. When we enrich the model by incorporating the roles of the steppe and the loess plateau, the Guanzhong Plain of Northwest China and Eastern Mongolia-Manchuria are added to the list of origins of the Chinese empire. This is broadly consistent with the historical record summarized in Table 3 of Appendix E. All ten dynasties that controlled most or all of China proper at their peaks originated north of the Yangtze River, and all had their capital cities in the north (with the exception of the Ming dynasty for several decades). Historically, there were long periods of political fragmentation in China: the Warring States period (475 BCE–221 BCE), the Six Dynasties period (220–589), the Five Dynasties and Ten Kingdoms period (907–960), and the Southern Song period (1127–1279). However, if a powerful Chinese state arose to establish stable rule in North China, it would often go on to subdue rival kingdoms and unify "all under heaven."

Europe. Figure 16 shows the evolution of the average size of the five largest polities in China and Europe in our preferred specification. In contrast to China, where one polity quickly dominates the rest, in Europe (including or excluding Eastern Europe), we typically observe

[27]The historical literature points to the reforms enacted by the Qin state, notably by Shang Yang. These included conscription, large-scale irrigation projects, and a system of land registration (Hui, 2005). However, other warring states also pursued these reforms.

the simultaneous emergence of several middle-sized polities. The size gap between the largest and fifth-largest European polities is never of the same order of magnitude observed in China. In other words, Europe is distinctively polycentric and develops into a series of medium-sized states surrounded by small polities.

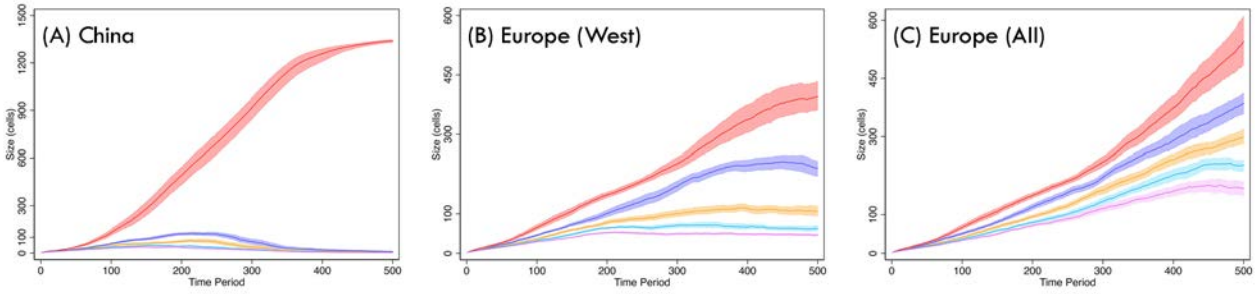

Figure 16: Land Area of the Five Largest Regimes in China and Europe (West, All).

This result is in line with European history from the Middle Ages onward. Scheidel (2019, pp. 338–339) notes that after the fall of Rome, Europe was composed of "multiple states that did not dramatically differ in terms of capabilities." This had significant implications for the balance of power (discussed below).

The closest that Europe came to being ruled by a single polity was during the Roman Empire. This was a unique development in European history; at no other point did a single polity come close to establishing stable rule over the majority of the European landmass or population. Numerous factors are important in explaining the rise of Rome: the Mediterranean Sea as a conduit to empire, Rome's peripheral position on the edge of the Eastern Mediterranean state system based around the Fertile Crescent, its early ability to incorporate the nearby population of Latium and to build an alliance system of nearby Italian cities, its unusual bellicosity (Harris, 1979, 1984), and favorable climatic conditions during the classical period (Braudel, 1972, 1949; Horden and Purcell, 2000; Harper, 2017; Scheidel, 2019). In Subsection 8, we use our model to study under what conditions a Mediterranean empire could emerge. We find that the rise of Rome likely depended on the highly contingent factors for which these historians have argued.

After the fall of the Roman Empire, the closest Europe came to being unified by a single ruler was during the 16th century under the Habsburg emperor Charles V. Importantly, for our purposes, Charles V did not acquire this empire by conquest, but by generations of successful marriages and dynastic luck. He also did not create a unified state, but ruled his disparate

kingdoms as separate entities. Our model does not directly speak to how the Habsburgs chanced on a European-wide empire. It does, however, speak to the difficulties Charles V had in managing his domains. Geography prevented Charles V from focusing attention on either facing the Ottomans in the Mediterranean, driving France out of Italy, or subduing Protestant German princes. The final admission of the power of geography came when, upon his abdication, Charles divided his territories between his son Philip II of Spain (r. 1556–1598) and his brother Ferdinand I (r. 1556–July 1564).

Beyond accounting for the Habsburgs' experience, our model also speaks to the failures of Louis XIV and Napoleon to successfully build a hegemonic state in Europe against a combination of several medium-size states led by Great Britain. Our model delivers many medium-size states not only because of the presence of mountain barriers in Europe, as stressed by Diamond (1997, 1998), but also because the most productive agricultural land in Europe is dispersed, rather than concentrated as in China.

The Balance of Power. Our model lacks strategic interactions: polities enter into conflicts and win or lose them based on exogenous probability distributions. For instance, we do not allow polities to think about issues such as state power investment, a dynamic path of conquest, or the formation of alliances—for instance, through strategic marriages, a common form of political consolidation in European history (Levine and Modica, 2013; Dziubinski et al., 2017).

The most important reason why we do this is computational. Introducing even a minimum of strategic thinking will complicate the model so much that simulations would become unfeasible given computing power and current algorithms.

However, we conjecture that strategic interactions will likely strengthen our results. A key idea in international relations is the balance of power (Morgenthau, 1948; Waltz, 1979; Mearsheimer, 2001). States form alliances against potential hegemons, limiting their ability to conquer neighboring polities. Examples of balancing in European history include the shifting compositions of the Greek poleis leagues,[28] the polyhedric structure of arrangements in the Italian peninsula during the Middle Ages and early modern period, or the alliances in Europe first against the Habsburgs and later against the House of Bourbon. More recently, balancing

[28]The oligarchic Corinth is a textbook example of a balancer, deftly switching between its alliances with Sparta, Athens, and Thebes to ensure none of its rivals became too powerful.

explains why the French Third Republic, probably the most democratic nation in Europe around 1914, could be the staunchest ally of Tsarist Russia, the epicenter of reaction, or why Churchill wrote: "If Hitler invaded Hell I would make at least a favourable reference to the Devil in the House of Commons" (Churchill, 1950, p. 370). Because Europe had different nuclei for the formation of states that could form the seed of multi-faced balancing coalitions, the balance of power was the predominant structure of international relations for much of its history, reinforcing the mechanisms in our model.

Why did the same balancing logic not prevail in China? Because the early formation of a large polity in northern China illustrated by our simulation triggered the opposite force to balancing: bandwagoning. In this situation, weaker states align themselves with the hegemon (or integrate), as resistance is futile in the absence of alternative nuclei. The Three Kingdoms period (220–280), which opened at the end of the Han dynasty, shows this point. The alliance between Wu and Shu could only resist Wei until the northern kingdom regained its strength. But once Wei was able to mobilize the resources of the northern plain, Wu and Shu were doomed. Our model suggests that the lack of geographical barriers in northern China and the potential for cumulative conquests in this core region of historical China as the reasons for bandwagoning. In other words, given the geographical features of China, balancing was likely never a feasible Nash equilibrium, but bandwagoning was, reinforcing the mechanisms in our model.

Feedback between Economic Growth and Political Fragmentation. To keep the model simple, we also abstract from how political fragmentation or unification might feed back into economic growth and, through it, into the power of different polities to conquer or defend. Abramson (2017) has argued that the economic prosperity that small independent polities, such as Venice or the United Provinces of the Netherlands, enjoyed thanks to Europe's polycentrism allowed them to punch above their weight militarily and survive for centuries. Eisenstadt and Rokkan (1973) defended the argument that the core of the modern European states appeared where there were no large urban centers that could assert their independence. Conversely, once a sufficiently large polity has emerged, its urban structure and the transportation network built around it can further unify the country (think about the role of London in England). Thus, these feedback channels will likely reinforce the main mechanisms in our simulations.

7 Africa and the Americas

In this section, we investigate the predictions of our model for state formation in Africa and the Americas. Due to length constraints, we discuss these extensions briefly here and leave their detailed discussions to the appendix.

Africa. Historically, state formation in Africa was different from state formation on other continents. No large, sustained agrarian state had emerged in sub-Saharan Africa outside Ethiopia before 1500, the calibrated end of our simulation (many states have risen and disappeared without long persistence over time). Panel A of Figure 17 shows how, by 1750, the region was still composed of many small states and communities.

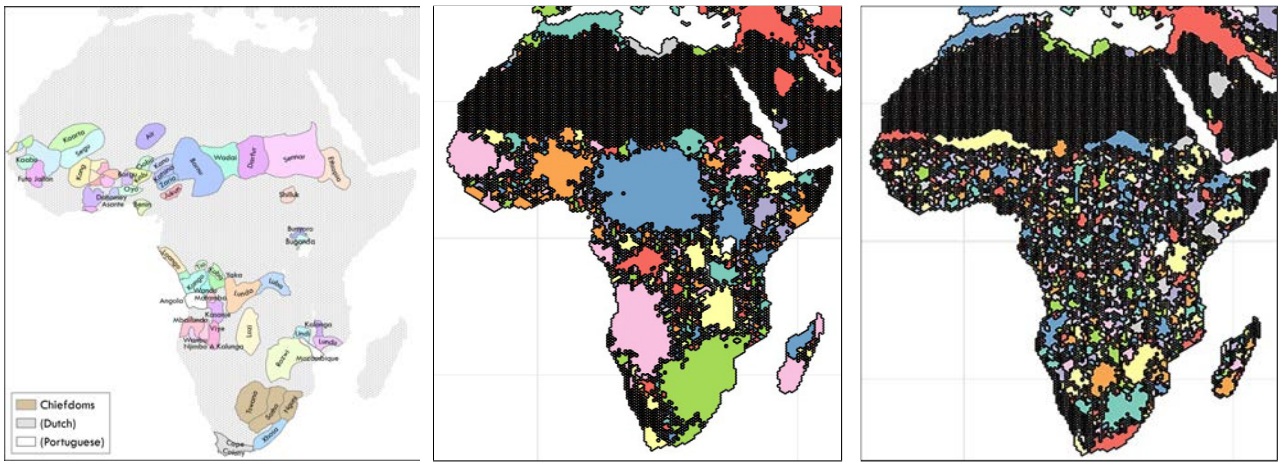

(A) Distribution of states in 1750 (Overy, 2004).

(B) Baseline specification: representative output ($t = 500$).

(C) Climate & timing adjusted: representative output ($t = 500$).

Figure 17: Accounting for the relative absence of large-scale states in Sub-Saharan Africa.

Our baseline simulations, however, suggest that Africa should be home to several large states (Panel B of Figure 17). While the prediction is off the mark, it is unsurprising. As we discussed earlier, the GAEZ v4 dataset overestimates productivities in hot regions like sub-Saharan Africa. In 1950, Africa's mean population density was 45% that of the world, but its mean GAEZ v4 attainable caloric yield is 2.2 times above the world's average. Because of this, in our baseline simulations, we observe political consolidation in every part of sub-Saharan Africa.

Scholars have highlighted sub-Saharan Africa's relative isolation from the rest of Eurasia in leading it onto a path of technological and agricultural development that was less conducive

to state formation (Childe, 1957; Goody, 1971; Diamond, 1997), and a climate-enabled disease environment that lowered population density (Weil, 2014; Alsan, 2015; Bellone, 2020). We consider these factors by delaying the start of the cells' ability to conquer other cells to $t = 150$ and by correcting GAEZ v4 productivity as in our preferred specification (see Appendix F for details). When we do so, Panel C of Figure 17 shows that our simulation results look much closer to what we observed historically (without having an impact on the process of state formation in Eurasia due to geographical distance).

The Americas. According to GAEZ v4, the Americas are home to the world's most productive lands. Each of the 50 hexagons with the highest attainable caloric yields in the world is in either present-day Argentina and the United States. As a result, in our baseline simulations, we generally observe empires emerging in Argentina and the eastern United States (Panel A of Figure 18), which is inconsistent with the historical observation that pre-Columbian state formation was most advanced in Mesoamerica and the Andes.

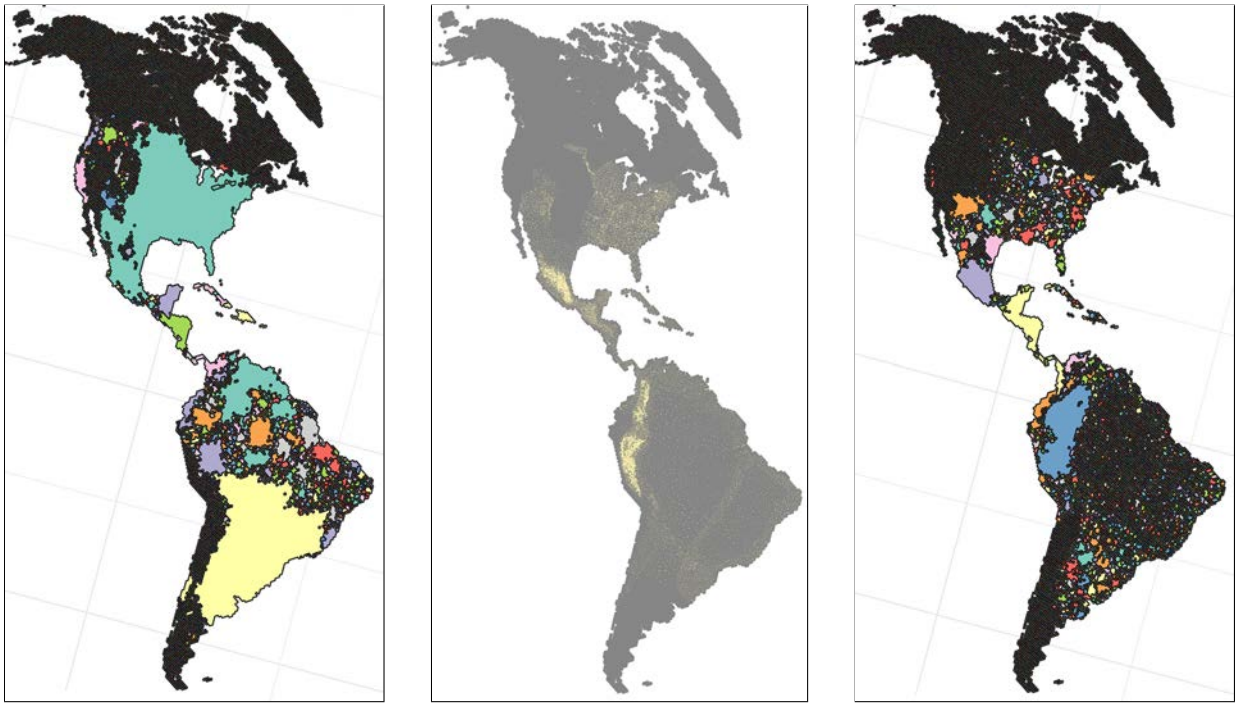

(A) Baseline specification: representative output ($t = 500$).

(B) Maize cultivation in 1500 (adapted from Fig. 1, Goodman and Galinat, 1988).

(C) Accounting for maize and guano: representative output ($t = 500$).

Figure 18: Locating the large states in pre-Columbian Americas.

This counterfactual result is driven by the fact that our use of GAEZ v4 assumes that maize,

the major indigenous crop in the Americas, is available throughout the continent from $t = 0$. Historically, this is inaccurate. While maize was domesticated from Balsas teosinte, a wild grass, in the Mexican plateau about 9000 years ago, its spread across the Americas was slow (Staller et al., 2006). Possible reasons include the wide climate and terrain variability across the vertically oriented American continent, which created obstacles to its adaptation across latitude and elevation. Also, the lack of iron tools in the Americas to deal with the prairie sod might have restricted maize cultivation in the fertile plains of the Midwest United States and northern Argentina (Hudson, 2004; Bamforth, 2021). For example, the earliest evidence of maize consumption in the middle Ohio valley is as late as 900 (Staller et al., 2006, p. 230). On the eve of the Columbian exchange, the crop was most intensely cultivated in the Mexican plateau and in neighboring Guatemala and Yucatán, as well as Peru (Panel B of Figure 18).

Furthermore, in the case of Peru, scholars have highlighted the role of guano, the accumulated feces of marine birds and bats. Guano was the richest organic source of nitrogen compounds known in the premodern world. Archaeological evidence suggests that Andean inhabitants understood the use of guano as a natural fertilizer as early as 2,000 BCE (Poulson et al., 2013). This was made possible by an abundance of guano-producing birds, including the Peruvian cormorant, the Peruvian pelican, and the Peruvian booby. Guano turned the relatively infertile Andean highlands and coastlines into some of the most productive fields in pre-Columbian Americas (Cushman, 2014) and, thus, it enabled the agricultural development and political ascendancy of the Inca Empire and its predecessors (Santana-Sagredo, 2021; Rodrigues and Micael, 2021).

We incorporate these insights by accounting for (1) the timing and spread of maize cultivation in the Americas and (2) the use of guano, a largely location-specific resource in the Cusco basin and its surroundings. As Panel C of Figure 18 illustrates, once we consider these factors in our simulations, the Americas cease to produce supersized polities. Now, relatively large states typically emerge on the Pacific coast and in the Andean highlands as well as in Mesoamerica, states that resemble the Triple Alliance and the Incan empire. As in the case of Africa, these modifications do not change the results of the simulations in Eurasia. See also Figure 35 in Appendix F.

Taking stock. The study of Africa and the Americas should not be understood as a claim that the fractured-land hypothesis applies everywhere and all the time. Instead, the study shows the power of our model as a measurement device: the model tells us where fractured land exerted a heavy influence on state formation and where it did not. Furthermore, our model suggests corrections one needs to introduce to match a concrete historical case.

8 Extensions

In this section, we consider several extensions of our model as external validity checks.

Exogenous Shocks and Dynastic Cycles. Introducing exogenous shocks allows us to probe the issue of path dependence. Are the patterns of state formation observed in the model generated by initial conditions? Or, to the contrary, can the introduction of large-scale shocks create changes in the overall distribution of polities?

The idea that external shocks explain the rise and fall of particular polities is an old one, but particularly popular in Chinese historiography, where the rise of empires is often interpreted through the lens of dynastic cycles (Usher, 1989; Chu and Lee, 1994). Recently, scholars have pointed to climate change as a cause of these dynastic cycles (see Zhang et al., 2006; Fan, 2010). Climatic factors have also been adduced as necessary in the rise and fall of the Roman Empire and widespread social upheavals in late medieval and early modern Europe (Lamb, 1982; Parker, 2013; Campbell, 2016).

We incorporate climatic and other random sociopolitical shocks by distinguishing between general system-wide and regime-specific crises. General shocks such as the collapse of Bronze Age empires c. 1177 BCE or the Little Ice Age of the 17th century are potentially significant as they have the potential to generate synchronized changes across a region—something observed by Lieberman (2003, 2009), who notes the "strange parallels" of synchronized administrative cycles across Eurasia. In contrast, regime-specific crises are modeled as localized shocks, such as the Twenty Years' Anarchy in the Byzantine Empire (695–717), the An Lushan Rebellion of Tang China (755–763), or the War of the Roses of 15th century England (one can think of the latter as occurring due to the crowning of the incompetent Henry IV). In our extension, these two types of crises occur randomly given exogenous probabilities.

In this version of the model, political cycles are muted in Europe, which never achieves complete unification despite short periods of a hegemonic state. By contrast, China intersects periods of sustained unification interrupted with periods of disunity, resembling the successive dynasties of Chinese history (which motivated the opening quote of this paper). The result echoes Root (2017, 2020), who contrasts patterns of network stability in China and Europe and argues that China's organization as a hub-and-spoke system was less resilient than Europe's polycentricity, and Ko et al. (2018), who show that the Chinese empire displayed greater volatility of population and economic output than Europe after the collapse of the Roman Empire.

The Mediterranean Sea. In our baseline simulations, we do not see political consolidation in Europe. But then: What about the Roman Empire? We can use our model to shed light on the conditions that were necessary to generate the Roman Empire and to explore why, after its collapse, no subsequent state ever came close to unifying as large a territory again.

In the first exercise, we improve the agricultural productivity of the area around the Mediterranean. This exercise is motivated by historians such as Harper (2017), who have pointed to the confluence of favorable climatic conditions that facilitated the rise of the Roman Empire. This exercise generates slightly larger polities in the Mediterranean, but it does not come close to causing a polity like the Roman Empire.

In the second exercise, we give Rome a military advantage. Classicists like Harris (1979, 1984) have argued that Republican Roman culture was uniquely bellicose and that this gave Rome an edge in war. This extension also does not generate anything like a Roman Empire.

Finally, we combine both extensions. In this case, we find larger empires emerging, another example of non-linear effects in our model. These Mediterranean-based empires, however, do not regularly extend beyond the Alps and, hence, do not resemble the full extent of the Roman Empire. This suggests that, while exogenous factors such as climate may have a played a role in the expansion of the Roman Empire, this event was both highly contingent (such as Rome's good fortune in gaining early control of the entire Mediterranean before many competing powers could appear), as many historians have observed, and also a one-off event that was not repeated.

State Formation across Eurasia. Consistent with the historical record, in our simulations, the formation of large states is pronounced in East Asia. As Scheidel (2019) notes, the

"easternmost macro-region, East Asia, has been characterized by much stronger dominance of hegemonic empire than any of the others." By contrast, Europe is distinctively polycentric (Figure 16). To what extent can our model also explain broader patterns of state formation across Eurasia beyond East Asia and Europe?

To investigate, we compute the size of the five largest regimes in Europe, East Asia, South Asia, Southeast Asia, and the Middle East. We observe a hegemonic state regularly emerge in China, northern India, and the Middle East (Figure 19). However, full political consolidation occurs nowhere else except in China. Inspecting the simulations, we can gauge, for example, why a single huge polity does not always conquer the entire Indian subcontinent. First, the Himalayas and the Hindu Kush in the north, the Thar Desert in the west, and the thick jungles of Burma and Gondwana in the east presented significant impediments in terms of either rugged terrain or low agricultural productivity that discouraged state expansion in these directions.[29] Second, the rugged Deccan plateau in southern India was a significant barrier to empire-building.[30] Third, the tropical climate of southern India, which historically posed difficulties in gathering and moving armies (Lieberman, 2003, 2009), further impeded the conquest of the south by the north.

Likewise, while we also observe large states arising in the Middle East, the process of political consolidation in the region is typically incomplete because of the region's relatively rugged terrain and large tracts of deserts in the region's interior.

In the case of Southeast Asia, the tropical climate, together with the rugged terrain, explains why, in our simulations, polities in the region are usually small and the political map is highly fragmented even compared with Europe.[31] In sum, comparing Figures 16 and 19, while China is

[29]While the thick jungles of Burma and Gondwana created unbridgeable outer limits to Mughal expansion (Gommans, 2002, p. 198), the mountains were not insurmountable to armies. The Mughals conducted mountainous expeditions into Kashmir (1561, 1585, 1588), Garhwal (1635, 1656), Baltistan (1637), and Ladakh and Tibet (1679–84). However, the lack of forage and food impeded the extension of permanent political authority north of India. As Gommans (2002, p. 23) puts it: "Indian armies were faced by tremendous logistical problems. One mid-18th-century source considered the Kabul area a land of snow: 'Men and cattle from India are not able to withstand the icy cold winds of that area. That is why it is difficult for the people of India to capture and occupy the Muslim countries of that area'." See also Nath (2019) for Mughal warfare and the South Asia environment.

[30]The Deccan plateau rises to over 1000 meters. It was the site of numerous conflicts between states from northern India and those from southern India. Multiple Hindu states in the Deccan could resist the expansion of Muslim empires such as the Mughals.

[31]Southeast Asia was less populous than other major regions of Eurasia until the 19th century and state formation took place later and under less favorable conditions there than elsewhere (Lieberman, 2003, 2009). There were periods that saw the formation of states with a considerable geographical scope such as the Khmer Empire in the 9th century, the Taoungoo Empire in the 16th century, or the Kingdom of Siam in the 18th and 19th centuries. But these larger states only retained regional hegemony for brief periods of time and the more common pattern was political fragmentation.

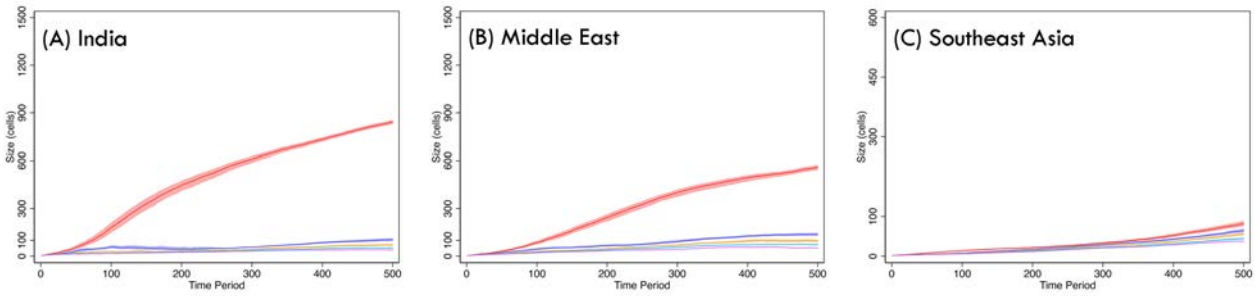

Figure 19: Land Area of Five Largest Regimes in India, Middle East, and Southeast Asia.

unique in its extremely robust tendency toward political unification, Europe's inclination toward polycentrism is also unparalleled.

9 Conclusion

This paper has developed a dynamic model to adjudicate among competing explanations of Europe's polycentrism and China's political centralization. Our analysis evaluates Jared Diamond's argument that Europe's mountain barriers and the shape of its coastline were responsible for its polycentrism, whereas Chinese geography encouraged political centralization. By developing a model of state formation that quantitatively incorporates the role of topography and agricultural productivity, we provide a rigorous formulation of the fractured-land hypothesis. Our simulations demonstrate that either topography or the location of productive land can generate political unification in China and persistent polycentrism in Europe.

We have also documented how the fractured-land hypothesis needs to be supplemented by additional mechanisms to account for the dynamics of state formation in Africa and the Americas and have suggested possible ways to do so, showing the power of our methodology. Indeed, we do not claim that the fractured-land hypothesis applies everywhere and all the time. More circumspectly, we argue that fractured land accounts for a large fraction of the variation in state formation in history, especially in Eurasia.

Finally, our model can be a starting point for additional explorations. For example, we could incorporate military technological change (Hoffman, 2015), investment in state capacity (Gennaioli and Voth, 2015; Johnson and Koyama, 2017; Becker et al., 2020), or epidemic diseases (McNeil, 1974; Voigtländer and Voth, 2013b). We could also add climatic change, migration, time-varying agricultural technology (new crops, irrigation systems), variation in transportation

capabilities (Bakker et al., 2018), or cultural aspects that feed back into the creation of states. For instance, after a state has been in existence for many periods, its inhabitants may have developed an "imagined community," which makes it harder to conquer and easier to maintain unified (Anderson, 1991). Think about how, in a few generations during the late Republic and the Principate, the conquered peoples of Italy started thinking about themselves as "Romans." Also, some cells may share a religion, which makes unification easier, or be separated by it, which makes conflict more likely.

In summary: it would be essential to evaluate the relative contributions of geographical endowment vs. human endowment to state formation. Although such a measurement is beyond the scope of the current (already lengthy) paper, our methodological approach is flexible in allowing for these and many other quantitative exercises and generating probability distributions of historical outcomes. We hope to see many of those extensions soon.

References

Abramson, S. F. (2017): "The Economic Origins of the Territorial State," *International Organization*, 71, 97–130.

Abulafia, D. (2011): *The Great Sea: A Human History of the Mediterranean*, Oxford: Oxford University Press.

Acemoglu, D., S. Johnson, and J. A. Robinson (2001): "The Colonial Origins of Comparative Development: An Empirical Investigation," *American Economic Review*, 91, 1369–1401.

——— (2002): "Reversal of Fortune: Geography and Institutions in the Making of the Modern World Income Distribution," *Quarterly Journal of Economics*, 117, 1231–1294.

——— (2005): "Institutions as a Fundamental Cause of Long-Run Growth," in *Handbook of Economic Growth*, ed. by P. Aghion and S. Durlauf, Elsevier, vol. 1 of *Handbook of Economic Growth*, chap. 6, 385–472.

Acharya, A. and A. Lee (2018): "Economic Foundations of the Territorial State System," *American Journal of Political Science*, 62, 954–966.

Ahlerup, P. and O. Olsson (2012): "The roots of ethnic diversity," *Journal of Economic Growth*, 17, 71–102.

Alesina, A. and E. Spolaore (1997): "On the Number and Size of Nations," *Quarterly Journal of Economics*, 112, 1027–1056.

——— (2003): *The Size of Nations*, Cambridge, MA: MIT Press.

——— (2005): "War, Peace, and the Size of Countries," *Journal of Public Economics*, 89, 1333–1354.

Alsan, M. (2015): "The Effect of the TseTse Fly on African Development," *American Economic Review*, 105, 382–410.

Anderson, B. (1991): *Imagined Communities: Reflections on the Origin and Spread of Nationalism*, Brooklyn: Verso.

Arbatli, C. E., Q. H. Ashraf, O. Galor, and M. Klemp (2020): "Diversity and Conflict," *Econometrica*, 88, 727–797.

Ashraf, Q. and O. Galor (2013): "Genetic Diversity and the Origins of Cultural Fragmentation," *American Economic Review*, 103, 528–33.

Ashraf, Q. H. and O. Galor (2018): "The Macrogenoeconomics of Comparative Development," *Journal of Economic Literature*, 56, 1119–1155.

Baechler, J. (1975): *The Origins of Capitalism*, Oxford: Basil Blackwell.

Bai, Y. and J. Kung (2011): "Climate Shocks and Sino-nomadic Conflict," *Review of Economics and Statistics*, 93, 970–981.

Bakker, J. D., S. Maurer, J.-S. Pischke, and F. Rauch (2018): "Of Mice and Merchants: Trade and Growth in the Iron Age," Working Paper 2018-05, Department of Economics, University of Konstanz.

Bamforth, D. B. (2021): *The Archaeology of the North American Great Plains*, Cambridge: Cambridge University Press.

Barfield, T. (1989): *The Perilous Frontier: Nomadic Empires and China*, Cambridge, MA: Basil Blackwell.

Becker, S. O., A. Ferrara, E. Melander, and L. Pascali (2020): "Wars, Taxation and Representation: Evidence from Five Centuries of German History," Manuscript.

Bellone, R. (2020): "The Role of Temperature in Shaping Mosquito-Borne Viruses Transmission," *Frontiers in Microbiology*, 11, 584846.

Braudel, F. (1972, 1949): *The Mediterranean, and the Mediterranean World in the Age of Phillip II, Vol. II*, Berkeley: University of California Press.

Campbell, B. M. (2016): *The Great Transition: Climate, Disease and Society in the Late-Medieval World*, Cambridge: Cambridge University Press.

Campbell, R. (2018): *Violence, Kinship and the Early Chinese State: The Shang and their World*, Cambridge: Cambridge University Press.

Carneiro, R. L. (1970): "A Theory of the Origin of the State," *Science*, 169, 733–738.

Chaudhry, A. and P. Garner (2006): "Political Competition Between Countries and Economic Growth," *Review of Development Economics*, 10, 666–682.

Chen, Q. (2015): "Climate Shocks, Dynastic Cycles and Nomadic Conquests: Evidence from Historical China," *Oxford Economic Papers*, 67, 185–204.

Childe, V. G. (1936): *Man Makes Himself*, New York: Spokesman.

——— (1957): "The Bronze Age," *Past & Present*, 2–15.

Chu, A. C. (2010): "Nation States vs. United Empire: Effects of Political Competition on Economic Growth," *Public Choice*, 145, 181–195.

Chu, C. Y. C. and R. D. Lee (1994): "Famine, Revolt, and the Dynastic Cycle: Population Dynamics in Historic China," *Journal of Population Economics*, 7, 351–378.

Churchill, W. S. (1950): *The Grand Alliance*, Boston: Houghton Mifflin.

Cline, E. H. (2014): *1177 B.C.: The Year Civilization Collapsed*, Princeton, NJ: Princeton University Press.

Clowes, G. S. L. (1932): *Sailing Ships: Their History and Development, as Illustrated by the Collection of Ship-models in the Science Museum. Part I: Historical Notes*, London: H.M.S.O.

Cowen, T. (1990): "Economic Effects of a Conflict-Prone World Order," *Public Choice*, 64, 121–134.

Crafts, N. (1977): "Industrial Revolution in England and France: Some Thoughts on the Question, "Why was England First"," *Economic History Review*, 30, 429–441.

Cunliffe, B. W. (2008): *Europe between the Oceans: Themes and Variations, 9000 BC–AD 1000*, New Haven: Yale University Press.

Cushman, G. (2014): *Guano and the Opening of the Pacific World: A Global Ecological History*, Cambridge: Cambridge University Press.

Department of the Army (2016): *TRADOC Regulation 350-29: Prevention of Heat and Cold Casualties*, Headquarters, United States Army.

Diamond, J. (1997): *Guns, Germs, and Steel*, New York: W.W. Norton & Company.

Diamond, J. M. (1998): "Peeling the Chinese Onion," *Nature*, 391, 433–434.

Dien, A. and K. Knapp, eds. (2019): *Cambridge History of China. Vol. 2: The Six Dynasties, 220—589*, Cambridge: Cambridge University Press.

Dincecco, M. and Y. Wang (2018): "Violent Conflict and Political Development over the Long Run: China versus Europe," *Annual Review of Political Science*, 341–358.

Downing, B. M. (1992): *The Military Revolution and Political Change: Origins of Democracy and Autocracy in Early Modern Europe*, Princeton, NJ: Princeton University Press.

Drews, R. (1993): *The End of the Bronze Age: Changes in Warfare and the Catastrophe ca. 1200 B.C.*, Princeton, NJ: Princeton University Press.

Driessen, P. and J. Deckers (2001): "Lecture Notes on the Major Soils of the World," World Soil Resources Reports 94, Food and Agriculture Organization.

Dupuy, T. N. (1979): *Numbers, Predictions and War: Using History to Evaluate Combat Factors and Predict the Outcome of Battles*, London: Macdonald and Jane's.

Dziubinski, M., S. Goyal, and D. E. N. Minarsch (2017): "The Strategy of Conquest," Cambridge Working Papers in Economics 1704, Faculty of Economics, University of Cambridge.

Eisenstadt, S. and S. Rokkan (1973): *Building States and Nations (Vol. 2)*, Thousand Oaks, CA: SAGE Publications.

Engel, J. H. (1954): "A Verification of Lanchester's Law," *Journal of the Operations Research Society of America*, 2, 163–171.

Fan, K. (2010): "Climatic change and Dynastic Cycles in Chinese History: a Review Essay," *Climatic Change*, 101, 565–573.

Frachetti, M. (2008): *Pastoralist Landscapes and Social Interaction in Bronze Age Eurasia*, Berkeley: University of California Press.

Fried, M. H. (1967): *The Evolution of Political Society: an Essay in Political Anthropology*, New York: Random House.

Fukuyama, F. (2011): *The Origins of Political Order*, London: Profile Books Ltd.

Galor, O. (2005): "From Stagnation to Growth: Unified Growth Theory," in *Handbook of Economic Growth*, ed. by P. Aghion and S. Durlauf, Elsevier, vol. 1, chap. 4, 171–293.

——— (2011): *Unified Growth Theory*, Princeton, NJ: Princeton University Press.

Galor, O. and O. Özak (2016): "The Agricultural Origins of Time Preference," *American Economic Review*, 106, 3064–3103.

Galor, O. and D. N. Weil (2000): "Population, Technology, and Growth: From Malthusian Stagnation to the Demographic Transition and Beyond," *American Economic Review*, 90, 806–828.

Gat, A. (2006): *War in Human Civilization*, Oxford: Oxford University Press.

Gennaioli, N. and H.-J. Voth (2015): "State Capacity and Military Conflict," *Review of Economic Studies*, 82, 1409–1448.

Gibbon, E. (2003): *The Decline and Fall of the Roman Empire*, New York: Modern Library.

Giráldez, A. (2015): *The Age of Trade: The Manila Galleons and the Dawn of the Global Economy*, Lanham: Rowman & Littlefield.

Goldewijk, K., A. Beusen, J. Doelman, and E. Stehfest (2017): "Anthropogenic Land Use Estimates for the Holocene–HYDE 3.2," *Earth System Science Data*, 9, 927–953.

Gommans, J. (2002): *Mughal Warfare*, London: Routledge.

Goodman, M. M. and W. C. Galinat (1988): "The History and Evolution of Maize," *Critical*

Reviews in Plant Sciences, 7, 197–220.

Goody, J. (1971): *Technology, Tradition and the State in Africa*, Oxford: Oxford University Press.

Greif, A. and G. Tabellini (2017): "The Clan and the Corporation: Sustaining Cooperation in China and Europe," *Journal of Comparative Economics*, 45, 1–35.

Grousset, R. (1970): *The Empire of the Steppes: a History of Central Asia*, New Brunswick: Rutgers University Press, translated by Naomi Walford.

Hajnal, J. (1965): "European Marriage Pattern in Historical Perspective," in *Population in History*, ed. by D. V. Glass and D. E. C. Eversley, London: Arnold, 201–213.

Hall, J. A. (1985): *Power and Liberties*, London: Penguin Books.

Harper, K. (2017): *The Fate of Rome*, Princeton, NJ: Princeton University Press.

Harris, W. V. (1979): *War and Imperialism in Republican Rome, 327–70 B.C.*, Oxford: Clarendon Press.

Harris, W. V., ed. (1984): *The Imperialism of Mid-Republican Rome*, University Park, PA: Pennsylvania State University Press.

Headquarters, Department of the Army (2017): *Foot Marches*, Department of Defense.

Hechter, M. and W. Brustein (1980): "Regional Modes of Production and Patterns of State Formation in Western Europe," *American Journal of Sociology*, 85, 1061–1094.

Hicks, J. (1969): *A Theory of Economic History*, Oxford: Oxford University Press.

Ho, P. (1975): *The Cradle of the East: An Inquiry into the Indigenous Origins of Techniques and Ideas of Neolithic and Early Historic China, 5000–1000 B.C.*, Chicago: University of Chicago Press.

Hodgson, M. G. S. (1954): "Hemispheric Interregional History as an Approach to World History," *Journal of World History*, 1, 715–23.

Hoffman, P. T. (2015): *Why Did Europe Conquer the World?*, Princeton, NJ: Princeton University Press.

Horden, P. and N. Purcell (2000): *The Corrupting Sea*, Oxford: Wiley Blackwell.

Huang, R. (1988): *China: A Macro History*, Armonk, NY: M.E. Sharpe.

Hudson, J. C. (2004): "Agriculture," in *Encyclopedia of the Great Plains*, ed. by D. J. Wishart, Lincoln: University of Nebraska Press.

Hui, V. T.-b. (2005): *War and State Formation in Ancient China and Early Modern Europe*,

Cambridge: Cambridge University Press.

Hume, D. (1752): *Political Discourses*, Edinburgh: A. Kincaid and A. Donaldson.

Iyigun, M., N. Nunn, and N. Qian (2017): "The Long-Run Effects of Agricultural Productivity on Conflict, 1400–1900," Working paper.

Jami, C. (2012): *The Emperor's New Mathematics: Western Learning and Imperial Authority During the Kangxi Reign (1662–1722)*, Oxford: Oxford University Press.

Jia, R., G. R. Roland, and Y. Xi (2020): "A Theory of Power Structure and Political Stability: China vs. Europe Revisited," Working paper.

Jiang, W., Y. Cheng, X. Yang, and S. Yang (2013): "Chinese Loess Plateau Vegetation since the Last Glacial Maximum and its Implications for Vegetation Restoration," *Journal of Applied Ecology*, 50, 440–448.

Johnson, N. D. and M. Koyama (2017): "States and Economic growth: Capacity and Constraints," *Explorations in Economic History*, 64, 1–20.

Jones, E. L. (2003): *The European Miracle*, Cambridge: Cambridge University Press, 3rd ed.

Jones, E. T. (2000): "River Navigation in Medieval England," *Journal of Historical Geography*, 26, 60–75.

Kaplan, J. O. and K. M. Krumhardt (2011): "The KK10 Anthropogenic Land Cover Change Scenario for the Preindustrial Holocene, Link to Data in NetCDF format," Supplement to: Kaplan, Jed O; Krumhardt, Kristen M; Ellis, Erle C; Ruddiman, William F; Lemmen, Carsten; Klein Goldewijk, Kees (2011): Holocene Carbon Emissions as a Result of Anthropogenic Land Cover Change. The Holocene, 21(5), 775–791.

Karayalcin, C. (2008): "Divided We Stand United We Fall: The Hume-North-John Mechanism for the Rise of Europe," *International Economic Review*, 49, 973–997.

Kennedy, P. (1987): *The Rise and Fall of the Great Powers, 1500–1980*, New York: Vintage Books.

Kitamura, S. and N.-P. Lagerlöf (2019): "Geography and State Fragmentation," *Journal of the European Economic Association*, 18, 1726–69.

Ko, C. Y., M. Koyama, and T.-H. Sng (2018): "Unified China; Divided Europe," *International Economic Review*, 59, 285–327.

Ko, C. Y. and T.-H. Sng (2013): "Regional Dependence and Political Centralization in Imperial China," *Eurasian Geography and Economics*, 54, 470–483.

Koyama, M., A. S. Rahman, and T.-H. Sng (2021): "Sea Power," *Journal of Historical Political Economy*, 1, 155–182.

Kremer, M. (1993): "Population Growth and Technological Change: One Million B.C. to 1990," *Quarterly Journal of Economics*, 108, 681–716.

Lagerlöf, N.-P. (2014): "Population, Technology and Fragmentation: the European Miracle Revisited," *Journal of Development Economics*, 108, 87–105.

Laitin, D. D., J. Moortgat, and A. L. Robinson (2012): "Geographic Axes and the Persistence of Cultural Diversity," *Proceedings of the National Academy of Sciences*, 109, 10263–10268.

Lamb, H. (1982): *Climate, History, and the Modern World*, London: Methuen.

Langdon, J. (1993): "Inland Water Transport in Medieval England," *Journal of Historical Geography*, 19, 1–11.

Lattimore, O. (1940): *Inner Asian Frontiers of China*, New York: American Geographical Society.

Levine, D. K. and S. Modica (2013): "Conflict, Evolution, Hegemony and the Power of the State," NBER Working Papers 19221, National Bureau of Economic Research.

Liberman, P. (1998): *Does Conquest Pay?: The Exploitation of Occupied Industrial Societies*, Princeton, NJ: Princeton University Press.

Lieberman, V. (2003): *Strange Parallels: Southeast Asia in Global Context, C. 800–1830. vol. 1: Integration on the Mainland*, Cambridge: Cambridge University Press.

——— (2009): *Strange Parallels: Southeast Asia in Global Context, C. 800–1830. Vol. 2, Mainland Mirrors: Europe, Japan, China, South Asia, and the Islands*, Cambridge: Cambridge University Press.

Lin, J. Y. (1995): "The Needham Puzzle: Why the Industrial Revolution Did Not Originate in China," *Economic Development and Cultural Change*, 43, 269–92.

Mackinder, J. H. (1942): "The Geographical Pivot of History," in *Democratic Ideals and Reality*, New York: H. Holt and Company.

Mayshar, J., O. Moav, and Z. Neeman (2017): "Geography, Transparency and Institutions," *American Political Science Review*, 111, 622–636.

Mayshar, J., O. Moav, and L. Pascali (2022): "The Origin of the State: Land Productivity or Appropriability?" *Journal of Political Economy*, forthcoming.

McLaughlin, R. (2010): *Rome and the Distant East: Trade Routes to the Ancient lands of Arabia, India and China*, London: Continuum.

McNeil, W. H. (1974): *Plagues and Peoples*, Oxford: Basil Blackwell.

McNeill, W. H. (2021): "The Steppe," in *Encyclopedia Britannica*, Encyclopædia Britannica, Inc.

Mearsheimer, J. J. (2001): *The Tragedy of Great Power Politics*, New York: W. W. Norton & Company.

Michalopoulos, S. (2012): "The Origins of Ethnolinguistic Diversity," *American Economic Review*, 102, 1508–39.

Mokyr, J. (2007): "The Market for Ideas and the Origins of Economic Growth in Eighteenth Century Europe," *Tijdshrift voor Sociale en Economische Geschidenis*, 4, 3–38.

——— (2016): *A Culture of Growth: The Origins of the Modern Economy*, Princeton, NJ: Princeton University Press.

Montesquieu, C. (1989): *The Spirit of the Laws*, Cambridge: Cambridge University Press, translated by Anne M. Cohler, Basia C. Miller, and Harold S. Stone.

Morgenthau, H. (1948): *Politics Among Nations: The Struggle for Power and Peace*, New York: Knopf.

Nath, P. (2019): *Climate of Conquest: War, Environment, and Empire in Mughal North India*, Oxford University Press India.

Neparáczki, E., Z. Maróti, and T. Kalmár (2019): "Y-Chromosome Haplogroups from Hun, Avar and Conquering Hungarian Period Nomadic People of the Carpathian Basin," *Scientific Reports*, 9, 16569.

Norkus, Z. (2019): "The Economic Output Growth of Baltic Countries in 1913–1938: A Quantitative Cross-Country Comparison," *Journal of Baltic Studies*, 50, 183–203.

Nunn, N. and D. Puga (2012): "Ruggedness: The Blessing of Bad Geography in Africa," *Review of Economics and Statistics*, 94, 20–36.

Olsson, O. and G. Hansson (2011): "Country Size and the Rule of Law: Resuscitating Montesquieu," *European Economic Review*, 55, 613–629.

Overy, R. (2004): *The Times Complete History of the World*, London: Times Books, sixth Edition.

Padfield, P. (1979): *Tide of Empires: Decisive Naval Campaigns in the Rise of the West*,

London: Routledge & Kegan Paul.

Parker, G. (1988): *The Military Revolution: Military Innovation and the Rise of the West, 1500–1800*, Cambridge: Cambridge University Press.

——— (2013): *Global Crises: War, Climate Change and Castrastrophe in the Seventeenth Century*, New Haven: Yale University Press.

Pavlik, J. B. and A. T. Young (2019): "Did Technology Transfer More Rapidly East–West than North–South?" *European Economic Review*, 119, 216–235.

Perdue, P. C. (2005): *China Marches West: The Qing Conquest of Central Eurasia*, Belknap Press of Harvard University Press.

Phillips, C. and A. Axelrod (2005): *Encyclopedia of Wars*, Facts On File.

Pirenne, H. (1925): *Medieval Cities: Their Origins and the Revival of Trade*, Princeton, NJ: Princeton University Press, translated by Frank D. Halsey.

Poulson, S. R., S. C. Kuzminsky, G. R. Scott, V. G. Standen, B. Arriaza, I. Muñoz, and L. Dorio (2013): "Paleodiet in Northern Chile through the Holocene: Extremely Heavy $\delta^{15}N$ Values in Dental Calculus Suggest a Guano-Derived Signature?" *Journal of Archaeological Science*, 40, 4576–4585.

Pounds, N. J. G. and S. S. Ball (1964): "Core-Areas and the Development of the European States System," *Annals of the Association of American Geographers*, 54, 24–40.

Przemieniecki, J. (2000): *Mathematical Methods in Defense Analyses*, American Institute of Aeronautics & Astronautics, 3rd ed.

Ramankutty, N. and J. Foley (2014): "Estimating historical changes in land cover: North American croplands from 1850 to 1992," *Global Ecology and Biogeography*, 381–396.

Ramankutty, N., J. Foley, J. Norman, and K. McSweeney (2002): "The Global Distribution of Cultivable Lands: Current Patters and Sensitivity to Possible Climate Change," *Global Ecology and Biogeography*, 11, 377–392.

Rickman, G. E. (1980): "The Grain Trade under the Roman Empire," *Memoirs of the American Academy in Rome*, 36, 261–275.

Rodrigues, P. and J. Micael (2021): "The Importance of Guano Birds to the Inca Empire and the First Conservation Measures Implemented by Humans," *International Journal of Avian Science*, 283–291.

Roland, G. (2020): "The Deep Historical Roots of Modern Culture: A Comparative Perspective,"

Journal of Comparative Economics, 48, 483–508.

Root, H. L. (2017): "Network Assemblage of Regime Stability and Resilience: Comparing Europe and China," *Journal of Institutional Economics*, 13, 523–548.

——— (2020): *Network Origins of the Global Economy: East vs. West in a Complex Systems Perspective*, Cambridge: Cambridge University Press.

Rosenberg, N. and L. J. Birdzell (1986): *How the West Grew Rich: The Economic Transformation of the Industrial World*, New York: Basic Books.

Rosenzweig, P. H. and S. L. Volpe (1999): "Iron, Thermoregulation, and Metabolic Rate," *Critical Reviews in Food Science and Nutrition*, 39, 131–148.

Sachs, J. D. (2001): "Tropical Underdevelopment," NBER Working Papers 8119, National Bureau of Economic Research.

Sanford, C. A., P. S. Pottinger, and E. C. Jong (2017): *The Travel and Tropical Medicine Manual. Fifth edition.*, Malta: Elsevier.

Santana-Sagredo, F. (2021): "'White Gold' Guano Fertilizer Drove Agricultural Intensification in the Atacama Desert from AD 1000," *Nature Plants*, 7, 152.

Scheidel, W. (2019): *Escape from Rome*, Princeton, NJ: Princeton University Press.

Scott, J. C. (2017): *Against the Grain*, Princeton, NJ: Princeton University Press.

Sellmann, J. (2002): *Timing and Rulership in Master Lü's Spring and Autumn Annals*, Albany: State University of New York Press.

Sha, X. (1972): *Essays in Geography [dili xue lunwen ji]*, Taipei: Commerical Press.

Skinner, G. W. (1977): *The City in Late Imperial China*, Stanford: Stanford University Press.

Spolaore, E. and R. Wacziarg (2016): "War and Relatedness," *Review of Economics and Statistics*, 98, 925–939.

Staller, J., R. Tykot, and B. Benz (2006): *Histories of Maize: Multidisciplinary Approaches to the Prehistory, Linguistics, Biogeography, Domestication, and Evolution of Maize*, Academic Press.

Surgeon General (2008): *JSP 539 Climatic Injuries in the Armed Forces: Prevention and Treatment, Amendment No 1*, Ministry of Defence, United Kingdom.

Talhelm, T., X. Zhang, S. Oishi, C. Shimin, D. Duan, X. Lan, and S. Kitayama (2014): "Large-Scale Psychological Differences Within China Explained by Rice Versus Wheat Agriculture," *Science*, 344, 603–608.

Tilly, C. (1990): *Coercion, Capital, and European States, AD 990–1990*, Oxford: Basil Blackwell.

Turchin, P. (2009): "A Theory for Formation of Large Empires," *Journal of Global History*, 4, 191–217.

Turchin, P., J. Adams, and T. Hall (2006): "East-West Orientation of Historical Empires and Modern States," *Journal of World-Systems Research*, 12, 219–229.

Turchin, P., T. E. Currie, E. A. L. Turner, and S. Gavrilets (2013): "War, Space, and the Evolution of Old World Complex Societies," *Proceedings of the National Academy of Sciences*, 110, 16384–16389.

Twitchett, D. and J. Fairbank, eds. (1986): *Cambridge History of China. Vol. 1: The Ch'in and Han Empires, 221 B.C.–A.D. 220*, Cambridge: Cambridge University Press.

Usher, D. (1989): "The Dynastic Cycle and the Stationary State," *American Economic Review*, 79, 1031–1044.

Voigtländer, N. and H.-J. Voth (2013a): "Gifts of Mars: Warfare and Europe's Early Rise to Riches," *Journal of Economic Perspectives*, 27, 165–186.

——— (2013b): "The Three Horsemen of Riches: Plague, War, and Urbanization in Early Modern Europe," *Review of Economic Studies*, 80, 774–811.

Waltz, K. N. (1979): *Theory of International Politics*, Long Grove, IL: Waveland Press In.

Weber, M. (1972): *Politics as a Vocation*, Philadelphia: Fortress Press.

Weil, D. (2014): "The Impact of Malaria on African Development over the Longue Durée," in *Africa's Development in Historical Perspective*, ed. by E. Akyeampong, J. Robinson, N. Nunn, and R. H. Bates, Cambridge: Cambridge University Press, 89–124.

Weiss, H. K. (1966): "Combat Models and Historical Data: The U.S. Civil War," *Operations Research*, 14, 759–790.

Whittlesey, D. (1944): *The Earth and the State: A Study of Political Geography*, New York: Henry Holt and Company.

Woodward, J. B. (2021): "History of Ships," in *Encyclopedia Britannica*, Encyclopædia Britannica, Inc.

Zhang, D. D., C. Jim, G. Lin, Y.-Q. He, J. J. Wang, and H. F. Lee (2006): "Climatic Change, Wars and Dynastic Cycles in China Over the Last Millennium," *Climatic Change*, 76, 459–477.

Online Appendices for "The Fractured-Land Hypothesis"

We now include a series of appendices with extra information regarding our main paper, "The Fractured-Land Hypothesis."

A Additional Information on Data

This appendix provides more details on the datasets listed in Table 2 that we use to construct our baseline specification and robustness checks.

Table 2: Data Sources

	Variable	Data	Source	Specification
1	Productivity (y)	Global Agro-Ecological Zoning (GAEZ) v4	FAO & IIASA (gaez.fao.org)	Baseline
2	Productivity (y)	Cropland Suitability Index	Ramankutty et al. (2002)	Alternative
3	Productivity (y)	History Database of the Global Environment (HYDE 3.1)	Goldewijk et al. (2017)	Alternative
4	Early development (r)	Digital Soil Map of the World (DSMW)	FAO (fao.org)	Baseline
5	Early development (r)	Harmonized World Soil Database (HWSD) v1.2	FAO (fao.org)	Alternative
6	Early development (r)	KK10 scenario of Anthropogenic Land Cover Change	Kaplan and Krumhardt (2011)	Alternative
7	Temperature (x_{hot}, x_{cold})	WorldClim 1.4 Paleoclimate for the Mid-Holocene	WorldClim (worldclim.org)	Baseline
8	Temperature (x_{hot}, x_{cold})	WorldClim 1.4 Climate Data (1960s)	WorldClim (worldclim.org)	Alternative
9	Ruggedness (x_{rugged})	90m SRTM digital elevation data	CGIAR-CSI (srtm.csi.cgiar.org)	All

A.1 Historical Resource Availability, y

Our primary source of historical resource availability is the Food and Agriculture Organization's Global Agro-Ecological Zones database version 4, or GAEZ v4 in short (Table 2, Row 1).[32] In that way, we follow a growing literature that has used the GAEZ dataset (in its different vintages) to investigate the historical origins of development. See, among others, Alesina et al. (2013), Galor and Özak (2016), and Mayshar et al. (2022). We employ the most recent vintage of GAEZ v4, released in 2021. Compared with previous versions, this vintage is based on higher-resolution data and improved methods (Fischer et al., 2021).

The database divides the world's land surface into grid-cells of size 5' latitude/longitude (approximately 75 km^2). The dataset reports the potential annual yields (in weight per unit of

[32] See https://gaez.fao.org/ for a complete description of the dataset.

area) of 53 crops for each grid-cell. Among these crops, we focus on cereal grains, which are appropriable and, hence, central to the rise of tax-levying states (Mayshar et al., 2017, 2022).

We follow Galor and Özak (2016) and (1) identify the major cereal grains that existed on every continent before the Columbian Exchange, (2) compute the GAEZ v4 yield of each of these crops for every cell of the continent, (3) convert the yields into calories using the National Nutrient Database for Standard Reference published by the U.S. Department of Agriculture, and (4) identify the highest calorie-yielding cereal for every cell and use it to determine the attainable caloric yield of the cell. Figure 5 shows the results of this exercise. Table 3 provides a complete list of the cereal grains in our dataset, their pre-Columbian distribution by continent, and their caloric contents.

Table 3: Cereal Grains: Pre-Columbian Availability and Caloric Content

Cereal Grain	Pre-Columbian Availability	Calorie ('000 per gram)
Barley	Asia, Europe, North Africa	3.52
Buckwheat	Asia	3.43
Foxtail Millet	Asia, Europe, North Africa	3.78
Indigo Rice	Asia, Sub-Saharan Africa	3.70
Maize	The Americas	3.65
Oat	Europe, North Africa	2.46
Pearl Millet	Asia, Africa	3.78
Sorghum	Asia, Africa	3.39
Rye	Europe	3.38
Rice (Wetland)	Asia, Sub-Saharan Africa	3.70
Wheat	Asia, Europe, North Africa	3.42

Source: Galor and Özak (2016) and USDA National Nutrient Database for Standard Reference.

GAEZ v4 data provide potential yields of different crops based on (1) two alternative assumptions of water supply (rain-fed and irrigation), (2) three different levels of input/management (low, medium, high), and (3) three 30-year historical reference periods (1961–1990, 1971–2000, and 1981–2010). On top of these, the dataset provides two different measures of crop yield: agro-climatic potential yield and agro-ecological attainable yield. Agro-climatic potential yield considers climatic factors such as temperature, precipitation, sunshine duration, wind speed, and humidity but does not account for soil and terrain conditions. Agro-ecological attainable yield considers all of these conditions.

We employ the hypothetical yield based on rain-fed, low-input agriculture to mitigate

concerns about the endogeneity of potential yields. We consider 1961–1990, the earliest period available, to minimize the impact of modern technology on our estimates. Finally, we choose agro-ecological attainable yield over agro-climatic potential yield because the latter's omission of soil and terrain considerations introduces a large systematic bias into its estimates.

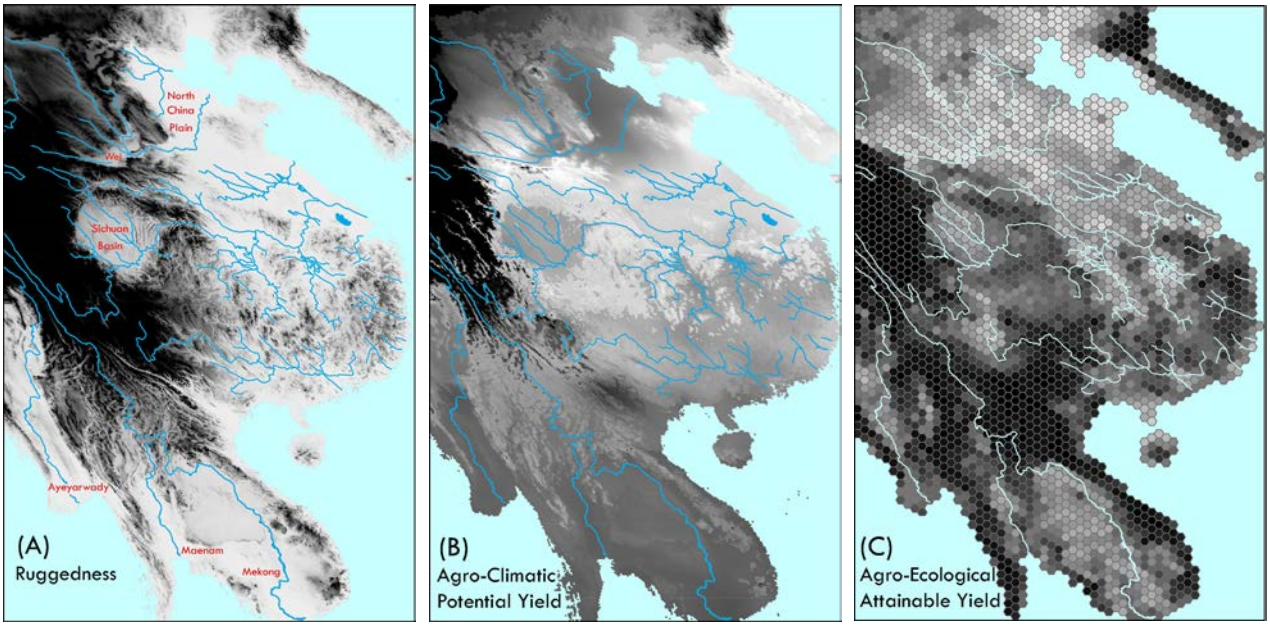

Figure 20: In Panel A, a darker shade implies a higher elevation. Panels B and C display the GAEZ v4 agro-climatic potential yield and agro-ecological attainable yield, respectively (darker implies lower productivity).

Figure 20 illustrates the bias. Panel A plots the terrain of East Asia, with a lighter shade representing lower ruggedness. Panel B depicts the agro-climatic potential yield (in calories), with a lighter shade representing higher productivity. Comparing the two panels shows that low-lying and flat areas in China are often less productive than more rugged areas. For instance, in Panel B, the Sichuan basin, historically referred to as "a land of plenty" (*tianfu zhiguo*) by the Chinese, is relatively barren compared to the mountains that enclose it. Likewise, the Wei River valley, which formed the power base of the Qin dynasty, and the North China plain, have lower agro-climatic potential yields than their more rugged surroundings. The problem is not limited to China. In Indochina, too, the plains of the Ayeyarwady (Myanmar), Maenam (Thailand), and Mekong (Vietnam, Laos, Cambodia) rivers have lower agro-climatic potential yields than their upstream hinterlands. These perverse patterns are likely driven by the monsoon in East Asia and the fact that mountainous areas generally experience higher rainfall during the summer monsoon season. Hence, we discard the agro-climatic potential yield in favor of the

agro-ecological attainable yield. Panel C shows that the agro-ecological attainable yield is lower in hilly areas than in the plains they envelop.

Using GAEZ v4 for historical research is not without problems since it is built by the FAO to improve land utilization and food security in today's world. It estimates productivities based on present-day (given our choices, 1961–1990) climatic, soil, and terrain conditions. While GAEZ v4 broadly provides an objective measure of historical resource availability, it may underestimate the productive advantage historically enjoyed by regions that developed early but subsequently suffered environmental degradation due to the overexploitation of resources. A glance at Figure 5 suggests that Mesopotamia and the Nile, Indus, and Wei River Valleys do not enjoy a significant productivity advantage over their neighbors, which contradicts the historical narratives built around other sources of information (archeological, documentary, etc.). For example, in the case of the Wei River, the largest tributary of the Yellow River, deforestation due to human exploitation contracted its network of tributaries, which became shallower or even dried up entirely over time (Mostern, 2016).

We could tackle this problem by modifying the GAEZ v4 estimates by incorporating additional insights. We do not follow that route because the possible underestimation of historical resource availability in China and other non-European regions that witnessed an early development of states biases our quantitative results against our main finding of faster political consolidation in China than in Europe. Correcting the potential bias would only strengthen the result.

Nonetheless, to ensure that our results are not overly dependent on GAEZ v4 data, we use two alternative measures of historical resource availability (Rows 2–3 of Table 2). First, we use the Cropland Suitability Index by Ramankutty et al. (2002), which measures the fraction of land suitable for agriculture. Like GAEZ v4, the Cropland Suitability Index gauges present-day agricultural conditions. We prefer GAEZ v4 over the Cropland Suitability Index because, among other things, the latter is coarser with a resolution of 5-minute by 5-minute latitude-longitude (as opposed to GAEZ v4's 30 arc-seconds by 30 arc-seconds resolution).

Second, in Appendix C.2, we construct an alternative y variable using the estimated population density in 0 CE in the History Database of the Global Environment (HYDE) version 3.1 (Goldewijk et al., 2017).[33] This measure is motivated by a simple Malthusian logic: before the Industrial Revolution, population density was directly linked to land productivity

[33]See https://www.pbl.nl/en/image/links/hyde.

and its ability to support dense populations (Ashraf and Galor, 2011). Unlike GAEZ v4 and the Cropland Suitability Index, HYDE is constructed as a historical dataset. However, its methodology, including the data employed to conduct hindcasting, has received substantial criticism from Guinnane (2021) and others, and, therefore, we do not use it as our baseline.

Nonetheless, as described in the main text (Panel A of Figure 11) and Appendix C (Panel C of Figure 23), our results are highly robust to switching from GAEZ v4 to the two alternative datasets. Besides these two exercises, we have replicated all our simulations (baseline, preferred, and checks) using these two alternative measures of y, and still find high consistency with our findings based on GAEZ v4. These additional results are available upon request.

A.2 Initial Level of Development, r

In our baseline specification, we use the percentage of land covered by alluvium as a proxy for early development advantage in 1000 BCE, r (Row 4 of Table 2). This choice is based on archaeological observations that wetlands played a central role in early sedentism (Pournelle, 2003; Hritz and Pournelle, 2015). The sedentary communities of Lower Mesopotamia, Jericho on the West Bank, Harrapan and Haripunjaya of India, Hemudu and Erlitou of China, Teotihuacan of Mexico, and Lake Titicaci of Peru were all wetland-based (Scott, 2017). It was also in alluvium-rich regions, including Mesopotamia (Tigris River), Egypt (Nile), the Indus Valley (Indus), and North China (Yellow River), that the world's first statelets emerged. As Scott (2017, p. 50) describes, the ecology of wetlands gave alluvium-rich areas an early advantage in agriculture and hence in the growth of complex societies.

In our baseline model, the productivity of cell i at $t = 0$ is $y_0 = r \cdot y_{GAEZ}$, where y_{GAEZ} is the highest attainable caloric yield from the pre-Columbian cereals derived from GAEZ v4. It then grows linearly at an increment of $\frac{y_{GAEZ} - r \cdot y_{GAEZ}}{500}$ per period between $t = 0$ and $t = 500$, so that $y_{500} = y_{GAEZ}$. Our baseline alluvial soil cover estimates are derived from the FAO Digital Soil Map of the World (DSMW). Following the approach adopted in GAEZ v4, we use the soil types of Fluvisols and Gleysols to represent alluvium.[34]

As a robustness check on the DSMW dataset, we use the FAO's Harmonized World Soil Database (HWSD) version 1.2 to compute the percentage of land covered by alluvial soils (Row

[34] As Fischer et al. (2021) spell out, "Fluvisols are by definition flooded by rivers," while "the soil profiles [of Gleysols] indicate regular occurrence of high groundwater tables through reduction (gley) features" (p. 116).

5 in Table 2). The HWSD has the advantage of being relatively new and more detailed than the DSMW. However, the HWSD is a harmonized dataset based on several data sources compiled by various agencies (FAO, the European Soil Bureau Network, the Chinese Academy of Sciences, etc.). We keep the DSMW as our baseline dataset to mitigate the potential heterogeneity left in the HWSD even after harmonization. However, we use the HWSD as a robustness check in Appendix C.2 (Figure 23). A comprehensive set of results using the HWSD in place of the DSMW to generate the baseline and preferred specifications as well as robustness checks in Figures 8–13 is available upon request.

Furthermore, to ensure that our results are not overly dependent on the use of alluvium share as a proxy for early development, we use the KK10 scenario of Anthropogenic Land Cover Change estimates from Kaplan and Krumhardt (2011) to generate another two alternative r variables as robustness checks (Row 6 of Table 2). The KK10 dataset has a spatial resolution of 5 arc-minutes or about 9 km. at the equator. It reconstructs estimates for anthropogenic land use from 8000 BP to 1850. The dataset has the advantage of not overly relying on one single factor (e.g., alluvium) to measure early development. In addition, when reconstructing the estimates, it assumes a negative relationship between land use per capita and population density, which is arguably an improvement over the assumption of constant land use per capita (as used in HYDE 3.1) in light of Boserup (1965).

However, like HYDE 3.1, the estimates in KK10 are reconstructed based on the hindcasting method, with its associated problems. Furthermore, using KK10 as our r measure is likely to underestimate the early development advantage of China vs. Europe for two reasons. First, its anthropogenic land-use estimates do not make a distinction between pasture and intensive agriculture. Hence, some areas outside the "cradles of civilization" (for example, parts of northwestern Europe) show an above-average fraction of land use, possibly due to the presence of pastoral activities. Since, unlike cropping, pastoral activities are not known to induce state formation, this bias would favor a false early emergence of large states in western Europe (although we do not see this phenomenon in our simulations). Second, as explained in Kaplan et al. (2011, pp. 777–8), to avoid overestimating human-induced land-use in tropical regions in prehistoric times, the KK10 dataset rescaled human-induced land-use estimates outside Europe downward. Despite these concerns, we continue to observe faster political consolidation in China than in Europe when using the KK10 human-induced land-use estimates as a proxy for early

development in Section 5.3 (Figure 11) and Appendix C.2 (Figure 23).

A.3 Temperature

Our baseline temperature variables are based on WorldClim 1.4 downscaled paleoclimate data for the Mid-Holocene, about 6000 years ago (Row 7 Table 2).[35] The dataset has a spatial resolution of 30 arc-seconds (about 900 m. at the equator). Like other climatic datasets investigating the past, the WorldClim Mid-Holocene is generated via simulations with a Global Climate Model (GCM). Given that the GCM processes are complex and every simulation is different (since weather is partially stochastic), we use the WorldClim 1.4 climate data for the 1960s to construct an alternative set of temperature variables for robustness checks (Row 8 of Table 2).

A.4 Ruggedness

Our ruggedness variable draws from the CGIAR-CSI GeoPortal's SRTM (Shuttle Radar Topography Mission) 90m Digital Elevation Dataset, which is based on data produced by NASA (Row 9 of Table 2). The NASA dataset covered slightly more than 80% of the globe. The CGIAR-CSI GeoPortal dataset, widely used in the GIS community, applies interpolation methods to fill the data voids. Reuter et al. (2007) detail the interpolation methods employed. The CGIAR-CSI dataset is organized into grid-cells of 5' x 5' and has a spatial resolution of about 90 m. at the equator.

B Summary of Specifications: Baseline and Alternatives

Table 4 summarizes all the specifications reported by Figures 8–12 in Section 5. The table shows that China and Europe are comparable in resource availability and fracturedness in our baseline and the various alternative specifications. If anything, China is slightly disadvantaged in both dimensions in most of the specifications. This observation highlights that it is not aggregate resource availability and fracturedness, but their geographical distributions, that drive China to unify relatively quickly while Europe develops into a polycentric system.

[35] See https://www.worldclim.org/data/v1.4/worldclim14.html and Hijmans et al. (2005) for details.

Panel A	Baseline Fig. 8, 9 (1)	No Climatic Obstacles Fig. 10A (2)	No Obstacles Fig. 10B (3)	Uniform Resource Fig. 10C (4)
y_0	(Soil)×(GAEZ)	(Soil)×(GAEZ)	(Soil)×(GAEZ)	0.5
y_{500}	(GAEZ)	(GAEZ)	(GAEZ)	0.5
α_{sea}	0.1	0.1	1	0.1
σ	0.333	0.333	1	0.333
$\theta_{rugged} \cdot x_{rugged}$ (90th pctl)	2	2	0	2
θ_{cold}	2	0	0	2
θ_{hot}	2	0	0	2
Resource (median y)				
–China$_{t=0}$	0.01	0.01	0.01	0.50
–China$_{t=500}$	0.53	0.53	0.53	0.50
–Europe$_{t=0}$	0.00	0.00	0.00	0.50
–Europe$_{t=500}$	0.60	0.60	0.60	0.50
Fracturedness (median $\Theta\mathbf{x}$)				
–China	1.41	0.95	0.00	1.41
–Europe	1.37	0.56	0.00	1.37

Panel B	No Obstacles + Uniform Resource Fig. 10D (5)	Alt. Y (CSI) Fig. 11A (6)	Alt. Initial Conditions Fig. 11B (7)	Alt. Conflict Mechanisms Fig. 12A, 12B (8)
y_0	0.5	(Soil)×(CSI)	(KK10)×(GAEZ)	(Soil)×(GAEZ)
y_{500}	0.5	(CSI)	(GAEZ)	(GAEZ)
α_{sea}	1	0.1	0.1	0.1
σ	1	0.333	0.333	0.333
$\theta_{rugged} \cdot x_{rugged}$ (90th pctl)	0	2	2	2
θ_{cold}	0	2	2	2
θ_{hot}	0	2	2	2
Resource (median y)				
–China$_{t=0}$	0.50	0.02	0.11	0.01
–China$_{t=500}$	0.50	0.72	0.53	0.53
–Europe$_{t=0}$	0.50	0.00	0.15	0.00
–Europe$_{t=500}$	0.50	0.66	0.60	0.60
Fracturedness (median $\Theta\mathbf{x}$)				
–China	0.00	1.41	1.41	1.41
–Europe	0.00	1.37	1.37	1.37

Table 4: Summary of specifications in Figures 8–12.

C Additional Robustness Tests

This appendix includes additional robustness tests on several parameter values and checks the effects of using alternative datasets and modifying the random contest function.

C.1 Parameters Θ and β

First, we vary the values of the parameter vector Θ, which measures the influence of the geographical and climatic characteristics on war outcomes. In the baseline, we set $\theta_{rugged} \cdot x^*_{rugged} = \theta_{hot} \cdot x^*_{hot} = \theta_{cold} \cdot x^*_{cold} = \theta = 2$, where x^*_{rugged}, x^*_{hot}, and x^*_{cold} represent

the 90th-percentile values of x_{rugged}, x_{hot}, and x_{cold} respectively. To explore a wide range of alternatives, we set θ to each integer between 0 and 8. For each integer value, we repeat the simulation 30 times, with which we create 10,000 bootstrap samples.

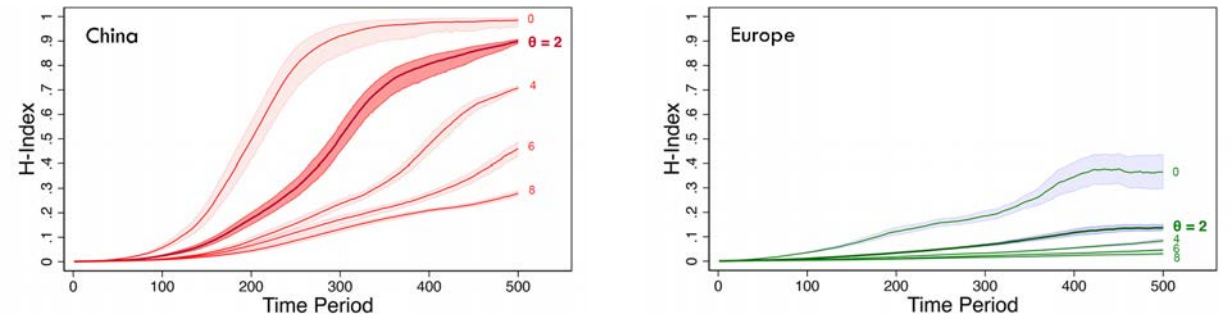

Figure 21: Varying θ between 0 and 8. For each value, we conduct the simulation exercise 30 times and display the average Herfindahl (unification) indices for China (left panel) and Europe (right panel). The shaded intervals depict the 0.95 bootstrap confidence interval.

Figure 21 reports the mean and the 95% confidence interval of Herfindahl (unification) indices for China (left panel) and Europe (right panel). When $\theta = 0$, geographical and climatic obstacles do not influence war outcomes. As θ increases, the likelihood of war ending with no victor or conquest increases as the influence of geoclimatic factors strengthens. While the Herfindahl indices of China and Europe decrease with θ, for all values of θ, China displays a stronger tendency toward political unification.

Second, we vary the value of the secession parameter β. In our baseline calibration, we set $\beta = 1 \times 10^{-5}$, a low value, to avoid biasing our results against Europe, which is more likely to produce states that are noncompact in shape due to its long coastline, or against the North European Plain, which has a funnel shape with a western portion that is long and relatively narrow. Figure 22 reports the results when we multiply β by 10, 5 , $\frac{1}{5}$, and $\frac{1}{10}$, respectively. For each value of β, we repeat the simulation 30 times, create 10,000 bootstrap samples, and compute the mean and the 95% confidence interval of Herfindahl indices for China and Europe.

When β is 10 times its baseline value, political consolidation in Europe is extremely sluggish. In this case, a polity that comprises the cells of Europe would have to annex territories at a rate of 900 cells (approximately 1 Iran or 20 Austrias) every 50 periods to prevent itself from shrinking. While China experiences slower political consolidation too, it continues to consolidate steadily and is able to achieve a high degree of unification at period 500. At lower values of β, unification continues to take place faster in China than in Europe.

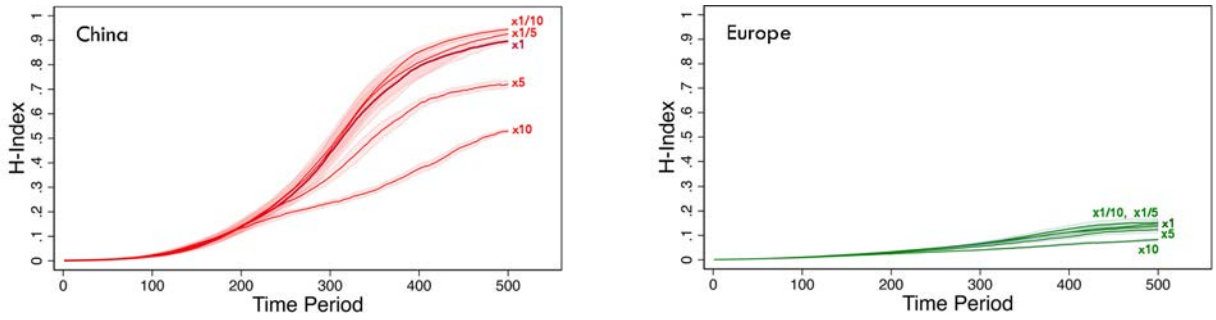

Figure 22: Varying β between 0.1 and 10 times its calibrated value. For each value, we conduct the simulation exercise 30 times and display the average Herfindahl (unification) indices for China (left panel) and Europe (right panel). The shaded intervals depict the 0.95 bootstrap confidence interval.

C.2 Alternative Datasets

Section 5.3 conducts two robustness tests using alternative datasets. First, we replace GAEZ v4 with Ramankutty et al. (2002)'s Cropland Suitability Index as our measure of historical resource availability. Second, we use Kaplan and Krumhardt (2011)'s KK10 Anthropogenic Land Cover Change data on 1000 BCE in lieu of alluvial soil cover as a proxy for early developmental advantage.

Figure 23 reports the results from conducting four more robustness checks with our datasets. In Panel A, we still rely on Kaplan and Krumhardt (2011)'s KK10 Anthropogenic Land Cover Change data to measure early developmental advantage (r). But now, we use the 0 CE instead of the 1000 BCE estimates. The purpose of doing so is two-fold: first, it is plausible that the 1000 BCE estimates may be noisier due to a relative dearth of evidence. Second, we would like to check if giving Europe a larger early developmental advantage (considering that the Mediterranean region was relatively developed in 0 CE) affects our findings. While we see a slight increase in the pace of political consideration in Europe, the same is also observed in China, which could be explained by a relatively developed North China in 0 CE. Thus, our findings remain intact.

Panel B uses the alluvial soil cover data of FAO Harmonized World Soil Database (HWSD) version 1.2 to measure early developmental advantage. Compared to the DSMW database used for our baseline, the HWSD is a harmonized dataset based on several data sources compiled by various agencies (FAO, the European Soil Bureau Network, the Chinese Academy of Sciences, etc.). Panel B shows that using the HWSD dataset has little noticeable effect on our results. We keep the DSMW as our baseline dataset to mitigate the potential heterogeneity left in the

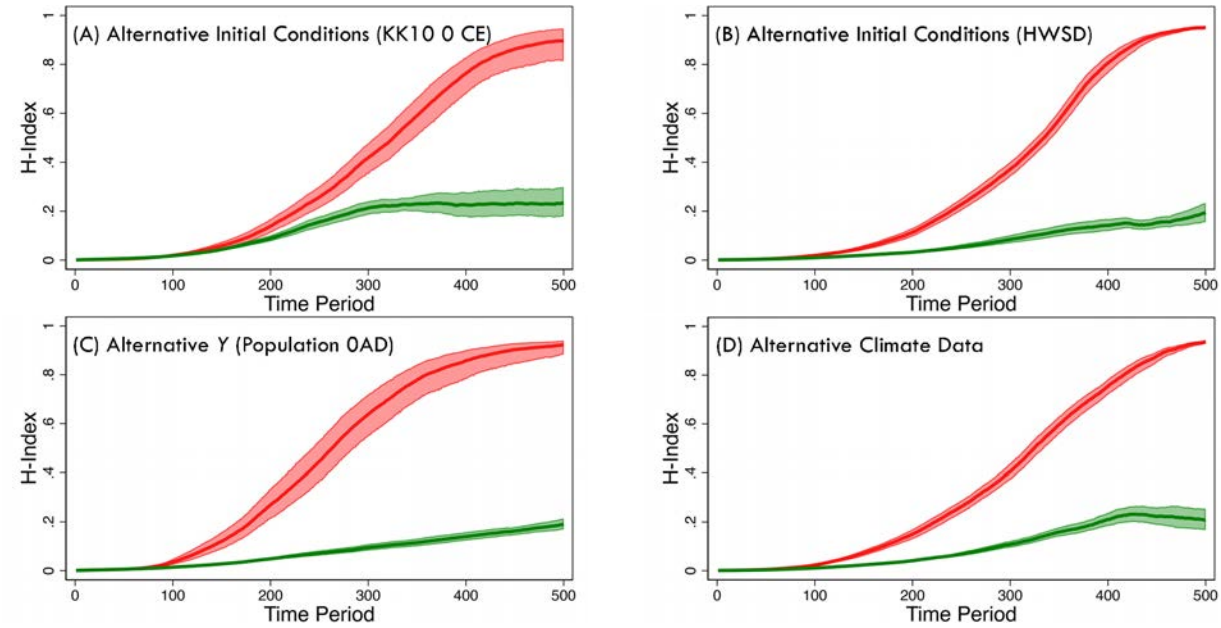

Figure 23: Data robustness checks. Panels A and B employ alternative datasets to capture initial conditions (r); Panel C uses an alternative measure for historical resource availability (y); Panel D uses an alternative data source to compute the temperature variables (x_{hot}, x_{cold}). For each specification, we conduct the simulation exercise 30 times and display the average Herfindahl (unification) indices for China (red) and Europe (green). The shaded intervals depict the 0.95 bootstrap confidence interval.

HWSD even after harmonization.

Panel C replaces GAEZ v4 with the population estimates in 0 CE of the History Database of the Global Environment (HYDE) version 3.1 as our measure of historical resource availability (y). We continue to observe faster political consolidation in China. For completeness, we also conduct robustness checks using the 1000 BCE, 500, and 1000 estimates from HYDE and obtain qualitatively similar results (available upon request).

Panel D uses the WorldClim 1.4 climate data for the 1960s to construct an alternative set of temperature variables instead of the WorldClim 1.4 downscaled paleoclimate data. Again, the results are similar to those in the baseline specification.

C.3 Alternative Conflict Mechanisms

In Section 5.3 of the main paper, we check whether modifying how wars take place in our model could affect our findings. In this subsection, we implement two more robustness checks on the conflict mechanisms. Both checks aim to investigate the effects of explicitly incorporating transport costs into our model.

In our baseline simulation, when a large polity that controls many cells engages a small polity in war, the former has a higher probability of winning according to the contest function given by equation (1). However, if the cells controlled by the large polity are extremely rugged, this might constrain the polity's ability to mobilize resources and lower its chances of winning. This concern is mitigated by the fact that productivity and ruggedness are highly correlated in the dataset. Hence, to keep the model conceptually and computationally simple, we do not factor in transport costs explicitly.

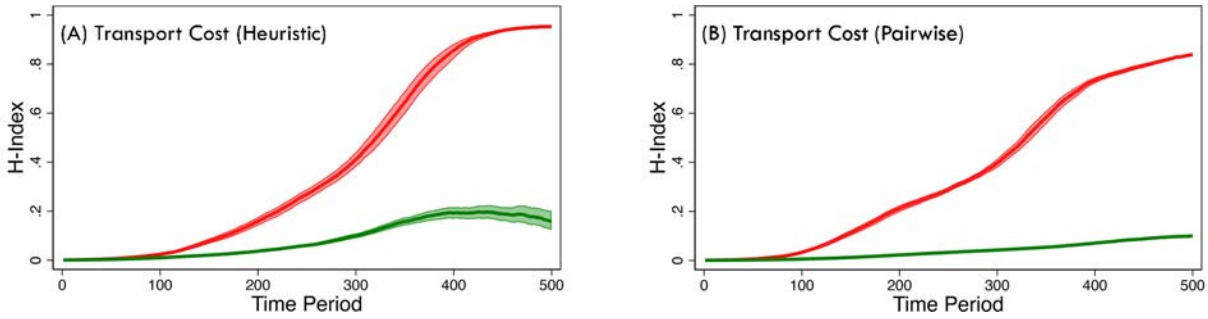

Figure 24: Varying the contest function. For each specification, we conduct the simulation exercise 30 times and display the average Herfindahl (unification) indices for China (red) and Europe (green). The shaded intervals depict the 0.95 bootstrap confidence interval.

However, as a heuristic check, in Panel A of Figure 24, we discount the productivity of every cell by its ruggedness when computing the aggregate productivity (Y) of a polity that enters into equation (1). The exercise in Panel B goes a step further. For any two cells in the world represented in Figure 2, we compute the least-cost route (or route of lowest ruggedness) between them. Now, if polity i fights a war in cell k, the aggregate resources that it devotes to the war (Y_i) are the sum of the productivity of every cell that polity i controls discounted by the ruggedness of the least-cost route between the cell and k. For both extensions, we continue to observe a faster pace of political consolidation in China than in Europe. The second extension, in particular, adds realism to the model at the cost of making it computationally cumbersome. This said, the results are reassuring.

D Enriching the Model

We now include additional details about the several extensions of our baseline model that we described in Sections 5 and 8 of the main text.

D.1 Major Rivers and Loess Soil

A river fosters the interdependence of its upstream and downstream areas. In particular, China was a riverine civilization that depended upon its rivers to serve as its primary means of transportation until the early 20th century (Skinner, 1977). This natural water system was complemented by the Great Canal, built in the Sui dynasty (581–618), which connected the Yangtze and Yellow rivers. However, a wide river also impedes movement between its two banks, especially during times of war. In some episodes of Chinese history, regimes in southern China successfully built defense lines along the Huai and Yangtze rivers to deter invasions from the north for prolonged periods (Sng et al., 2018).

To capture the dual roles of rivers, we identify the world's groundwater resources using the BGR-UNESCO "Major River and Lake Basins of the World" dataset. We set the obstacle value $\Theta \cdot x$ to zero when cells along the same river come into contact and increase the obstacle value $\Theta \cdot x$ by two when a riverine cell comes into conflict with a non-riverine cell. We simulate this extension 30 times to create 10,000 bootstrap samples. Panel A of Figure 13 shows the new results, which are roughly the same as in the baseline specification, with only a slightly slower unification of China.

Historians have also observed that regular flooding along the Yellow River gave North China a head start in state development because flood management problems increased tensions between upstream and downstream states along the Yellow River and accelerated the emergence of a unified regime through intense warfare (Huang, 1988). Our model does not consider this factor, but doing so would likely increase the pace of unification in China further.

However, the flood-prone Yellow River might have contributed to early state formation in China in another way: its floods replenished the soil and allowed agriculture to develop early and remain sustainable even with limited farming knowledge (Ho, 1975). Notably, the Chinese loess plateau, one of the world's largest loess regions with a land area larger than Germany, was looped by the Yellow River along the river's middle reaches. Loess, a fine-grained, windblown sediment, is stoneless and, hence, easy to work on even with primitive tools. Its well-aerated nature further makes it excellent for cereal cultivation (Catt, 2001). In the Guanzhong basin, adjacent to and overlapping with the loess plateau, the combination of an abundance of loess and alluvial soils and easy access to water from the Yellow River and its tributaries made it an

extremely productive agricultural zone in ancient China. It was from Guanzhong, centered on the city of Xi'an, where the Qin dynasty extended its power to complete the first unification of China in the 3rd century BCE.

Panel B of Figure 13 incorporates the hypothesis postulated in Scott (2017) that loess and alluvium were the only soils capable of sustaining a dense concentration of grain cultivation in early history by computing, for every hexagon in the world, the fraction of area covered by deep loess deposits (greater than 100 meters) and adding it to r, the parameter that measures early development (recall that in the baseline, r measures the fraction of area covered by alluvial soil). The exercise generates faster unification in China, but our main findings remain unchanged.

D.2 The Eurasian Steppe

We incorporate the Eurasian steppe into our model in two separate exercises, reported by Panels C and D of Figure 13.

The first exercise deals with the historical roles of the Eurasian steppe as (i) a conduit between Asia and Europe; and (ii) a source of military threats to sedentary societies in Eurasia. Scholars have observed that the steppe exerted a profound influence on Eurasian history (Lattimore, 1940, 1947; Barfield, 1989; Di Cosmo, 1994). With a string of oasis towns connecting the belt of grassland stretching from Hungary through Central Asia to Manchuria, the steppe served as a "highway of grass" that facilitated the movement of people, goods, technology, and disease across Eurasia (Frachetti, 2008, p. 7).

Also key was the influence of the steppe in intensifying Eurasian (and North African) warfare. For instance, Turchin et al. (2013) argue that the steppe shapes agrarian societies in two ways: (i) through the destruction of less powerful polities; and (2) through the diffusion of military technologies that make conflict more destructive (such as chariots, horse archers, and stirrups). These technologies hinged on the availability and quality of horses. In premodern times, horses were an invaluable military asset, a powerful war machine likened to modern tanks (Ropa and Dawson, 2020). Control of horses allowed some states to develop highly mobile cavalry forces that could easily outflank infantry units and charge down routed opponents.

Importantly, horses were a location-specific resource. Equine domestication began in the Eurasian steppe and steppe horses were especially stocky and vigorous (Zheng, 1984). Moreover,

only an extensive expanse of grassland could support a high density of horses and correspondingly a high concentration of skills in breeding and riding them. Thus, states near the Eurasian steppe fielded larger and better cavalry forces, giving them an advantage in war (Barfield, 1989; Gat, 2006; Turchin et al., 2013).

Scholars have also shown that climate played a crucial role in the conflicts between the steppe nomads and their agricultural neighbors (Bai and Kung, 2011). A cold and arid climate often triggered steppe invasions and drove waves of steppe peoples west into eastern Europe and south into the Middle East, India, or China. The ecological conditions in the steppe east of the Altai Mountains, where temperature swings were greater than anywhere else, were especially fragile and prone to fluctuations (McNeill, 2021).

Thus, traditional scholarship links the Huns, whose migration into Eastern Europe precipitated the movement of barbarian peoples that eventually destroyed the Western Roman Empire, to the Xiongnu, a nomadic confederation that dominated the eastern steppe during the Han dynasty of China (Gibbon, 2003; Neparáczki et al., 2019). Other scholars find a continuity between the Avars who assaulted the Byzantine Empire in the 6–8th centuries and the Rourans in the eastern steppe (Róna-Tas and Berta, 2011). Indeed, recent research on the genetic origins of the Avars suggests they were of East Asian origins (Csáky et al., 2020). The movement of the Avars westward might have resulted from the formation of Turkic tribal confederacies in the Eastern steppe. These Turkic peoples also pushed west over time (notably the Göktürks and the Bulgars), invading central Asia, Anatolia, and the Iranian plateau in the 10th–11th centuries. It is notable too that the Mongols, whom we discuss below and who briefly created the largest land empire ever witnessed in history, came from the eastern steppe.

Motivated by the previous discussion, Panel C of Figure 13 extends the baseline model to account for the role of the steppe as a "highway of grass" by reducing the obstacle value $\Theta \cdot x_k$ by one if cell k is a part of the Eurasian steppe, effectively halving the overall $\Theta \cdot x_k$ in the steppe. In addition, we introduce a parameter ψ into the contest function (1) and rewrite it as:

$$\pi_{i,win} = \frac{\psi_i \cdot Y_{i,t}}{(\psi_i \cdot Y_{i,t} + \psi_j \cdot Y_{j,t}) \times (1 + max\{\Theta \cdot \mathbf{x}_k, \Theta \cdot \mathbf{x}_{\overline{k}}\}} \tag{5}$$

where $\psi_i = 3$ if regime i originates as a cell in the eastern steppe and $\psi_i = 1$ otherwise. The extension assumes that a regime that originates from the eastern steppe is more proficient in

war because it had better access to horses and it was socially conditioned and militarized by the ecology of the eastern steppe to seek survival through conquest (Di Cosmo et al., 2009). A $\psi_i = 3$ is the largest plausible difference, as steppe armies were on occasion defeated by sedentary populations.

As before, we simulate this extension 30 times to create 10,000 bootstrap samples. Panel C of Figure 13 shows that even by reducing the geographical barriers in the steppe cells and making the eastern steppe cells three times better at conflict, the main results of the paper remain unchanged.

Recall that our baseline model assumes that state formation rests on the economic foundation of cereal production as estimated by GAEZ v4. But, although some agrarian production was present, the steppe was dominated by pastoral nomadism (Barfield, 1989). Thus, we further refine our baseline model by setting the productivities of all steppe cells uniformly to one-third of the median productivity level of the cells in China. In that way, we consider the steppe as a homogeneous grassland biome dominated by pastoralism.

Considering (i) the population density disparity between China and Inner Asia historically,[36] and (ii) the land-intensive nature of pastoral nomadism,[37] our assumption likely overestimates energy production in the steppe. We allow for this overestimation to compensate for the fact that pastoral nomadism likely enhanced the military potential of steppe regimes through channels not fully captured by caloric production.

Panel D of Figure 13 shows the result of this exercise. Again, we continue to see that China unifies quickly while Europe remains fragmented after 500 periods.

Several features of these two exercises deserve emphasis. First, our aim is to better capture the dynamics of the steppe from circa 1,000 BCE to circa 1500. The purpose of our model is to generate pattern predictions and not to forecast specific or one-off events. In general, steppe confederacies were able to create sizable but short-lived polities that occupied territory on the edge of the Eurasian steppe. This was true of the Huns, Avars, and Magyars in central Europe; the Khazars in Ukraine; the Turkic polities of Anatolia; the various Uyghur kingdoms; and

[36] Jia Yi, a 2nd century BCE scholar, estimated that the Xiongnu confederation of the steppe comprised approximately 300,000 households during his time. By contrast, the contemporary Han dynasty controlled 10 million households or 50 million heads at the peak of its power (Twitchett and Fairbank, 1986, Table 15).

[37] On average, raising livestock requires approximately 100 times as much land as crop cultivation to produce the same amount of calories (Poore and Nemecek, 2018).

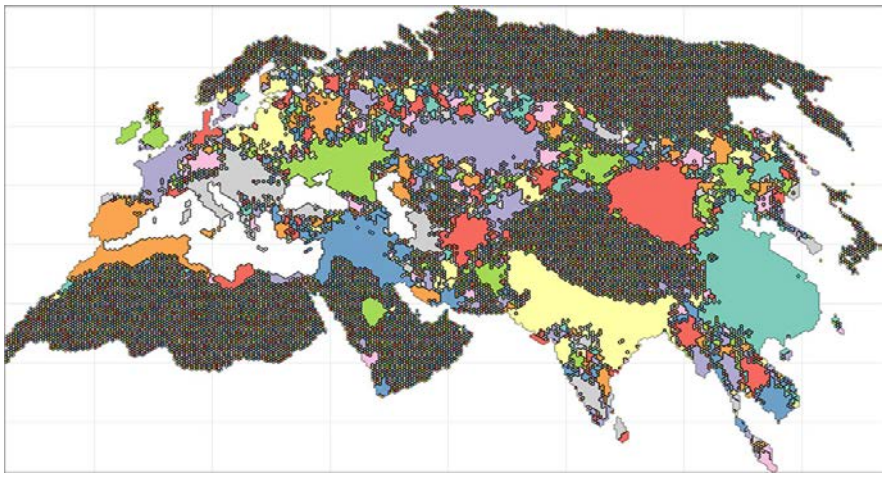

Figure 25: Preferred specification: Representative simulation at t=500.

later, the Golden and Great Hordes and their successor states such as the Crimean, Qasim, and Kazakh Khanates. In the above exercises, we observe patterns comparable to those that we see historically. Large steppe-based confederations do emerge. Figure 25 illustrates a representative map of the preferred specification simulation after 500 periods. In this simulation, there are large polities very much like the eastern (Blue Horde) and western (White Horde) wings of the Golden Horde and the Oirats spanning a large part of the eastern and western steppe.

Second, neither of these exercises generates an empire comparable to the Mongol Empire at its largest extent. This is unsurprising. The rise of the Mongol Empire has been attributed to a number of contingent and one-off factors. Traditional scholarship places great weight on the personality and achievements of Temüjin or Genghis Khan. More recent work places emphasis on a unique set of climatic factors (Hvistendahl, 2012; Pederson et al., 2014). Hvistendahl (2012, p. 1598) summarizes this as follows:

> [A]s Genghis Khan began consolidating power, weather conditions appear to have substantially improved—and to nomads who rely on access to lakes for watering animals, that would have made all the difference. In times of abundant rain, pastoralists thrive, Hessl says: Very little human effort is needed to "create large amounts of meat that is mobile, that can be used for war, and that can be used to transport things." Whole herds can be tended by children—leaving the men free to fight.
>
> If more rainfall boosted grassland productivity and overall energy output, that could

> help explain why the Mongols were able to transition from a "chieftain society, where positions are hereditary" to managing a complex state covering a vast empire, Di Cosmo says: "A centralized state requires more resources." The horses and food accumulated on the steppe would have enabled the Mongols to set out for China in pursuit of gold and silk—and from there on to more distant lands.

Thus, we add another variant to our preferred specification, which includes the two steppe modifications discussed above. We assume that the boost in grassland productivity in the 13th century can be represented by an increase in the caloric yield of cells in the eastern steppe by a factor of three, i.e., we set the productivity of every cell in the eastern steppe to the median productivity of China. That is, the steppe is as productive as China, three times better militarily, and distances are effectively halved.

This exercise generates large steppe polities but with a low probability. For instance, out of 30 simulations of this specification, we observe a single empire spanning the steppe only once (Figure 26). In comparison, Figure 27 illustrates a more representative map at $t = 500$ of this specification. Instead of a single empire spanning the steppe, we see polities that arguably resemble the four khanates of the Mongol Empire (Figure 28).

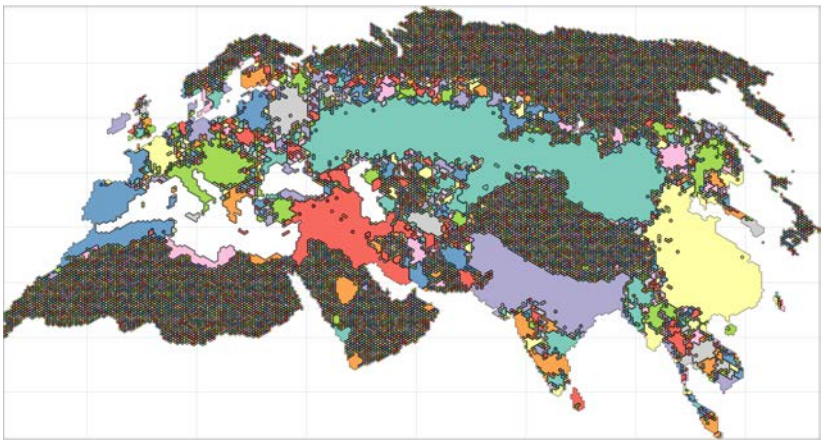

Figure 26: Improved steppe climate: One simulation at t=500.

We interpret these results as a relatively good performance of the model. First, the Mongol Empire was both unique and short-lived. The Mongols began to invade other polities after 1206. It was only in 1221 that they succeeded in conquering the Khwarazmian empire in central Asia. After that point, Mongol expansion was very rapid. But the empire was permanently divided in 1259 as Kublai Khan expanded into the rest of Song China, founding the Yuan dynasty,

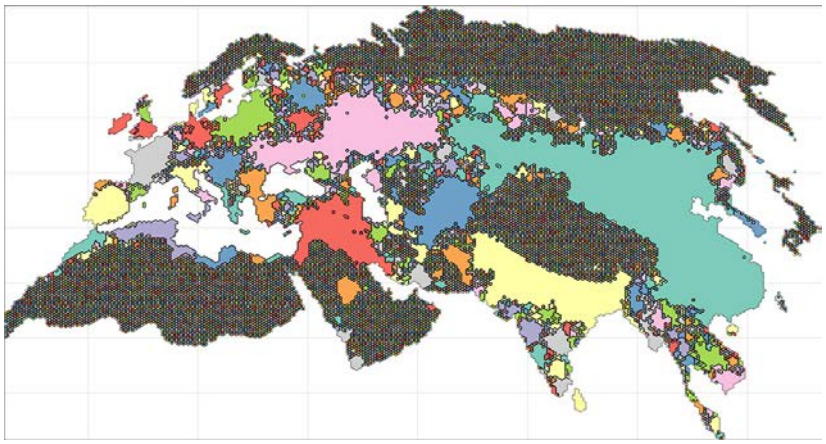

Figure 27: Improved steppe climate: Another simulation at t=500.

Figure 28: The Four Khanates of the Mongol Empire.

while the Golden Horde, Chagatai Khanate, and Ilkhanate became independent. All in all, a single Mongol empire spanning the entire Eurasian steppe lasted for around *25 years* out of the 2,500 years of our time period or around 1% of the time. It would be a problem for our model if it systematically generated steppe polities as large as the Mongol Empire, as it would be counterfactual.

Second, our exercise teaches that beyond favorable climatic conditions, additional factors (for instance, the organizational genius of Genghis Khan or other factors that have been overlooked in the literature thus far) also played a critical role in the rise of the Mongol Empire. More generally, it shows that a confluence of exceptional and accidental circumstances would be required for a pan-Eurasian steppe empire to emerge in history, which explains why it was such a rare and short-lived event.

D.3 Climatic Shocks and Dynastic Cycles

To further account for contingency in history and to study the role of large exogenous events such as natural disasters or incompetent leaders on the rise and fall of polities, we modify the model by extending our simulation range to 4000 periods and allowing random shocks to occur each period. Specifically, we consider two kinds of negative shocks: a general shock that affects all polities (e.g., the Little Ice Age), and a regime-specific shock (e.g., the ascension of a weak ruler such as Charles II of Spain, r. 1665–1700, or the Chongzhen Emperor, r. 1627–1644, or the predisposition of the Carolingians to divide their lands among different heirs). Thus, we call these events "climatic shocks" and "dynastic cycles."

We set the probability of a general shock occurring at $\frac{1}{1000}$ and the probability of a regime-specific shock occurring at $\frac{1}{200}$. Thus, on average, a general shock occurs once every 1000 periods, and each polity independently experiences a specific shock once every 200 periods. When a shock occurs, the regime disintegrates into its constituent cells. These two frequencies are mostly irrelevant since nearly all of our parameter values are time-invariant, and they just determine how often we will observe a collapse of existing state systems.

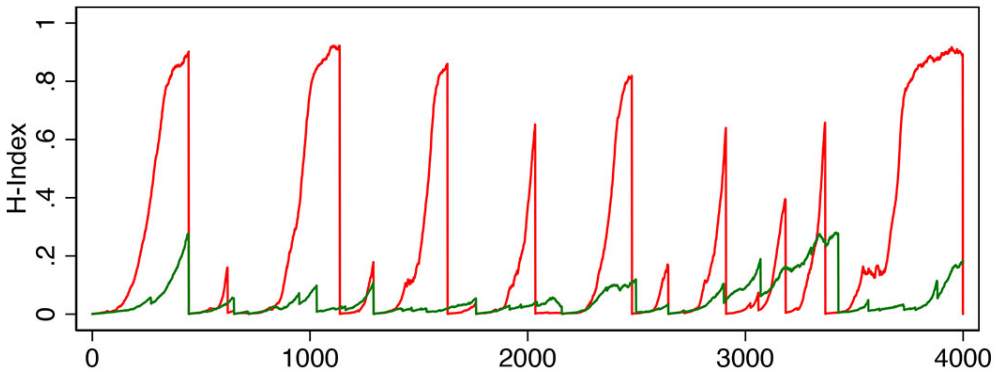

Figure 29: This figure depicts one realization of a 4,000-period simulation where we allow for both general shocks (prob. 0.001) and regime-specific shocks (prob. 0.02) occurring.

Figure 29 depicts the Herfindahl indices for China and Europe from a representative simulation. China experiences periods of sustained unification interrupted by periods of disunity, resembling the patterns of dynastic rise and fall so often depicted in Chinese historiography. Some periods of unified rule are short-lived; others persist for many periods. By contrast, political cycles are relatively muted in Europe. Europe never achieves full unification in this realization of the model. There are periods of heightened military conquests that rest on one state becoming

hegemonic in Europe, but these are always transitory; polycentrism remains persistent.

D.4 The Mediterranean Sea

Historically, the Roman Empire controlled the Mediterranean region for centuries. But in our baseline calibration, we observe a low level of political consolidation in the Mediterranean (Panel A of Figure 30 and Panel A of Figure 31). Here, we expand on our discussion in the main text of how our model can account for the emergence of the Roman Empire.

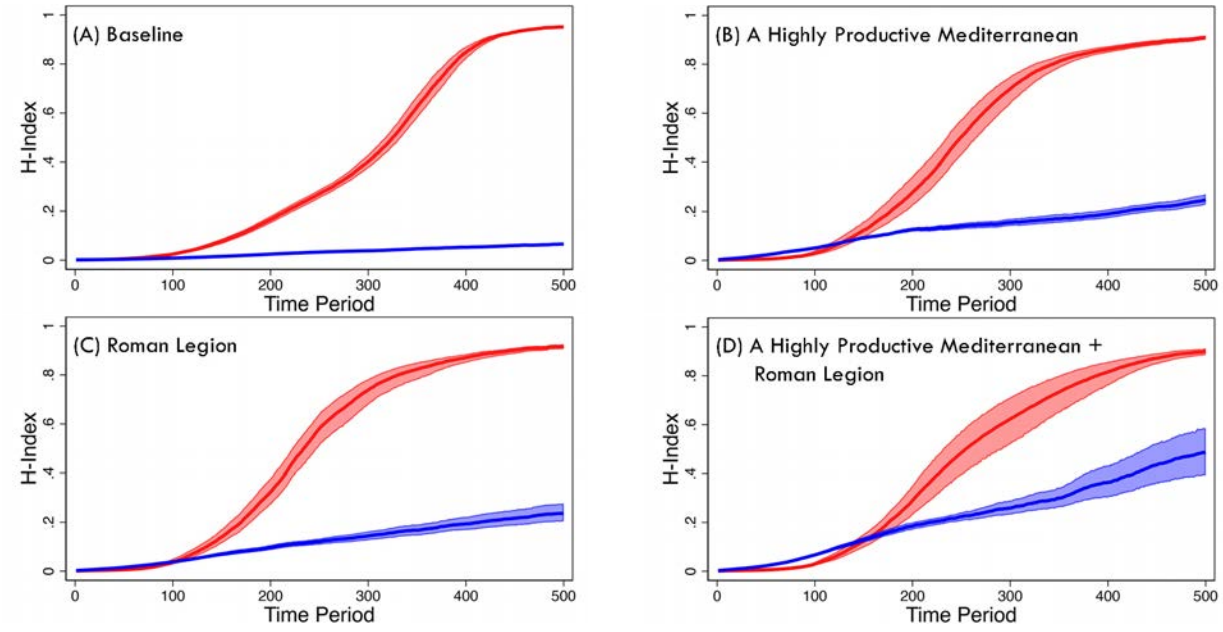

Figure 30: Political consolidation in China (red) and the Mediterranean (blue) under various scenarios.

Historians see the Roman Empire as a unique event (see, for instance, Scheidel, 2019, 35–48). Indeed they have suggested several idiosyncratic factors that may have been responsible for its emergence. First, the Roman economy was built on its access to the extremely productive North African agriculture during the Classical period, when the region was wetter than today (Murphey, 1951; Reale and Dirmeyer, 2000). As a consequence, the provinces of Egypt and Africa (modern-day Algeria, Morocco, and Tunisia) were the "bread baskets" of the empire.[38]

Conditions across the western Mediterranean were so favorable to cereal agriculture between 200 BCE and 150 that this period has been referred to as the Roman Climate Optimum. Wheat

[38] See Rickman (1980). According to Linn (2012, pp. 305–306), "[S]ince the first century BCE, whenever Rome was shut off from North African grain, a shortage typically had ensued . . . All these instances demonstrate two facts about the relationship between North Africa and the city of Rome: (1) North Africa was the lifeline for the city of Rome; (2) warfare commonly led to a food crisis in Rome because of transport blockages."

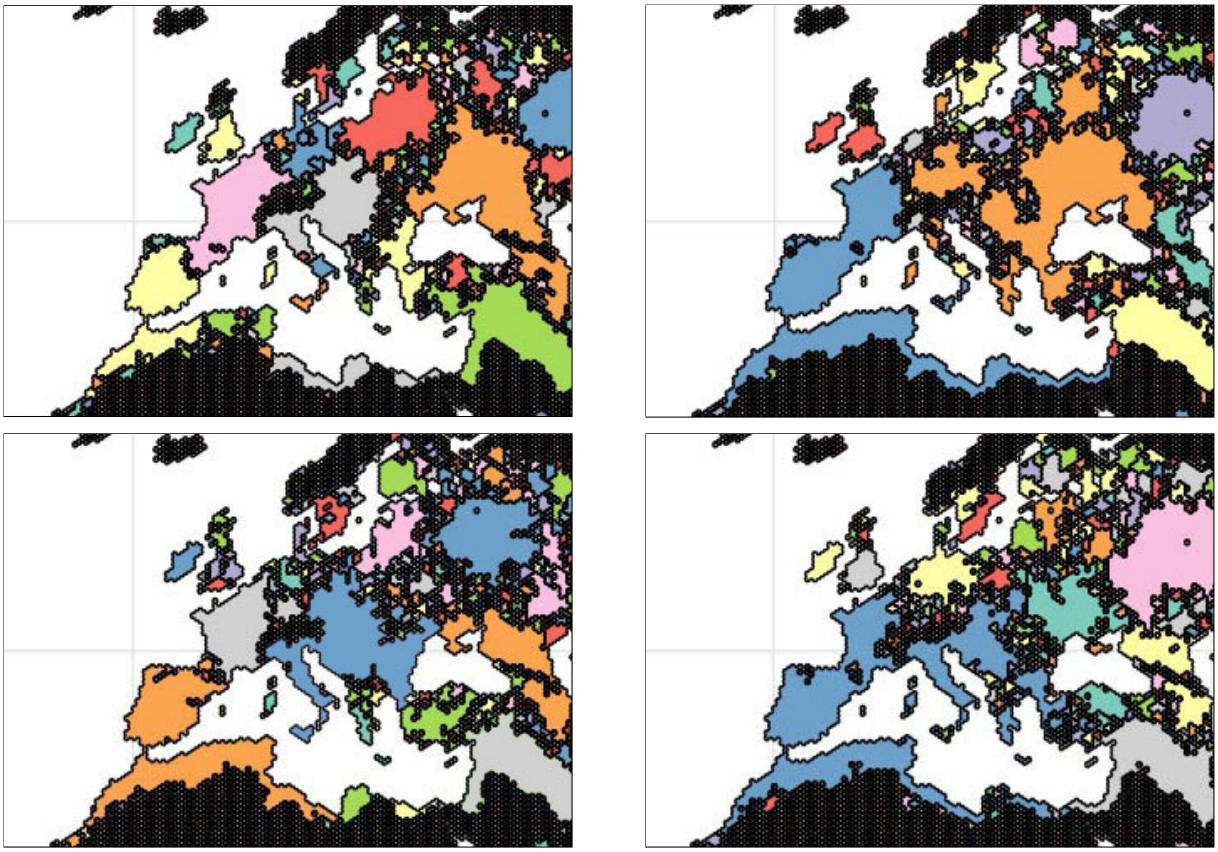

Figure 31: Representative simulations at period 500 for (A) the baseline calibration; (B) a high productivity Mediterranean; (C) military superiority of Latium; and (D) high productivity Mediterranean and military superiority of Latium.

agriculture responds favorably to higher temperatures, particularly in the growing season. And the climate in the Mediterranean was warmer, wetter, and more stable than it has been in preceding or succeeding periods and "a potent incubator of growth" that "fueled the agricultural engine of the economy" (Harper, 2017, p. 52).

A second relevant factor is the political and military culture of Rome. Scholars have highlighted cultural features that may have been specific to Rome and may help explain its success. Among those, we can highlight the martial ethos of Roman society and Roman politics that encouraged politicians to seek electoral successes through external wars (Harris, 1979, 1984; Rosenstein, 2007). Scheidel (2019, pp. 72–74) summarizes some of this in his depiction of Republican Rome as a machine for perpetual war. Another unique feature of Rome was its ability to integrate new citizens. Rome was generous in extending citizenship, and this ensured that it had a steady supply of young men to fight in its armies (see Scheidel, 2019, pp. 65–68).

Motivated by this scholarship, we consider several extensions to the model. In Panel B of

Figure 30, we increase the productivity of every cell surrounding the Mediterranean Sea by a factor of 1.25, or to the median productivity of Europe, whichever is higher. We observe an increase in political consolidation. Nonetheless, the mean Herfindahl index remains low and reaches only around 0.2 at its peak. Moreover, this extension does not generate an empire that resembles the Roman Empire. Indeed, in some simulations Italy remains highly fragmented (see, for a specific example, Panel B of Figure 31).

Next, in Panel C of Figure 30, we give regimes originating from Latium, which formed the core of the Roman city state, an advantage in war. As in the steppe extension, we use Equation 5 as the contest function of regime i if the regime originates as a cell in Latium and set $\psi_i = 3$. As before, in each case, we repeat the simulations 30 times and create 10,000 bootstrap samples. In this extension, we do see greater political centralization around Italy. It is not uncommon to see polities emerge that control large parts of Italy and the Balkans over time. However, the mean Herfindahl index remains relatively low, and we do not observe anything like the Roman Empire (see, for example, Panel C of Figure 31).

Finally, in Panel D of Figure 30, we combine both extensions. In this instance, we observe a non-linear increase in the mean Herfindahl index, which reaches 0.5 at period 500. Even so, the degree of political consolidation remains low compared with China. Indeed, while we now obtain relatively large states emerging around the Mediterranean (see, for example, Panel D in Figure 31), they only rarely correspond to the Roman Empire's boundaries.

Overall, this exercise suggests that the political unification of the Mediterranean in Roman times depended on highly contingent historical factors. This accounts for why no subsequent regime could unify a large proportion of Europe.

D.5 State Formation Across Eurasia

Beyond China and Europe, to what extent can our model explain broader patterns of political fragmentation across Eurasia? Figures 16 and 19 use our preferred model to compute the five largest polities originating in China, Europe (in two definitions: west of the Hajnal line and west of the Urals), South Asia, Middle East, and Southeast Asia. As before, we run 30 simulations and compute the bootstrap mean and confidence intervals with 10,000 samples with replacement. In our simulations, the formation of large states is most pronounced in East Asia. Importantly,

Europe is also distinctive. No other part of the world develops a robust system of medium-sized polities. It is this particular form of polycentricity that Mokyr (2016), Scheidel (2019), and others posit was critical to Europe's economic rise.

To illustrate further, we compute the Herfindahl indices of the five largest polities in these regions. Figure 32 confirms that the formation of large polities is most pronounced in China. After about 250 periods, the rise of one large state dwarfing all other Chinese states becomes apparent and unstoppable. To a lesser extent, we also see large hegemonic states emerging regularly in India and the Middle East. In the case of India, the trend emerges even earlier than in China, but it generally loses momentum over time, and full unification is never achieved. Closer scrutiny reveals that large states always originate from the north (for example, the Maurya, Harsha, and Gupta Empires). This is consistent with what we observe historically. Large polities or empires often emerged in North India. But until the Mughal Empire and the British Raj, they did not come close to unifying the Indian subcontinent.

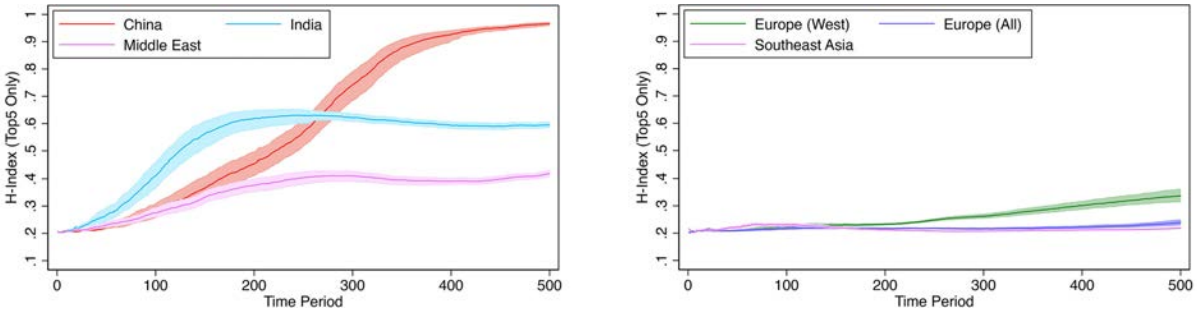

Figure 32: Herfindahl indices of the five largest polities in different Eurasian regions.

In the case of the Middle East, we also observe considerable political consolidation, but nowhere close to the full political unification seen in China. One particular episode that is not easily generated by our model is the rapid Arab conquests of the 7th century. This is not surprising, as the episode has long been regarded as a unique event by historians.[39] The success of the Arab conquest of the entire Sasanian Empire and much of the Byzantine Empire in the mid-7th century has been attributed to three factors: (i) the weaknesses of the Sasanian and Byzantine Empires due to war and plague-induced population losses; (ii) religious divisions with the Byzantine Empire between the dominant Chalcedonian Church and Monophysitism; (iii) the religious cohesion, or *asabiyyah*, of the first Muslims. These factors, particularly the role of

[39]For example, Kennedy (2001, p. 2) observes that "Despite the mass of words, the full explanation for Muslim victory still eludes us."

religion, are not in our model, but could be added in future research.

At the same time, the Abbasid Caliphate was brittle. By 900, it had partitioned into nine components (Scheidel, 2019, p. 140). Our simulations typically produce several mid-size states in the Middle East that can be interpreted as the different successor states of the Caliphate.

Consistent with historical observations, in our simulations we generally do not observe the rise of hegemonic states in Europe and Southeast Asia. In all three cases, the Herfindahl indices are remarkably stable through the 500 periods, hovering at around 0.2, which implies that the largest polities in these regions are consistently evenly matched (the Herfindahl index value of five equal-sized polities is exactly 0.2). However, the similarity between Europe and Southeast Asia is somewhat superficial. As Figure 19C illustrates, the largest states in Southeast Asia are absolutely small. Even at $t = 500$, we generally do not observe any polity amassing more than 100 hexagons (an area slightly smaller than modern-day Laos). In Europe, the largest polities grow and become sizable over time (Panels B and C in Figure 16), but because they grow in tandem, no single power becomes dominant over time. No power acquires the capability to overwhelm all its neighbors singlehandedly. For this reason, the trend is almost flat when we compute the Herfindahl indices for the five largest European states in Figure 32.

E The Expansion of China in History

Historically, China as a political entity emerged in the middle and lower reaches of the Yellow River. In the 2nd century BCE, the Han dynasty's territorial reach did not encompass China's southeastern coast or the Lingnan region and the Yungui plateau (Figure 33). Successive regimes gradually absorbed these regions into the Chinese empire, but the process took centuries and, for a long time, Chinese rulers maintained only nominal suzerainty in much of these regions.

Table 3 summarizes the unified regimes in China and their origins. Qin, the first dynasty, originated from the Wei River, a tributary of the Yellow River. The founding emperor of the Former Han dynasty and his closest aides, including the founding prime minister Xiao He, rebelled against the Qin empire near their home county of Pei north of the Huai River. The Later Han dynasty was founded by Liu Xiu, who received support from local magnates from his native region of Nanyang in the Middle Yangtze River Basin. The founder of the Western Jin was a usurper of the Cao Wei regime, which unified northern China from Xiuchang in the lower

reaches of the Lower Yellow River. Sui and Tang were offshoots of Toba Wei, a proto-Turkic regime originally based in Pingcheng, about 250 km west of present-day Beijing. Northern Song was a usurper state of Later Zhou, which originated from Ye in the Lower Yellow River. The Yuan and Qing rulers were nomadic or semi-nomadic people from the Eurasian steppe. The Ming dynasty, the only unified regime that had ruled China from a capital city south of the Yangtze River, could be traced to the Red Turban rebels who were active in the Huai and Lower Yangtze regions toward the end of the Yuan dynasty.

Figure 33: Early Han Dynasty

Table 3: Major Unifications of China

Dynasty	Period	Origins
Qin	221–206 BCE	Middle Yellow River
Former Han	202 BCE–8	Lower Yellow River
Later Han	25–220	Middle Yangtze
Western Jin	280–316	Lower Yellow River
Sui	581–618	Middle Yellow River
Tang	618–907	Middle Yellow River
Northern Song	960–1127	Lower Yellow River
Yuan	1206–1368	Eastern Mongolia
Ming	1368–1644	Huai River/Lower Yangtze
Qing	1644–1912	Manchuria

In summary, eight unified Chinese regimes started in northern China: either in the Yellow River Basin or in the steppe north of it. Two regimes originated from the Yangtze River Basin. None came from the regions further south (Yungui, Lingnan, and the Southeast Coast). This observation is consistent with our simulation results in Figure 15.

F Africa and the Americas

In this section, we provide further details of the predictions of our model regarding Africa and the Americas.

F.1 Africa

In the main text, we highlighted that scholars have advanced numerous accounts to explain why large agrarian states did not emerge in sub-Saharan Africa prior to 1500.

One group of explanations focuses on the slow diffusion of technology due to Africa's geography. First, the rarity of copper in many parts of Africa constrained the development of metallurgy and the use of metal tools on the continent (Childe, 1957). The oldest securely dated smelting furnaces in sub-Saharan Africa can be dated to 400–200 BCE, almost a millennium after the end of the Bronze Age and the beginning of the Iron Age in Eurasia (Killick, 2015). Diamond (1997) argues that the verticality of the African continent plus the barrier posed by the Sahara desert, which dried up about 5,400 years ago, prevented many technologies from spreading into sub-Saharan Africa. Consequently, land was less productive in sub-Saharan Africa than in Eurasia (Goody, 1971; Webb, 2006). This was partly due to the absence of tools such as the plow and wheeled transport (Goody, 1971). Furthermore, without artificial fertilizers, the fertility of the land often dropped off dramatically, thereby encouraging slash and burn agricultural and pastoralism rather than intensive cultivation, which hindered the formation of centralized states.

A complementary group of explanations emphasizes Africa's climate and disease environment. High temperatures in many parts of sub-Saharan Africa mean that insect vectors are very active (Bellone, 2020). Two important examples of parasite-caused diseases are malaria, spread by mosquitoes, and sleeping sickness and nagana, spread by the tsetse fly. Malaria has played an important role in limiting population growth in sub-Saharan Africa. The tsetse fly is responsible for the parasite that causes nagana in domesticated animals. This meant that historically there was a dearth of large livestock in areas affected by the tsetse fly. Alsan (2015) documents how this factor impeded the development of intensive agriculture and state formation. Weil (2014), too, suggests that Africa's disease environment can explain why it had fallen behind Eurasia in terms of population, urbanization, and state development by 1500.

To capture the effect of the slow diffusion of intensive agricultural technologies on state formation in sub-Saharan Africa, we modify our preferred specification and allow cells in this region to annex each other only from $t = 150$ (which would correspond to c. 250 BCE) onward. In addition, recall that our preferred specification is formulated to address GAEZ v4's overestimation of historical productivities in hot and cold regions and should capture, albeit imperfectly, some effects of climate on Africa's historical resource availability.

Unlike the baseline specification, where we see large empires emerging in almost every part of Africa over time (left panel of Figure 34 and Panel B of Figure 17), in the modified

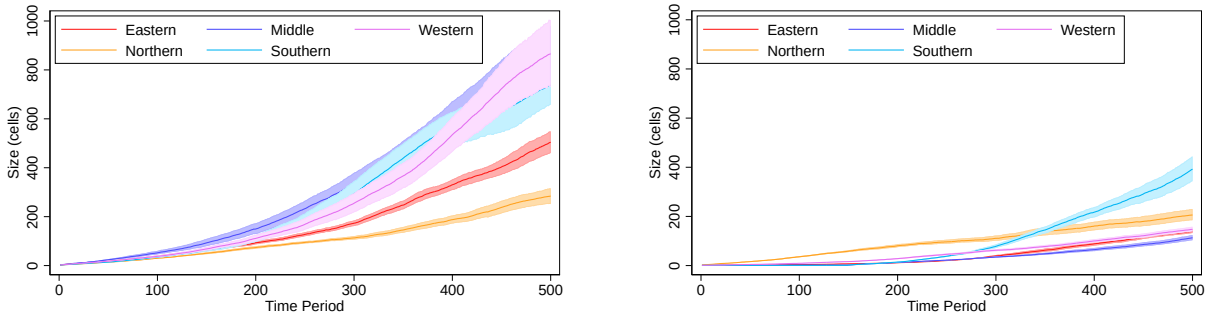

Figure 34: Left panel: baseline simulations. Right panel: preferred specification.

preferred specification (right panel of Figure 34), the largest states in Africa are relatively small. Only southern Africa—home to the historical kingdom centered on the Great Zimbabwe (c. 11th–15th century) and the 19-century Zulu kingdom—occasionally produces states larger than 300 hexagons (approximately the size of France).

F.2 The Americas

The isolation of the Americas from Eurasia and Africa determined that, until the Columbian Exchange, its development depended solely on its local agricultural and technological innovations. Only one of the major cereals cultivated today, maize, is indigenous to the Americas. The other six (barley, oats, rice, rye, sorghum, and wheat) belonged exclusively to the "Old World" throughout our period of study. The absence of iron tools in the Americas before 1500 meant that the major maize-producing areas today, including Iowa, Illinois, and northern Argentina, were marginal in maize cultivation due to the difficulties in clearing the tough-rooted sod covering the prairies and savannas (Hudson, 2004).[40] Maize cultivation in these otherwise highly fertile plains depended on slash-and-burn techniques, which could only support low population densities.

Furthermore, as in Africa, Diamond (1997) argues that the North-South orientation of the Americas slowed the diffusion of crops as climatic conditions varied across latitude (see also Turchin et al., 2006). The first Europeans who traveled to the Americas observed that maize grown in different places varied widely in appearance, reflecting their distinct isozymes (Goodman and Galinat, 1988). While this reflects the amazing ability of maize to adapt to a wide range of environments and climatic conditions, the adaptation process was time consuming.

[40] In the absence of iron tools, the Indigenous peoples used bison scapulae and bone tools, which wore out quickly, to work their gardens (Bamforth, 2021).

On the eve of the Columbian Exchange, several millennia after maize was domesticated, Mexico and neighboring Guatemala remained the main maize areas of the Americas, alongside Peru, where maize might have been independently domesticated (Kistler et al., 2018).

Peru deserves a separate mention. As Figure 5 illustrates, attainable yields based on rainfed, low-input cultivation in Peru are quite low, both in highland Peru and its coastal deserts. Without modern agricultural techniques, these lands appear incapable of supporting a large premodern state like the Inca Empire. However, the local peoples had access to guano, the desiccated manure of seabirds rich in nitrates and phosphates. Known as "white gold" to many in an industry that is worth $1.1 billion annually (Plazas-Jiménez and Cianciaruso, 2020), guano had been used as a natural fertilizer for several millennia (Poulson et al., 2013).

Guano was highly valued by the Incas. To safeguard its supply, the Inca kings undertook harsh measures, including imposing death penalties for those who killed a bird or disturbed a bird's nest (de la Vega, 1609, (1961); Rodrigues and Micael, 2021). Alexander von Humboldt, a Prussian scientist who visited Peru in 1802 and whose writings helped make guano known to the world, remarked upon realizing guano's properties that he now knew the secret to the glory of the Inca Empire and its predecessors: their possession of large amounts of guano that allowed their deserts to blossom (Cushman, 2014). Importantly, guano was a location-specific asset. Not only was Peru blessed with an abundance of guano-producing birds, including the Peruvian cormorant, the Peruvian pelican, and the Peruvian booby, but the relative lack of precipitation along the Peruvian coast was also critical by allowing guano to accumulate and bake instead of being washed away by rain (Szpak et al., 2012). By contrast, although Europe has many seabird colonies too, high rainfall levels mean that European guano is of inferior quality due to severe leaching of valuable nitrates.

We incorporate these insights by extending our baseline model in two ways. First, we account for the timing and spread of sedentary agriculture in the Americas based on Weatherwax (1954, Figure 18) and Blake (2015, Figure 6.1) and allow cells in the Americas to annex each other only after the adoption of maize cultivation. Next, we identify the guano-bearing regions of South America based on Cushman (2014, Map 1). Next, as in the steppe and the Mediterranean extensions, we increase the attainable yield of cells in these regions by a factor of 1.25, or to the median productivity of South America, whichever is higher. Panel C of Figure 18 illustrates how, once we consider these factors, the Americas cease to produce super-sized polities. Conforming

to historical observations, we see that the larger states in the Americas typically emerge in the Pacific coast and Andean highlands, Guatemala and the Yucatán Peninsula, and the Mexican plateau, home to the Inca, Maya, and Aztec societies, respectively (Panel C of Figure 18; Figure 35). Figure 35 presents the same information, but now in terms of Herfindahl indeces of political unification.

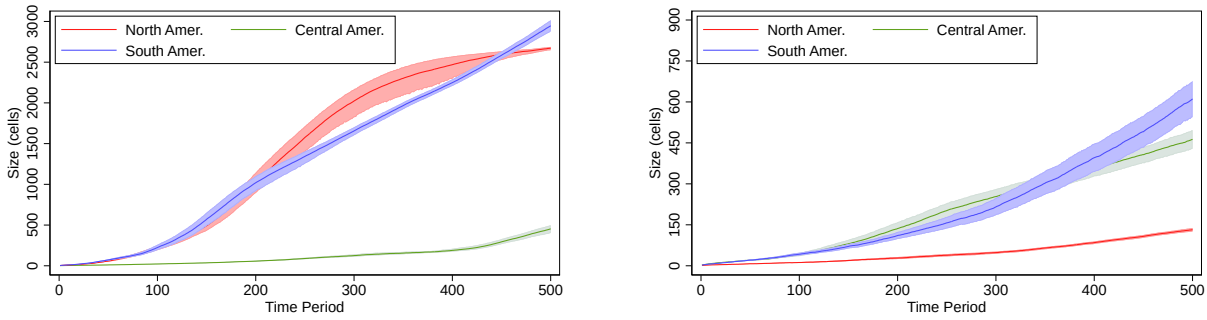

Figure 35: State formation in the Americas. Baseline simulations (left panel) vs. simulation adjusted by the spread of corn (right panel) eastern United States (North America) and Argentina (South America).

Appendix References

Alesina, A., P. Giuliano, and N. Nunn (2013): "On the Origins of Gender Roles: Women and the Plough," *Quarterly Journal of Economics*, 128, 469–530.

Alsan, M. (2015): "The Effect of the TseTse Fly on African Development," *American Economic Review*, 105, 382–410.

Ashraf, Q. and O. Galor (2011): "Dynamics and Stagnation in the Malthusian Epoch," *American Economic Review*, 101, 2003–41.

Bai, Y. and J. Kung (2011): "Climate Shocks and Sino-nomadic Conflict," *Review of Economics and Statistics*, 93, 970–981.

Bamforth, D. B. (2021): *The Archaeology of the North American Great Plains*, Cambridge: Cambridge University Press.

Barfield, T. (1989): *The Perilous Frontier: Nomadic Empires and China*, Cambridge, MA: Basil Blackwell.

Bellone, R. (2020): "The Role of Temperature in Shaping Mosquito-Borne Viruses Transmission," *Frontiers in Microbiology*, 11, 584846.

Blake, M. (2015): *Maize for the Gods: Unearthing the 9,000-Year History of Corn*, Berkeley: University of California Press.

Boserup, E. (1965): *The Conditions of Agricultural Growth: The Economics of Agrarian Change Under Population Pressure*, Chicago: Aldine.

Catt, J. (2001): "The Agricultural Importance of Loess," *Earth-Science Reviews*, 54, 213–229.

Childe, V. G. (1957): "The Bronze Age," *Past & Present*, 2–15.

Csáky, V., D. Gerber, I. Koncz, G. Csiky, B. G. Mende, B. Szeifert, B. Egyed, H. Pamjav, A. Marcsik, E. Molnár, G. Pálfi, A. Gulyás, B. Kovacsóczy, G. M. Lezsák, G. Lőrinczy, A. Szécsényi-Nagy, and T. Vida (2020): "Genetic Insights into the Social Organisation of the Avar Period Elite in the 7th Century AD Carpathian Basin," *Scientific reports*, 10, 948–948.

Cushman, G. (2014): *Guano and the Opening of the Pacific World: A Global Ecological History*, Cambridge: Cambridge University Press.

de la Vega, G. (1609, (1961)): *The Royal Commentaries of the Incas*, New York: Avon Books, edited by Alain Gheerbrant and translated by Maria Jolas.

Di Cosmo, N. (1994): "Ancient Inner Asian Nomads: Their Economic Basis and Its Significance in Chinese History," *The Journal of Asian Studies*, 53, 1092–1126.

Di Cosmo, N., A. Frank, and P. B. Golden, eds. (2009): *Cambridge History of Inner Asia: The Chinggisid Age*, Cambridge: Cambridge University Press.

Diamond, J. (1997): *Guns, Germs, and Steel*, New York: W.W. Norton & Company.

Fischer, G., F. Nachtergaele, H. van Velthuizen, F. Chiozza, G. Franceschini, M. Henry, D. Muchoney, and S. Tramberend (2021): *Global Agro-Ecological Zones (GAEZ v4)—Model Documentation*, Rome: FAO.

Frachetti, M. (2008): *Pastoralist Landscapes and Social Interaction in Bronze Age Eurasia*, Berkeley: University of California Press.

Galor, O. and O. Özak (2016): "The Agricultural Origins of Time Preference," *American Economic Review*, 106, 3064–3103.

Gat, A. (2006): *War in Human Civilization*, Oxford: Oxford University Press.

Gibbon, E. (2003): *The Decline and Fall of the Roman Empire*, New York: Modern Library.

Goldewijk, K., A. Beusen, J. Doelman, and E. Stehfest (2017): "Anthropogenic Land Use Estimates for the Holocene–HYDE 3.2," *Earth System Science Data*, 9, 927–953.

Goodman, M. M. and W. C. Galinat (1988): "The History and Evolution of Maize," *Critical Reviews in Plant Sciences*, 7, 197–220.

Goody, J. (1971): *Technology, Tradition and the State in Africa*, Oxford: Oxford University Press.

Guinnane, T. (2021): "We Do Not Know the Population of Every Country in the World for the past Two Thousand Years," CESifo Working Paper Series 9242, CESifo.

Harper, K. (2017): *The Fate of Rome*, Princeton, NJ: Princeton University Press.

Harris, W. V. (1979): *War and Imperialism in Republican Rome, 327–70 B.C.*, Oxford: Clarendon Press.

Harris, W. V., ed. (1984): *The Imperialism of Mid-Republican Rome*, University Park, PA: Pennsylvania State University Press.

Hijmans, R. J., S. E. Cameron, J. L. Parra, P. G. Jones, and A. Jarvis (2005): "Very High Resolution Interpolated Climate Surfaces for Global Land Areas," *International Journal of Climatology*, 25, 1965–1978.

Ho, P. (1975): *The Cradle of the East: An Inquiry into the Indigenous Origins of Techniques*

and Ideas of Neolithic and Early Historic China, 5000–1000 B.C., Chicago: University of Chicago Press.

Hritz, C. and J. Pournelle (2015): "Feeding History: Deltaic Resilience, Inherited Practice, and Millennial-Scale Sustainability in an Urbanized Landscape," in *Viewing the Future in the Past: Historical Ecology Applied to Environmental Issues*, ed. by H. T. F. II, D. J. Goldstein, and L. M. Paciulli, Columbia: University of South Carolina Press.

Huang, R. (1988): *China: A Macro History*, Armonk, NY: M.E. Sharpe.

Hudson, J. C. (2004): "Agriculture," in *Encyclopedia of the Great Plains*, ed. by D. J. Wishart, Lincoln: University of Nebraska Press.

Hvistendahl, M. (2012): "Roots of Empire," *Science*, 337, 1596–1599.

Kaplan, J. O. and K. M. Krumhardt (2011): "The KK10 Anthropogenic Land Cover Change Scenario for the Preindustrial Holocene, Link to Data in NetCDF format," Supplement to: Kaplan, Jed O; Krumhardt, Kristen M; Ellis, Erle C; Ruddiman, William F; Lemmen, Carsten; Klein Goldewijk, Kees (2011): Holocene Carbon Emissions as a Result of Anthropogenic Land Cover Change. The Holocene, 21(5), 775–791.

Kaplan, J. O., K. M. Krumhardt, E. C. Ellis, W. F. Ruddiman, C. Lemmen, and K. K. Goldewijk (2011): "Holocene Carbon Emissions as a Result of Anthropogenic Land Cover Change," *The Holocene*, 21, 775–791.

Kennedy, H. (2001): *The Armies of the Caliphs: Miltary and Society in the Early Islamic State, Warfare and History*, New York: Routledge.

Killick, D. (2015): "Invention and Innovation in African Iron-smelting Technologies," *Cambridge Archaeological Journal*, 25, 307–319.

Kistler, L., S. Y. Maezumi, J. G. de Souza, N. A. S. Przelomska, F. M. Costa, O. Smith, H. Loiselle, J. Ramos-Madrigal, N. Wales, E. R. Ribeiro, R. R. Morrison, C. Grimaldo, A. P. Prous, B. Arriaza, M. T. P. Gilbert, F. de Oliveira Freitas, and R. G. Allaby (2018): "Multiproxy Evidence Highlights a Complex Evolutionary Legacy of Maize in South America," *Science*, 362, 1309–1313.

Lattimore, O. (1940): *Inner Asian Frontiers of China*, New York: American Geographical Society.

——— (1947): "Inner Asian Frontiers: Chinese and Russian Margins of Expansion," *Journal of Economic History*, 7, 24–52.

Linn, J. (2012): "The Roman Grain Supply, 442–455," *Journal of Late Antiquity*, 5, 298–321.

Mayshar, J., O. Moav, and Z. Neeman (2017): "Geography, Transparency and Institutions," *American Political Science Review*, 111, 622–636.

Mayshar, J., O. Moav, and L. Pascali (2022): "The Origin of the State: Land Productivity or Appropriability?" *Journal of Political Economy*, forthcoming.

McNeill, W. H. (2021): "The Steppe," in *Encyclopedia Britannica*, Encyclopædia Britannica, Inc.

Mokyr, J. (2016): *A Culture of Growth: The Origins of the Modern Economy*, Princeton, NJ: Princeton University Press.

Mostern, R. (2016): "Sediment and State in Imperial China: The Yellow River Watershed as an Earth System and a World System," *Nature + Culture*, 11, 121–147.

Murphey, R. (1951): "The Decline of North Africa since the Roman Occupation: Climatic or Human?" *Annals of the Association of American Geographers*, 41, 116–132.

Neparáczki, E., Z. Maróti, and T. Kalmár (2019): "Y-Chromosome Haplogroups from Hun, Avar and Conquering Hungarian Period Nomadic People of the Carpathian Basin," *Scientific Reports*, 9, 16569.

Pederson, N., A. E. Hessl, N. Baatarbileg, K. J. Anchukaitis, and N. Di Cosmo (2014): "Pluvials, droughts, the Mongol Empire, and modern Mongolia," *Proceedings of the National Academy of Sciences*, 111, 4375–4379.

Plazas-Jiménez, D. and M. V. Cianciaruso (2020): "Valuing Ecosystem Services Can Help to Save Seabirds," *Trends in Ecology & Evolution*, 35, 757–762.

Poore, J. and T. Nemecek (2018): "Reducing Food's Environmental Impacts through Producers and Consumers," *Science*, 360, 987–992.

Poulson, S. R., S. C. Kuzminsky, G. R. Scott, V. G. Standen, B. Arriaza, I. Muñoz, and L. Dorio (2013): "Paleodiet in Northern Chile through the Holocene: Extremely Heavy $\delta^{15}N$ Values in Dental Calculus Suggest a Guano-Derived Signature?" *Journal of Archaeological Science*, 40, 4576–4585.

Pournelle, J. (2003): "Marshland of Cities: Deltaic Landscapes and the Evolution of Early Mesopotamian Civilization," Dissertation, University of California, San Diego.

Ramankutty, N., J. Foley, J. Norman, and K. McSweeney (2002): "The Global Distribution of Cultivable Lands: Current Patters and Sensitivity to Possible Climate Change,"

Global Ecology and Biogeography, 11, 377–392.

Reale, O. and P. Dirmeyer (2000): "Modeling the Effects of Vegetation on Mediterranean Climate during the Roman Classical Period: Part I. Climate History and Model sSnsitivity," *Global and Planetary Change*, 25, 163–184.

Reuter, H. I., A. Nelson, and A. Jarvis (2007): "An Evaluation of Void-Filling Interpolation Methods for SRTM Data," *International Journal of Geographical Information Science*, 21, 983–1008.

Rodrigues, P. and J. Micael (2021): "The Importance of Guano Birds to the Inca Empire and the First Conservation Measures Implemented by Humans," *International Journal of Avian Science*, 283–291.

Róna-Tas, A. and A. Berta (2011): *West Old Turkic. Turkic Loanwords in Hungarian*, Wiesbaden: Harrassowitz.

Ropa, A. and T. Dawson, eds. (2020): *The Horse in Premodern European Culture*, New York: De Gruyter.

Rosenstein, N. (2007): "Military Command, Political Power, and the Republican Elite," in *A companion to the Roman army*, ed. by P. Erdkamp, Oxford: Blackwell, 132–147.

Scheidel, W. (2019): *Escape from Rome*, Princeton, NJ: Princeton University Press.

Scott, J. C. (2017): *Against the Grain*, Princeton, NJ: Princeton University Press.

Skinner, G. W. (1977): *The City in Late Imperial China*, Stanford: Stanford University Press.

Sng, T.-H., P. Z. Chia, C.-C. Feng, and Y.-C. Wang (2018): "Are China's provincial boundaries misaligned?" *Applied Geography*, 98, 52–65.

Szpak, P., J.-F. Millaire, C. D. White, and F. J. Longstaffe (2012): "Influence of Seabird Guano and Camelid Dung Fertilization on the Nitrogen Isotopic Composition of Field-Grown Maize (Zea mays)," *Journal of Archaeological Science*, 39, 3721–3740.

Turchin, P., J. Adams, and T. Hall (2006): "East-West Orientation of Historical Empires and Modern States," *Journal of World-Systems Research*, 12, 219–229.

Turchin, P., T. E. Currie, E. A. L. Turner, and S. Gavrilets (2013): "War, Space, and the Evolution of Old World Complex Societies," *Proceedings of the National Academy of Sciences*, 110, 16384–16389.

Twitchett, D. and J. Fairbank, eds. (1986): *Cambridge History of China. Vol. 1: The Ch'in and Han Empires, 221 B.C.–A.D. 220*, Cambridge: Cambridge University Press.

Weatherwax, P. (1954): *Indian corn in old America*, New York: Macmillan.

Webb, J. L. A. (2006): "Ecology and Culture in West Africa," in *Themes in West Africa's History*, ed. by E. Akyeampong, Ohio: Ohio University Press, 33–51.

Weil, D. (2014): "The Impact of Malaria on African Development over the Longue Durée," in *Africa's Development in Historical Perspective*, ed. by E. Akyeampong, J. Robinson, N. Nunn, and R. H. Bates, Cambridge: Cambridge University Press, 89–124.

Zheng, P. (1984): "Livestock Breeds of China," Animal Production and Health Papers 46, Food and Agriculture Organization.